2007

Predicting water quality effects on bay anchovy (Anchoa mitchilli) growth and production in Chesapeake Bay: linking water quality and individual-based fish models

Aaron Thomas Adamack
Louisiana State University and Agricultural and Mechanical College

PREDICTING WATER QUALITY EFFECTS ON BAY ANCHOVY (*ANCHOA MITCHILLI*) GROWTH AND PRODUCTION IN CHESAPEAKE BAY: LINKING WATER QUALITY AND INDIVIDUAL-BASED FISH MODELS

A Dissertation

Submitted to the Graduate Faculty of the
Louisiana State University and
Agricultural and Mechanical College
in partial fulfillment of the
requirements for the degree of
Doctor of Philosophy

in

Department of Oceanography and Coastal Sciences

by
Aaron Thomas Adamack
B.Sc., University of British Columbia, 1999
M.S., Louisiana State University, 2003
August, 2007

ACKNOWLEDGEMENTS

After nearly eight years of graduate school there are a number of people that I need to thank for their help, guidance and friendship. I will start off by thanking my advisor, Dr. Kenneth Rose for his guidance over the past several years and his patience in getting me through two degrees (M.S. and a Ph. D.). I believe that the training that I have received from Kenny over the past several years will serve me well throughout my future career in science. Unfortunately, despite his guidance there is little hope for my having a future career in basketball. I also thank Kenny for providing me with the opportunity to present my research in Italy.

I would like to thank my committee members, Dr. Jim Cowan, Dr. Dubravko Justic, Dr. Carl Cerco, Dr. Barry Moser, Dr. James Geaghan, Dr. Ronald Malone and Dr. John Hargreaves for their insight and guidance. I would like to extend a special thank you to Dr. Jim Cowan who has served as a committee member for both my Masters degree and my Ph. D. I appreciate all of the time that he has spent looking at my work and the enthusiasm that he has shown for my results. I have also enjoyed the stories he has told and the wisdom he has shared during the "smoke and jokes" and shrimp and crawfish boils. Thank you to Dr. James Geaghan for agreeing to fill in on my committee after Dr. Moser passed away, despite being on dozens of other committees.

There are several people that I wish to thank for making contributions that without which, I could not have done this research. Dr. Winston Lung and Dr. Alex Nice, both of the University of Virginia, provided me with the output from their CE-QUAL-W2 water quality model for the Patuxent River. Dr. Denise Breitburg, of the Smithsonian Environmental Research Center, facilitated this collaboration and also provided much of the anchovy field data that was used for the simulations. Dr. Sarah Kolesar of the Office of Naval Research also provided some of her

anchovy field data. Dr. Carl Cerco provided me with access to the source code for the CE-QUAL-ICM water quality model. Dr. Cerco and Mark Noel, both of the U.S. Army Corps of Engineers Waterways Research Station, were very helpful, providing me with guidance on the use and modification of the water quality model. Dr. Ed Houde and Dr. Tom Miller, both of the Chesapeake Bay Laboratory, provided me with access to field data from the TIES and CHESFIMS projects respectively. Additionally, Dr. Houde provided me with a number of insights into the movement behavior and biology of bay anchovy in Chesapeake Bay.

I could not have gotten through graduate school without the friendship and support of a number of people. My parents Tom and Bev Adamack, my sister Denene, and my grandma Helen Adamack have all provided me with lots of love, support and guidance throughout my academic career. I owe a big thanks to several members of the Rose Lab: Dr. Cheryl Murphy, Shaye Sable, Susanne Hoeppner, Dr. Julie Neer, and Dr. Brian Roth, for their friendship, support and interesting times. Thanks to Kristen Laursen for providing me with her friendship and support. Finally, I would like to thank several friends who have aided and abetted me in my efforts to procrastinate during the last couple of years: Angela Schrift, Joe and Melissa Baustian, Brian Milan, Carey Lynn Perry, Mike McDonough, Kate Carpenter Hoefer, Susanne Hoeppner, Sean and Emily Keenan, Aaron and Dr. Pam Podey, Dr. Kevin and Piper Boswell, Dr. Dave and Janelle Wells, Dr. Ted Switzer, Dave Lindquist, Kirsten Simonsen, and Jody Callihan. I apologize if I have missed anyone.

Along the way, I've received financial support from a number of different organizations. LSU's Coastal Fisheries Institute provided me with a graduate research assistantship throughout my time at LSU. I received funding for travel from an EPA STAR grant (*R 82945801*) and from LSU's Department of Oceanography and Coastal Sciences and the Graduate School.

TABLE OF CONTENTS

ACKNOWLEDGEMENTS ii

ABSTRACT vi

CHAPTER 1: GENERAL INTRODUCTION 1
1.1 Introduction 1
1.2 Dissertation Overview 4
1.3 References 7

CHAPTER 2: SIMULATING THE EFFECTS OF HYPOXIA ON BAY ANCHOVY (*ANCHOA MITCHILLI*) EGG AND LARVAL MORTALITY IN THE PATUXENT RIVER USING COUPLED WATERSHED, WATER QUALITY, AND INDIVIDUAL-BASED MODELS 11
2.1 Introduction 11
2.2 Methods 16
2.2.1 Watershed Model 16
2.2.2 Water Quality Model 18
2.2.3 Determination of Water Column Structure and Associated DO Concentrations 21
2.2.4 Individual-Based Model 22
2.2.5 Simulations 30
2.3 Results 31
2.3.1 Water Column Structure and DO Concentrations 31
2.3.2 Egg Mortality Rates 37
2.3.3 Larval Mortality Rates 40
2.4 Discussion 43
2.5 References 51

CHAPTER 3: COUPLING HYDRODYNAMIC, WATER QUALITY, AND INDIVIDUAL–BASED MODELS TO SIMULATE THE EFFECTS OF CHANGES IN NUTRIENT LOADINGS ON BAY ANCHOVY IN CHESAPEAKE BAY 56
3.1 Introduction 56
3.2 Methods 60
3.2.1 Chesapeake Bay Water Quality Model 60
3.2.2 Bay Anchovy Model 65
3.2.3 Modifications to the Eutrophication Model to Accommodate Bay Anchovy 80
3.2.4 Simulations 81
3.3 Results 90
3.3.1 Assessment of Calibration Using Baseline Simulations 90
3.3.2 Effects of Water Year and Recruitment Level in Baseline Simulations 97
3.3.3 Effects of Nutrient Loadings 108
3.3.4 Kinesis Versus Random Movement 116
3.4 Discussion 120
3.4.1 Effects of Nutrient Loadings and Caveats 120
3.4.2 Density Dependence and Water Years 124
3.4.3 Kinesis Versus Random Movement 125
3.4.4 Summary and Future Directions 126

3.5 References 128

CHAPTER 4: GENERAL CONCLUSIONS 134
4.1 References 139

VITA 141

ABSTRACT

Water quality in the Chesapeake Bay and the Patuxent River has decreased since the 1950s due to an increase in nutrient loadings. Increased nutrient loads have caused an increase in the extent and duration of hypoxic conditions. Restoration via large-scale reductions in nutrient loadings is now underway. How reducing nutrient loadings will affect water quality is well predicted; however the effect on fish is generally unknown as most water quality models do not include trophic levels higher than zooplankton. I combined two water quality models with bay anchovy models (*Anchoa mitchilli*) to examine the effects of changes in nutrient loadings on anchovy survival and growth. An individual-based predation model was statically linked to Patuxent River watershed land-use and water quality models, and used to simulate the effects of changes in watershed land-use, Chesapeake Bay boundary condition nutrient loadings, and water year types on the summertime survival of daily anchovy egg and larval cohorts. I found that changes in Patuxent watershed land-use had little effect on egg and larval survival, while reduced nutrient loadings at the Chesapeake Bay boundary condition increased egg survival but reduced larval survival in June. The second analysis dynamically coupled a spatially-explicit, individual-based population dynamics model of juvenile and adult anchovy to the 3-dimensional Chesapeake Bay water quality model. Growth rates of individual anchovy within water quality model cells were calculated using a bioenergetics equation. Zooplankton densities from the water quality model provided prey for anchovy consumption, and anchovy consumption was an additional mortality term on zooplankton. Anchovy mortality was size-dependent. Anchovy movement depended on water temperature, dissolved oxygen, and zooplankton concentrations. Multi-year simulations with fixed annual recruitment were performed under decreased, baseline, and increased nutrient loadings scenarios. Increasing nutrient loadings had small effects on

survival, but increased anchovy growth and therefore biomass. Anchovy growth exhibited compensatory density dependence. The results of both analyses showed that anchovy responses to changed nutrient loadings were complex and depended on life stage. Full-life cycle, spatially-explicit population models that are dynamically coupled to water quality models are needed to truly predict the effects of changes in nutrient loadings on fish populations.

CHAPTER 1: GENERAL INTRODUCTION

1.1 Introduction

Many estuaries throughout the world are experiencing increasing nutrient inputs to their surface waters (Nixon 1995, Rabalais et al. 2002, Cloern 2001). This increase in the supply of nutrients has been primarily driven by increasing human population, especially in coastal areas (Diaz 2001, Cloern 2001). Humans affect the supply of nutrients to estuaries through the release of treated and untreated sewage, the use of fertilizers for agriculture, changes in non-point source runoff via alterations to land-use patterns, and atmospheric deposition of oxidized-nitrogen from the burning of fossil fuels (Nixon 1995, Cloern 2001).

Increases in the supply of nutrients to estuaries can have both beneficial and negative effects on estuarine fish populations (Caddy 1993). Increased nutrient supplies can be beneficial by stimulating primary and secondary production (Nixon 1995), which may lead to an increase in the supply of food for fish (Caddy 1993). However, increases in turbidity from increased phytoplankton and macro algae growth can lead to the loss of sea grass beds (McGlathery 2001, Kemp et al. 2005) that are valuable as fish habitat (Lubbers et al. 1990). Also, if the nutrient supply becomes overly enriched, it may lead to the formation of oxygen depleted waters. Hypoxic water is often defined as having a dissolved oxygen concentration less than 2 mg liter^{-1} and anoxic water is functionally defined as less than 0.2 mg liter^{-1} (Kemp et al. 2005). The formation of anoxic and hypoxic waters affects fish both directly and indirectly (Breitburg et al. 2001, 2003A). Exposure to anoxic and hypoxic conditions may directly cause fish mortality through suffocation. The eggs and larvae of fish are more vulnerable to direct mortality due to hypoxia than juveniles and adults, as they are less able to avoid hypoxic conditions and they are less tolerant of hypoxia (Breitburg et al. 2001). Indirectly, anoxia and hypoxia may affect fish by

altering their spatial distribution which may alter the degree of spatial overlap between prey and predators and may force fish out of their preferred habitats. In this dissertation, I will be focusing on the effects of anoxia and hypoxia due to eutrophication on bay anchovy (*Anchoa mitchilli*), a small, pelagic, forage fish species, in the Chesapeake Bay and one of its tributaries, the Patuxent River, located in Maryland, USA.

The Chesapeake Bay (Bay) is the largest estuary in the United States, and is located in the mid-Atlantic coastal region (Kemp et al. 2005). The Bay is nearly 300 km long and is 5.5 km wide at its narrowest point and nearly 60 km wide at its widest point. A relatively narrow (1 to 4 km) and deep (20 to 30 m) central channel runs along the main stem of the Bay; however the majority of the Bay has a depth of less than 10 m. The Bay's largest tributary is the Susquehanna River, which provides over half of its freshwater inflow. Salinity in the Bay ranges from 0 ppt at its head where the Susquehanna enters to 30 ppt at its mouth of the Bay on the Atlantic Ocean. The differences in the salinities of the riverine inflow and water entering from the Atlantic Ocean leads to vertical stratification of the water column, which limits mixing between the surface and bottom layers. The vertical stratification of the water column has resulted in the Bay being susceptible to the formation of hypoxia in the bottom layer (Hagy et al. 2004).

The Patuxent River is located between Baltimore, MD and Washington, DC, on the west side of the Chesapeake Bay. It is one of the larger tributaries of the Bay, draining a 2,290 km^2 watershed (Breitburg et al. 2003B). The Patuxent River estuary may experience hypoxia due to density stratification isolating the bottom-layer from the surface or from the inflow of hypoxic water from the Chesapeake Bay. Of the Bay's tributaries, the Patuxent River experiences the second most frequent occurrence of hypoxic conditions (duration and extent), following only the Potomac River (Hagy et al. 2004, Fisher et al. 2006).

Areas of hypoxic and anoxic conditions have been present, at least seasonally, in the Chesapeake Bay and some of its tributaries since the time of European settlement (Cooper and Brush 1991). Hypoxia was first noticed in the deeper waters of the Bay in the 1930s (Newcombe and Horner 1938). At that time, low levels of dissolved oxygen were observed in the main channel with the oxygen levels occasionally approaching anoxia. In the 1950s, hypoxic conditions were present in the deeper portions of the main channel in the mid-Bay region (Officer et al. 1984). Since the 1950s, the extent of hypoxic conditions have increased greatly, as nutrient loadings to the Bay have increased due to a rapidly growing population, increased fertilizer use by agriculture, and changes in land-use (Officer et al. 1984, Hagy et al. 2004). By the 1980s, the extent of hypoxic conditions had expanded to cover much of the bottom waters of the Bay. In 1983, the first Chesapeake Bay agreement was signed. In 1987, a revised Chesapeake Bay agreement was signed, requiring a 40% reduction by the year 2000 in the nitrogen and phosphorus loadings entering the Bay's mainstem (Powledge 2005).

In 2000, a new Chesapeake Bay agreement was signed, outlining restoration plans for Chesapeake Bay that included an on-going effort to reduce nitrogen and phosphorus loadings and a new initiative to reduce sediment loading into the Bay (Chesapeake Bay Program 2007). By 2010, the objective of the restoration program is to "Correct the nutrient- and sediment-related problems in the Chesapeake Bay and its tidal tributaries sufficiently to remove the Bay and the tidal portions of its tributaries from the list of impaired waters under the Clean Water Act". It is not clear what achieving this goal of reduced nutrient and sediment loadings to the Bay will mean for fish growth, population dynamics, and food web interactions (Kemp 2004). The models used to simulate water quality in the Chesapeake Bay (CE-QUAL-ICM) and the Patuxent River (CE-QUAL-W2) did not explicitly include fish in their simulations (Cerco and

Cole 1993, Cerco and Noel 2004, Nice 2006). The CE-QUAL-ICM water quality model only included trophic levels up to zooplankton, while the CE-QUAL-W2 model stopped at phytoplankton.

In this dissertation, I link fish population models with the Chesapeake Bay and the Patuxent River water quality models to simulate the effects of changes in nutrient loading on bay anchovy growth and survival. Bay anchovy is one of the dominant fish species in the Bay and the Patuxent River in terms of both abundance and biomass (Baird and Ulanowicz 1989, Houde et al. 1989, Jung and Houde 2003), and is a major trophic link between the zooplankton and piscivorous fish (Baird and Ulanowicz 1989, Hartman and Brandt 1995). Baird and Ulanowicz (1989) found that bay anchovy consumed about 15-18% of zooplankton production in Chesapeake Bay during the summer and fall, which represented about 70-90% of all the zooplankton consumed by planktivorous fish. In turn, bay anchovy were the source of 60-90% of the energy intake of carnivorous fish that fed on bay anchovy during the summer, fall, and spring seasons. Finally, bay anchovy is a well studied species having been the subject of several, long-term investigations (e.g. Houde et al. 1989, Luo and Brandt 1993, Rilling and Houde 1999, Rose et al. 1999, Cowan et al. 1999, Breitburg et al. 2003A, Jung and Houde 2003, 2004A,B).

1.2 Dissertation Overview

In Chapter 2, I simulate the effects of changes in Patuxent River watershed land-use and changes in nutrient loadings from its downstream boundary at Chesapeake Bay on anchovy egg and larval cohort survival rates in four spatial segments of the lower Patuxent River. The effects of changes in Patuxent River watershed land-use on point and non-point source stream and nutrient discharges to the Patuxent River were simulated by Weller et al. (2003) using a watershed model. Output from the watershed model was then used as an input to the Patuxent

River water quality model initially developed by Lung and Bai (2003), and further modified by Nice (2006). Nice (2006) used the linked watershed and water quality models to simulate the effects of water years (wet and dry), changes in Patuxent River watershed land-use (decreased, baseline and increased), and changes in downstream (Chesapeake Bay) boundary condition nutrient loadings (decreased, baseline and increased) on Patuxent River water quality. I use the daily outputs of temperature, salinity, and dissolved oxygen concentrations from the water quality model to determine the vertical structure (thicknesses of the surface, pycnocline, and bottom layers), and dissolved oxygen concentrations in each layer, for each day in June and in July for a dry year and a wet year for each of the four spatial segments. Water column structure and dissolved oxygen concentrations are used as inputs to a 3-layer individual-based model that predicts the survival of bay anchovy eggs and larvae. For each day in June and July, I use the individual-based predation model to simulate the survival and movement of bay anchovy eggs and larvae and their gelatinous predators (*Mnemiopsis leidyi* and *Chrysaora quincherra*) among the surface, pycnocline, and bottom layers. Sizes and densities of bay anchovy and their predators are specified using field data summarized by Breitburg et al. (2003A). Simulations of egg cohort survival are for one day as anchovy eggs hatch approximately 24 hours after spawning (Chesney and Houde 1989; Zastrow and Houde 1991); simulations of larval cohort survival are for 7 days. The simulations are used to obtain monthly summaries of daily mortality rates of anchovy egg and larval cohorts under combinations of changes in Patuxent watershed land-use, changes in downstream boundary conditions at Chesapeake Bay, and under wet, and dry water years.

In Chapter 3, I dynamically couple the 3-dimensional Chesapeake Bay water quality model with a bay anchovy population model to simulate the effects of changes in nutrient

loadings on juvenile and adult anchovy growth, survival, and biomass. The water quality and anchovy models are run simultaneously, using stored hydrodynamics output for wet, normal, and dry years. Growth rates of individual anchovy within the water quality model cells are calculated using a bioenergetics equation. Zooplankton densities from the water quality model provide prey for anchovy consumption, and anchovy consumption was an additional mortality term on zooplankton. The nutrients from zooplankton consumed by anchovy are recycled within the water quality model. Anchovy mortality is assumed to be size-dependent, with additional mortality terms included for exposure to hypoxia, starvation, and old age. Anchovy movement is simulated using a kinesis movement model (Humston et al. 2000, Humston 2001). Horizontal movement of anchovy depends upon water temperature and zooplankton densities, while vertical movement depends upon water temperature and dissolved oxygen. Ten year simulations with fixed annual recruitment (low or high) are performed under decreased, baseline, and increased nutrient loading scenarios. Additional simulations are done to compare the kinesis movement model to a random movement model. Anchovy growth, survival, and biomass are compared among the three nutrient loading scenarios and between the two movement models.

In the final chapter, I summarize the major results of the Patuxent River and Chesapeake Bay simulations. I discuss the implications of my modeling results and some of the caveats about why the results should be interpreted with caution. I address the limitations of the current anchovy models and suggest the next steps for expanding my analyses and the two individual-based models to increase the realism and confirm the robustness of modeling results.

Reducing nutrient loadings into estuaries is expensive (~$19 billion for Chesapeake Bay, Chesapeake Bay Program 2007) and an understanding of the full food-web effects of contemplated nutrient reductions are needed to properly evaluate their utility and to decide

among alternative management actions. There is a great need for spatially-explicit, full life cycle fish population and community models that are coupled to water quality and hydrodynamics models, and this need will only increase in the future as increasing human population continues to cause eutrophication in coastal waters. Fully-coupled fish and water quality models are also needed for fisheries management (Runge et al. 2003), and for forecasting the effects of climate change on small pelagic fish (Lett et al. submitted). My analyses offer two examples for coupling fish models to water quality models. Such analyses are feasible and should be pursued if we are to effectively manage our estuaries and coastal fisheries.

1.3 References

Baird, D. and R. E. Ulanowicz. 1989. The seasonal dynamics of the Chesapeake Bay ecosystem. Ecological Monographs 59: 329-364

Breitburg, D. L., L. Pihl, and S. E. Kolesar. 2001. Effects of low dissolved oxygen on the behavior, ecology and harvest of fishes: A comparison of Chesapeake Bay and Baltic-Kattegat systems. p. 241-268 *In* Rabalais, N. N. and R. E. Turner. Coastal Hypoxia: Consequences for Living Resources and ecosystems. American Geophysical Union, Washington, D.C.

Breitburg, D. L., A. Adamack, K. A. Rose, S. E. Kolesar, M. B. Decker, J. E. Purcell, J. E. Keister, J. H. Cowan Jr.. 2003A. The pattern and influence of low dissolved oxygen in the Patuxent River, a seasonally hypoxic estuary. Estuaries 26: 280-297

Breitburg, D. L., T. E. Jordan, D. Lipton. 2003B. Preface – from ecology to economics: Tracing human influence in the Patuxent River estuary and its watershed. Estuaries 26: 167-170

Caddy, J. F. 1993. Toward a comparative evaluation of human impacts on fishery ecosystems of enclosed and semi-enclosed seas. Reviews in Fisheries Science 1: 57-95

Cerco, C. and T. Cole. 1993. Three-dimensional eutrophication model of Chesapeake Bay. Journal of Environmental Engineering 119: 1006-1025

Cerco, C. F. and M. R. Noel. 2004. Process-based primary production modeling in Chesapeake Bay. Marine Ecology Progress Series 282: 45-58

Chesapeake Bay Program. 2007. http://www.chesapeakebay.net. Annapolis, Maryland

Chesney, E. J. and E. D. Houde. 1989. Laboratory studies on the effect of hypoxic waters on the survival of eggs and yolk-sac larvae of the bay anchovy, *Anchoa mitchilli*. P. 184-191. *In* E. D.

Houde, E. J. Chesney, T. A. Newberger, A. V. Vasquez, C. E. Zastrow, L. G. Morin, H. R. Harvey, and J. W. Gooch, (eds.), Population Biology of Bay Anchovy in mid-Chesapeake Bay. Final Report to Maryland Sea Grant Ref. No. (UM-CEES) CBL 89-141. Solomons, Maryland.

Cloern, J. E.. 2001. Our evolving conceptual model for the coastal eutrophication problem. Marine Ecology Progress Series 210: 223-253

Cooper, S. R. and G. S. Brush. 1991. Long-term history of Chesapeake Bay anoxia. Science 254: 992-996

Cowan, J. H. Jr., K. A. Rose, E. D. Houde, S-B Wang and J. Young. 1999. Modeling effects of increased larval mortality on bay anchovy population dynamics in the mesohaline Chesapeake Bay: Evidence for compensatory reserve. Marine Ecology Progress Series 185: 133-146

Diaz, R. J.. 2001. Overview of hypoxia around the world. Journal of Environmental Quality. 30: 275-281

Fisher, T. R., J. D. Hagy III, W. R. Boynton, and M. R. Williams. 2006. Cultural eutrophication in the Choptank and Patuxent estuaries of Chesapeake Bay. Limnology and Oceanography 51: 435-447

Hagy, J. D., W. R. Boynton, C. W. Keefe, and K. V. Wood. 2004. Hypoxia in Chesapeake Bay, 1950-2001: Long-term change in relation to nutrient loading and river flow. Estuaries 27:634-658

Hartman, K. J. and S. B. Brandt. 1995. Trophic resource partitioning, diets and growth of sympatric estuarine predators. Transactions of the American Fisheries Society 124: 520-537

Houde, E. D., E. J. Chesney, T. A. Newberger, A. V. Vazquez, C. E. Zastrow, L. G. Morin, H. R. Harvey, and J. W. Gooch. 1989. Population Biology of Bay Anchovy in Mid-Chesapeake Bay. Solomons, Maryland

Humston, R. J. S. Ault, M. Lutcavage, D. B. Olson. 2000. Schooling and migration of large pelagic fishes relative to environmental cues. Fisheries Oceanography 9: 136-146

Humston, R. 2001. Development of movement models to assess the spatial dynamics of marine fish populations. PhD dissertation. University of Miami, Coral Gables, Florida

Jung, S. and E. D. Houde. 2003. Spatial and temporal variabilities of pelagic fish community structure and distribution in Chesapeake Bay, USA. Estuarine, Coastal and Shelf Science 58: 335-351

Jung, S. and E. D. Houde. 2004A. Production of bay anchovy *Anchoa mitchilli* in Chesapeake Bay: Application of size-based theory. Marine Ecology Progress Series 281: 217-232

Jung, S. and E. D. Houde. 2004B. Recruitment and spawning-stock biomass distribution of bay anchovy (*Anchoa mitchilli*) in Chesapeake Bay. Fishery Bulletin 102: 63-77

Kemp, W. M. 2004. Coupling water quality and upper trophic level modeling for Chesapeake Bay: A planning workshop. U.S. EPA Chesapeake Bay Program Conference Room Annapolis, Maryland

Kemp, W. M., W. R. Boynton, J. E. Adolf, D. F. Boesch, W. C. Boicourt, G. Brush, J. C. Cornwell, T. R. Fisher, P. M. Glibert, J. D. Hagy, L. W. Harding, E. D. Houde, D. G. Kimmel, W. D. Miller, R. I. E. Newell, M. R. Roman, E. M. Smith, and J. C. Stevenson. 2005. Eutrophication of Chesapeake Bay: Historical trends and ecological interactions. Marine Ecology Progress Series 303: 1-29

Lett, C., K. A. Rose, B. A. Megrey. *Submitted*. Biophysical models of small pelagic fish.

Lubbers, L., W. R. Boynton, and W. M. Kemp. Variations in structure of estuarine fish communities in relation to abundance of submersed vascular plants. Marine Ecology Progress Series 65: 1-14

Lung, W. S. and S. Bai. 2003. A water quality model for the Patuxent estuary: Current conditions and predictions under changing land-use scenarios. Estuaries 26: 267-279

Luo, J. and S. B. Brandt. 1993. Bay anchovy *Anchoa mitchilli* production and consumption in mid-Chesapeake Bay based on a bioenergetics model and acoustic measures of fish abundance. Marine Ecology Progress Series. 98: 223-236

McGlathery, K. J.. 2001. Macroalgal blooms contribute to the decline of seagrass in nutrient-enriched coastal waters. Journal of Phycology 37: 453-456

Newcombe, C. L., and W. A. Horne. 1938. Oxygen-poor waters in Chesapeake Bay. Science 88: 80-81

Nice, A. J. 2006. Developing a fate and transport model for arsenic in estuaries. Ph.D. Dissertation, University of Virginia, Charlottesville, Virginia

Nixon, S. W.. 1995. Coastal marine eutrophication: A definition, social causes, and future concerns. Ophelia 41: 199-219

Officer, C. B., R. B. Biggs, J. L. Taft, L. E. Cronin, M. A. Tyler, and W. R. Boynton. 1984. Chesapeake Bay anoxia: origin, development, and significance. Science 223:22-26

Powledge, F.. 2005. Chesapeake Bay restoration: A model of what?. BioScience 55: 1032-1038

Rabalais, N. N., R. E. Turner, Q. Dortch, D. Justic, V. J. Bierman Jr., and W. J. Wiseman Jr.. 2002. Nutrient-enhanced productivity in the northern Gulf of Mexico: past present and future. Hydrobiologia 475/476: 39-63

Rilling, G. C. and E. D. Houde. 1999. Regional and temporal variability in growth and mortality of bay anchovy, *Anchoa mitchilli*, larvae in Chesapeake Bay. Fishery Bulletin 97: 555-569

Rose, K. A., J. H. Cowan Jr., M. E. Clark, E. D. Houde, and S-B Wang. 1999. An individual-based model of bay anchovy population dynamics in the mesohaline region of Chesapeake Bay. Marine Ecology Progress Series. 185: 113-132

Runge, J. A., P. J. S. Franks, W. C. Gentleman, B. A. Megrey, K. A. Rose, F. E. Werner, B. Zakardjian. 2004. Diagnosis and prediction of variability in secondary production and fish recruitment processes: developments in physical-biological modeling (Chapter 13), *In* Robinson, A. R. and K. H. Brink (eds). The global coastal ocean: Multi-scale interdisciplinary processes, The Sea, 13: 413-473

Weller, D. E., T. E. Jordan, D. L. Correll, and Z.-J. Liu. 2003. Effects of land-use change on nutrient discharges from the Patuxent River watershed. Estuaries 26: 244-266

Zastrow, C. E., E. D. Houde, and L. G. Morin. 1991. Spawning fecundity, hatch-date frequency and young-of-the-year growth of bay anchovy *Anchoa mitchilli* in mid-Chesapeake Bay. Marine Ecology Progress Series 73: 161-171

CHAPTER 2: SIMULATING THE EFFECTS OF HYPOXIA ON BAY ANCHOVY (*ANCHOA MITCHILLI*) EGG AND LARVAL MORTALITY IN THE PATUXENT RIVER USING COUPLED WATERSHED, WATER QUALITY, AND INDIVIDUAL-BASED MODELS

2.1 Introduction

Patuxent River water quality and water column structure are both affected by changes in Patuxent River watershed land-use, Chesapeake Bay water quality at the downstream boundary, and inter-annual variability in rainfall (Jordan et al. 2003, Weller et al. 2003, Lung and Bai 2003, Nice 2006, Fisher et al. 2006). Land-use in the Patuxent River watershed has changed dramatically over the past 150 years, from an area that in the 1850s was primarily used for agriculture (~85% agriculture and 15% forested) to a mix of forested (51.6%), agriculture (28.5%) residential (15.5%), and urban (4.3%) areas in 1994 (D'Elia et al. 2003). Changes in Patuxent River watershed land-use and farming practices, and the accompanying increases in human population size, have resulted in a 2 to 5-fold increase in nitrogen (N) and phosphorus (P) inputs during the period of 1970-2004, and may have caused a 4 to 20 times increase in N and P over the last 350 years (Fisher et al. 2006). It is expected that rapid population growth in the watershed will cause land-use patterns to continue to change into the future (Bockstael and Irwin 2003, Chesapeake Bay Program http://www.chesapeakebay.net/). Since the 1980s, there have been efforts to reduce nutrient loads entering the Patuxent River. The Chesapeake Bay initiative led to the banning of phosphate in laundry detergents in Maryland in 1984, and the removal of phosphorus at wastewater treatment plants in 1986 (Lung and Bai 2003, Fisher et al. 2006). Biological nitrogen removal began at the eight major wastewater treatment plants along the Patuxent River in 1991.

Chesapeake Bay water quality affects the water quality in the Patuxent River via tidal exchange of nutrients at the downstream boundary (Boynton et al. 1995, Boesch et al. 2001,

Fisher et al. 2006). Water quality in Chesapeake Bay has declined over the past century due to the effects of cultural eutrophication, the loss of submerged aquatic vegetation, and the effects of overfishing (Kemp et al. 2005). While Chesapeake Bay has experienced hypoxia, at least occasionally, since the 1700s (Cronin and Vann 2003), cultural eutrophication in the Bay has caused the frequency, intensity, duration, and extent of hypoxia to increase over the past century (Boesch et al. 2001, Hagy et al. 2004). In some portions of the Bay, hypoxic or anoxic conditions are now present year round. Since 1983, there has been an ongoing effort to improve water quality in Chesapeake Bay and its tributaries (including the Patuxent River) through the reduction of nutrient and suspended sediment loadings (Powledge 2005, Kemp et al. 2005, http://www.chesapeakebay.net/).

Inter-annual variability in rainfall affects the magnitude of nutrient loadings to the Patuxent River from its watershed (Jordan et al. 2003; Weller et al. 2003). These localized nutrient loadings from land can affect the extent and timing of the onset of hypoxia in the same way as nutrients imported into the Patuxent from the Chesapeake Bay (Hagy et al. 2004). In addition, freshwater inputs from the local area can affect the degree of stratification (i.e. water column structure), which can amplify the effects of increased nutrient loadings by reducing the mixing between the oxygenated surface layer and the hypoxic bottom layer, thereby increasing the volume of hypoxic water and the duration of hypoxic conditions. During wet years, stratification and nutrient loads were both predicted to increase in the Patuxent River (Lung and Bai 2003, Jordan et al. 2003, Weller et al. 2003, Nice 2006). Hagy et al. (2004) concluded that wet years lead to an earlier onset and larger volume of hypoxic water compared to dry years.

Water column dissolved oxygen (DO) concentrations can affect the mortality rates of fish eggs and larvae through both direct and indirect effects (Breitburg 1994, Breitburg et al. 1999,

2003A). Fish eggs frequently suffer direct mortality when DO concentrations are below 3 mg liter^{-1} for 12 or more hours (Breitburg et al. 2003A). Mortality rates may be indirectly affected by changes in DO concentrations due to changes in the vertical distributions of fish larvae and their predators from avoidance of low DO (Breitburg et al. 1999, 2003A). Changes in the vertical distribution of fish and their predators may either increase or decrease fish mortality rates, depending on whether the spatial overlap of the fish and their predators increase or decrease (Keister et al. 2000, Breitburg et al. 1999, 2003A). Low DO also may increase larval mortality rates by slowing larval growth (Breitburg et al. 1999, 2003A), thereby extending the length of time larvae are exposed to high predation rates (Houde 1987).

In this chapter, I use a series of statically linked models (Figure 2.1) to predict how changes in Patuxent River watershed land-use, Chesapeake Bay water quality, and inter-annual variation in rainfall would affect the survival of bay anchovy eggs and larvae during June and July in the lower Patuxent River (Figure 2.2). A combination of field data and predictions from a Patuxent River watershed model (Jordan et al. 2003, Weller et al. 2003) were used to set inputs of nutrients and water flow to the river (Nice 2006). Predictions of point-source and non-point source discharges from the watershed model were then used as inputs to a Patuxent River water quality model. The Patuxent River water quality model was a hydrodynamic module coupled to a water quality module. The hydrodynamics module provided the transport rates among the river segments comprising the Patuxent River. The water quality module used the transport rates, plus biological and chemical processes, to simulate the daily concentrations of 21 constituents in each of the segments over two year simulations. In this analysis, I used the temperature, salinity, and DO outputs from the water quality module for June and July for segments in the lower Patuxent where bay anchovy are found. I used the temperature and salinity to determine the vertical

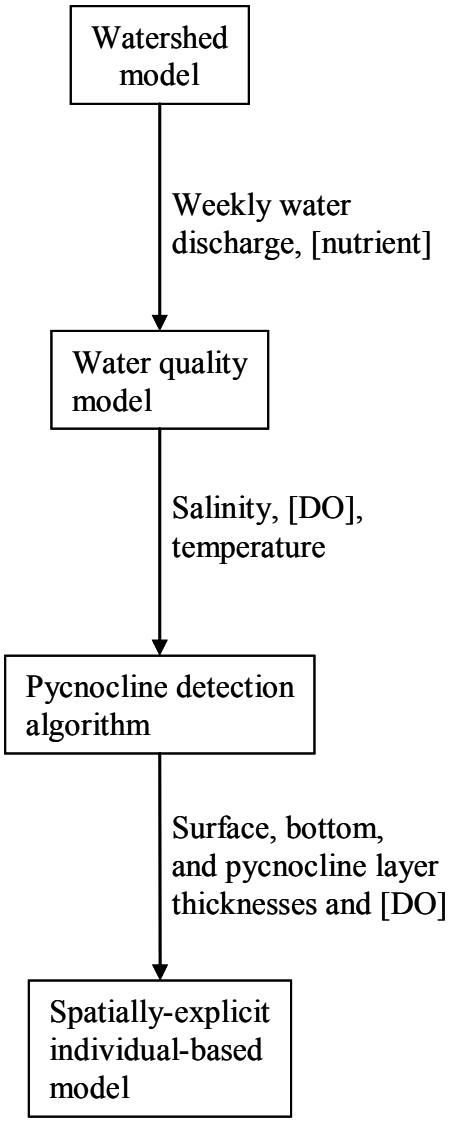

Figure 2.1 Relationship between the watershed model, the water quality model, the pycnocline detection algorithm and the spatially-explicit, individual-based predation model. Variables listed beside the arrows indicate the information that is transferred from the preceding model to the subsequent model.

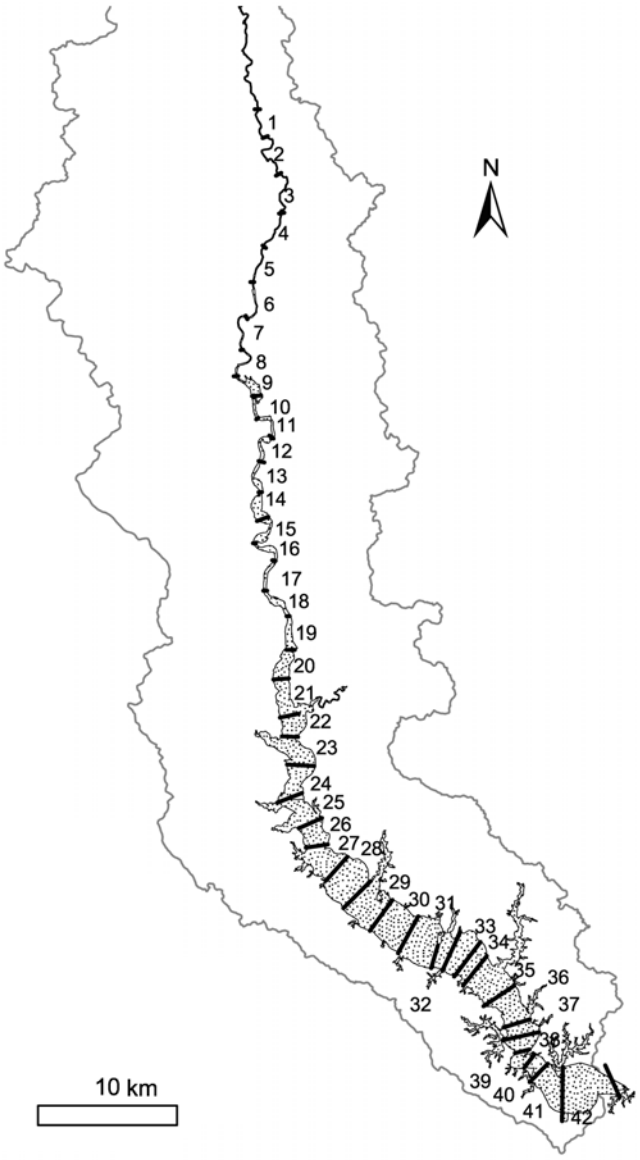

Figure 2.2 The Patuxent River estuary and the spatial segments used in the water quality modeling (from Weller et al. 2003).

structure of the water column on each day in each segment, and then averaged DO for each layer on each day. Daily water column structure and daily layer-specific DO concentrations are then used as inputs to the individual-based 3-layer model of bay anchovy egg and larval stage survival. One-day egg and seven-day larval mortality rates were predicted, beginning on each day of the month, under water quality simulations of wet and dry years, reduced, baseline, and increased Chesapeake Bay boundary conditions, and reduced, current, and increased land-use in the Patuxent River watershed.

2.2 Methods

2.2.1 Watershed Model

The Patuxent River watershed model, developed by Weller et al. (2003), is an empirical model that integrates non-point source discharges, point source discharges, and reservoir management to predict watershed discharges of water, sediment, organic carbon, silicate, nitrogen, and phosphorus to the Patuxent River proper. Weekly data on non-point source material discharges and stream flow were collected for 23 watersheds within the Patuxent River drainage basin (15 watersheds) and the adjacent Rhode River basin (7 watersheds) from July 27, 1997 through August 4, 1999 (Jordan et al. 2003). Separate linear statistical models were fit to the material discharge data and stream flow using a two stage process (Weller et al. 2003). Each model used week (104 weeks), geological province (Piedmont or Coastal Plain), proportion of the watershed that was cropland, and proportion of the watershed that was developed land as independent variables. Week and geological province were treated as classification variables. In the first stage of model fitting, material discharges and stream flow were fit to full models which included the independent variables and their interaction terms. In the second stage, reduced models that only included significant terms from the full models were fit to the material

discharge data and stream flow data. Total r^2 values for the fitted reduced models of material discharge, with the exception of NH_4, ranged from 0.62 to 0.83. The total r^2 value for the reduced model of NH_4 was 0.18. The non-point source stream flow model had a total r^2 of 0.87.

The reduced statistical models were used to predict non-point source flows and material concentrations for 23 watershed sections comprising the entire Patuxent River basin (Weller et al. 2003). Point source flows, reservoir releases, and nutrient concentrations were specified weekly and added to the predicted non-point source values to get total flows and material concentrations from each watershed section. Total flows and concentrations from the sections were then apportioned among 42 tributaries for the water quality model based upon the fraction of estuary surface in each section.

Weller et al. (2003) generated combined non-point and point source loadings to the 42 tributaries for use in the water quality model for three land-use scenarios and two types of rainfall years (six total combinations). The three land-use scenarios were: current land-use, increased land-use (doubled the proportion of developed land area and point-source discharges in each section over current values), and reduced land-use (halved cropland, developed land and point source discharges from current values). Doubling the developed land and point-source discharges resulted in the average annual total nitrogen load to the Patuxent River increasing by 155%, and the average annual total phosphorus load increasing by 146% (Weller et al. 2003). Halving cropland, developed land, and point-source discharges resulted in the average annual total nitrogen load to the Patuxent River decreasing to 53% of the current land use level and the average annual total phosphorus load decreasing to 57%. Rainfall years were based upon two years of rainfall data collected during the two-year watershed sampling period. Annual precipitation was 122 cm during the first year and 71 cm during the second year (Jordan et al.

2003). Compared to a 160-yr precipitation record (mean precipitation = 108 ± 21.8 cm, Correll et al. 1999), the first year was considered a wet year and the second year was considered a dry year.

2.2.2 Water Quality Model

The CE-QUAL-W2 water quality model is a two-dimensional (longitudinal-vertical) water quality model that was initially developed by the US Army Corps of Engineers (Cole and Wells 2000), and was subsequently modified by Lung and Bai (2003) and by Nice (2006) to model water quality in the Patuxent River. The water quality model divided the river into 163 longitudinal segments at the surface, each with a length of 613 m (Nice 2006). Each segment was then divided into 1 m vertical layers for a total of 1,993 spatial cells. The model uses finite difference techniques to calculate elevations and velocities by solving the laterally averaged free-water surface (continuity) equation and two laterally averaged momentum equations (Cole and Wells 2000). Within the CE-QUAL-W2 modeling framework, the hydrodynamic and mass transport modules are linked to a water quality module (Nice 2006).

The water quality module simulated 21 constituents in each of the cells, including salinity, temperature, DO, total nitrogen, and total phosphorous (Nice 2006). Constituents were moved among cells using advective and dispersive transport from the hydrodynamics module, and were affected by biological processes that were computed for each cell (internal sources and sinks). Major processes represented include photosynthesis, sediment diagenesis, water column nutrient kinetics, and dissolved oxygen kinetics. Photosynthesis was dependent upon nutrient concentrations, temperature, light availability, and season. The effects of temperature and light varied longitudinally, representing differences in the types of phytoplankton inhabiting saline and fresh water portions of the Patuxent River and differences in suspended solids concentrations. Season was used to account for temporal differences in turbidity. Sediment

diagenesis was dependent upon deposition of organic matter to the sediments, temperature, and nutrient and dissolved oxygen concentrations. Water column nutrient kinetics was a function of temperature, photosynthesis, and inputs and outputs of nutrients. Dissolved oxygen kinetics were a function of photosynthesis, temperature, reaeration rate (which varied longitudinally), and carbonaceous oxygen demand.

Important boundary conditions for the hydrodynamics and water quality modules included tributary inputs of nutrients, flow, temperature, dissolved oxygen, and chlorophyll *a* from the Patuxent River watershed, time varying climatic data, and Chesapeake Bay boundary conditions including temperature, salinity, nutrient loads, and tidal water elevations (Nice 2006). Tributary inputs of nutrients and flow were set using output from the watershed model (Weller et al. 2003) described above. Freshwater flows from the upper Patuxent River were set using data from a USGS gauging station located on MD Route 50 near Bowie, Maryland (river kilometer 100). Tributary dissolved oxygen, temperature, and chlorophyll *a* were obtained from data collected as part of the Chesapeake Bay Program. Chlorophyll *a* for tributaries that were not explicitly monitored was set conservatively to zero. Time varying climatic data included air temperature, wind speed, wind direction, and cloud cover; these data were obtained from a weather station at the Baltimore International Airport. Chesapeake Bay downstream boundary condition data for temperature, salinity, dissolved oxygen, and nutrients were set using data from bimonthly sampling at the Patuxent River water quality monitoring station LE1.4. Tidal water levels at Solomon's Island in the lower Patuxent Estuary were obtained from the National Oceanic and Atmospheric Administration's (NOAA) Center for Operational Oceanographic Products and Services (NOAA 2003).

The Patuxent River water quality model was calibrated through the use of vertical, longitudinal, and temporal comparisons of predicted temperature, salinity, chlorophyll *a*, DO, and nutrients to field data collected at water quality monitoring stations along the length of the Patuxent River. Temporal and vertical comparisons were made between the predicted values of the model constituents and field data from station LE1.1 located near Broomes Island and from station TF1.1 also known as "Nottingham". Longitudinal comparisons compared the predicted values of the constituents to field data at the stations located along the main axis of the Patuxent River. Calibration results of particular relevance to the bay anchovy simulations include the finding that temporal and spatial predictions of temperature and salinity had error measurements of less than 10% while bi-monthly predictions of the vertical distribution of DO at Broomes Island for the two-year simulations had error measurements of less than 12%. Overall, the model was successful in reproducing the pattern of the spatial and temporal trends of temperature, salinity, chlorophyll *a*, DO and nutrients (Nice 2006).

In addition to the three land-use scenarios and dry versus wet years simulated by the watershed model, three downstream boundary conditions were examined with the water quality model (Nice 2006). The baseline boundary condition simulation used observed field conditions in the mainstem of the Chesapeake Bay during the period August 1997 through July 1999. The nutrient concentrations were then halved (0.5×) and increased by 50% (1.5×). Boundary conditions for temperature, salinity, and DO were held constant. A total of 18 combinations of the 3 land-use scenarios, 2 water year types, and 3 Chesapeake Bay boundary conditions were simulated using the water quality model.

2.2.3 Determination of Water Column Structure and Associated DO Concentrations

The dimensions of the 3-layer water column and the mean DO concentration in each layer, were determined for each day during June and during July for segments 30, 32, 34, and 36 (Figure 2.2) using water temperatures, salinity, and DO outputted from the water quality model. June and July daily values were determined for each of the 18 combinations of 3 land-use scenarios, 3 Chesapeake Bay boundary conditions, and 2 water year types.

The vertical thicknesses of each of the three layers (surface, pycnocline, and bottom) were determined each day for each segment using a pycnocline detection algorithm. The algorithm divided the water column into the three layers based upon the vertical rate of change in water density (Appendix D, EPA 2003), which was computed from water quality model predictions of salinity and water temperature. The depth of the surface layer was estimated using a density gradient threshold of 0.1 kg m^{-4}, while the depth of the bottom layer was estimated as the last depth interval having a density gradient greater than 0.2 kg m^{-4}. The vertical structure of the water column was insensitive to land use scenarios and Chesapeake Bay boundary conditions, so daily water column structure was determined for dry and wet years only. I applied the pycnocline detection algorithm to each of the 9 simulations (3 land-use and 3 boundary conditions) for the dry year and the 9 simulations for the wet year, and then determined the thickness of the three layers for each day in June and in July by examining plots and smoothing over the 9 different estimates for each day. The fraction of the volume of the water column in each layer was then computed each day based upon the volume of water in each segment using the volumes of the 1-meter vertical cells in each segment (Nice 2006).

Averaged DO concentrations in the surface, pycnocline, and bottom layers of each segment were then determined for each day by assigning each vertical cell to a layer and then

averaging the DO concentrations in cells within a layer. The DO values of each cell were weighted by the volume of the cell.

2.2.4 Individual-Based Model

The individual-based model tracked the daily location, encounters with gelatinous predators, and mortality of individual fish eggs or fish larvae in the same 3-layer (surface, pycnocline, and bottom) water column estimated from the water quality model. The individual-based model was a modified version of the model described in Breitburg et al. (2003A). The water column was defined by the thickness of each of the 3 layers, the total volume of the modeled box (Table 2.1), and the bottom-layer DO concentrations, as estimated from the output of the Patuxent River water quality model. Individual predators (ctenophores and medusae) were specified, and used to determine daily encounters and capture (i.e., predation) of individual anchovy eggs and larvae. On each day during June and during July, each individual anchovy egg or larva was evaluated for growth, whether it had been eaten by any of the predators in that layer, and movement among the three vertical layers in the water column. The thicknesses of the layers and their DO concentrations, and locations of the individual predators in each layer, changed daily.

The initial number and sizes of individual prey (fish eggs or larvae) and predators (sea nettles and ctenophores) were based upon field data (Table 2.1). The lengths of each individual larval prey (mm) and predator (body length for ctenophores; bell diameter for medusae) were then generated from normal probability distributions with specified means, standard deviations, and minimum and maximum values. Minimum and maximum values were specified to eliminate unrealistic values from the initial distributions of lengths.

Table 2.1 Initial values used for spatially-explicit individual-based predation model simulations. Different ctenophore densities and sizes were used for larval and egg simulations as ctenophores smaller than 25 mm were too small to capture larvae (Kolesar unpublished data). The length of the smallest ctenophores captured was 10 mm.

	Egg Predation		Larval Predation	
Simulation duration	1 d		7 d	
Volume of simulated water column (m^3)	2000		2000	
	June	July	June	July
Initial prey density (no. m^{-3})	100	100	50	50
Mean and standard deviation initial prey length (mm)	1.0, 0.0	1.0, 0.0	2.8, 0.5	2.8, 0.5
Minimum and maximum initial prey starting length (mm)	1.0, 1.0	1.0, 1.0	2.3, 3.2	2.3, 3.2
Ctenophore density (no. $m^{-3} \geq 10$ mm length)	3.7	2.5	na	na
Ctenophore density (no. $m^{-3} \geq 25$ mm length)	na	na	1	2.5
Ctenophore length ≥ 10 mm (mean, SD mm)	21, 12	58, 19	na	Na
Ctenophore length ≥ 25 mm (mean, SD mm)	na	na	36, 13	59, 20
Minimum and maximum ctenophore length (mm)	10, 90	10, 106	25, 90	25, 106
Sea nettle density (no. m^{-3})	0.0	0.05	0.0	0.05
Sea nettle bell diameter (mean, SD mm)	Na	69, 37	Na	69, 37
Minimum and maximum sea nettle bell diameter (mm)	Na	25, 170	na	25, 170

Length of each individual larva was increased each day (growth) based on an assigned growth rate (0.23 mm d^{-1}). The lengths of eggs (assumed to be 1 mm) and predator lengths remained constant throughout the simulation. Growth and reproduction of gelatinous predators during the summer was crudely represented by the differences assumed for predator numbers and sizes between June and July (Table 2.1).

Predation mortality was evaluated each day for each surviving individual egg or larva. The mean number of encounters of each prey (larvae or eggs) with each individual predator was computed using the Gerritsen-Strickler formulation (Gerritsen and Strickler 1977), modified to account for the non-negligible size of fish egg and larvae prey (Bailey and Batty 1983). Only predators in the same layer as the prey were evaluated. The mean number of encounters in a day between a prey and each predator in the same layer ($\overline{E}$) was computed as:

$$\overline{E} = \pi(R_L + R_P)^2 \times C \times (10^{-9}/V) \quad (2.1)$$

$$C = \frac{D_L^2 + 3D_P^2}{3D_P} \text{ if } D_P > D_L$$

$$C = \frac{3D_L^2 + D_P^2}{3D_L} \text{ if } D_P < D_L$$

where C is the foraging rate (mm s^{-1}), R_P is the encounter radius of the predator (mm), R_L is the encounter radius of the larva (mm), D_P is the distance swum in a day by the predator (mm), D_L is the distance swum in a day by the larva prey (mm), and V is the modeled volume of the layer (m^3). Swimming speeds and encounter radii for prey and predators were adapted from previous applications of the predator-prey encounter model (Table 2.2). The actual number of encounters was generated from a Poisson distribution with $\overline{E}$ as the mean. Whether an encounter lead to a successful capture was then determined from capture success. Ctenophore capture probability of larvae increased with ctenophore length and decreased with increasing larval length (Figure

Table 2.2 Encounter radii and distances swum in a day for larval bay anchovy, ctenophores, and sea nettles from Cowan and Houde (1992), and capture probability relationships of ctenophores and sea nettles eating bay anchovy larvae modified from Cowan and Houde (1992).

Parameter	Larval bay anchovy	Ctenophore	Sea nettle
Encounter Radius (mm)	$\frac{2 \cdot L_L}{\pi^2}$	$0.33 \cdot L_C$	$0.5 \cdot L_{SN}$
Distance Swum (mm)	$1.5L_L \cdot 46800$	$0.025 \cdot L_C \cdot 86400$	$1.2 + 0.04 \cdot L_{SN} \cdot 86400$
Realized Capture Probability	N/A	$0.813 - 4.416\frac{L_L}{L_C}$	$0.505 + 4.653\frac{L_L}{L_{SN}} - 66.215\left(\frac{L_L}{L_{SN}}\right)^2 + 155.377\left(\frac{L_L}{L_{SN}}\right)^3$

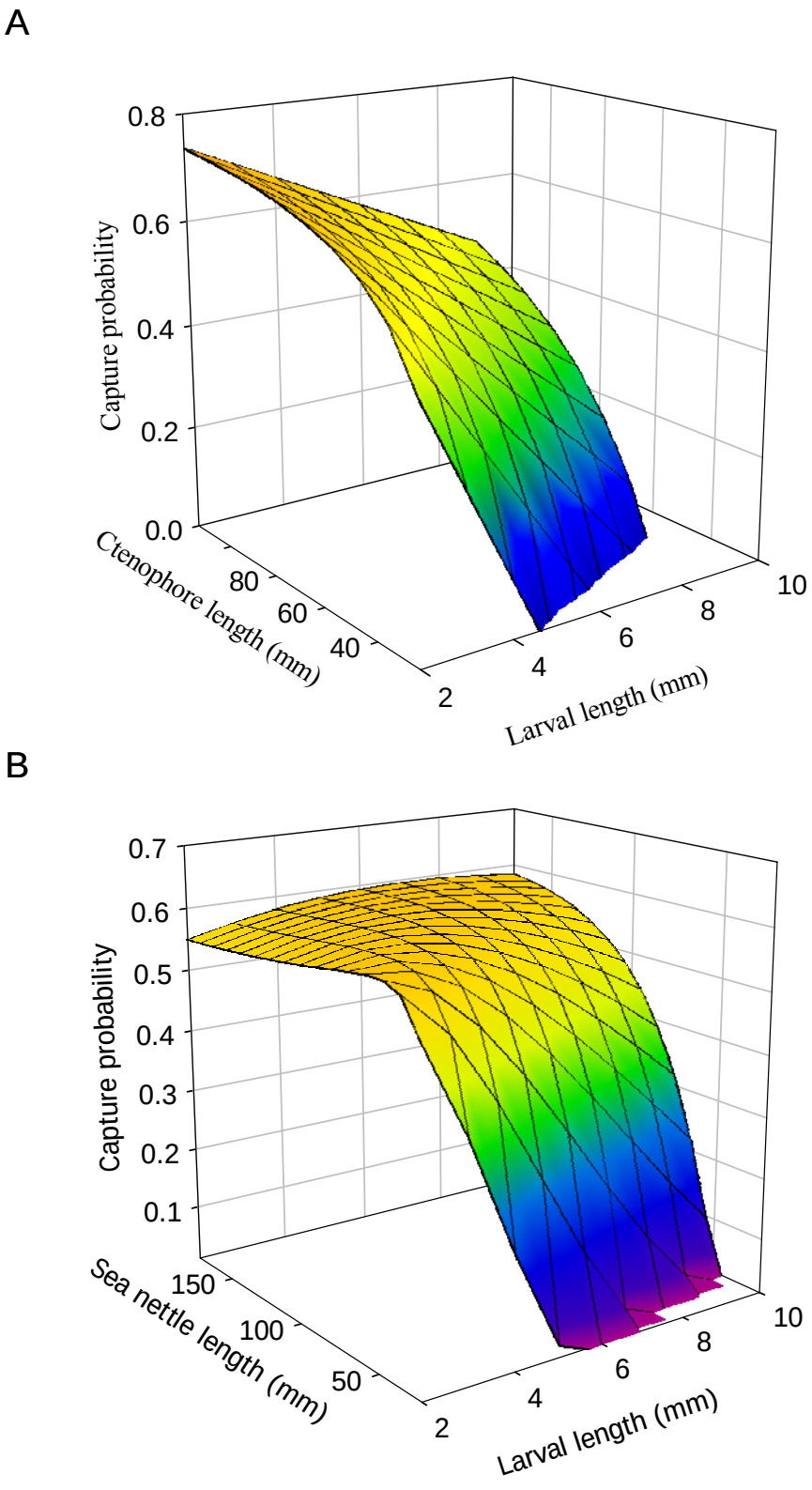

Figure 2.3 Capture probabilities of ctenophore and sea nettle predators preying upon larval bay anchovy. (A) Ctenophore (B) Sea nettle.

2.3A); sea nettle capture probability of larvae increased to a maximum with increasing sea nettle length and decreased slightly with increasing larval length (Figure 2.3B).. Predator capture probability was assumed to be 0.8 for eggs as prey. Finally, the realized number eaten by a predator was generated from a binomial distribution with actual number encountered as the number of trials and capture success as the probability of a success. A larva or egg was considered eaten if any of the predators in the layer had at least one successful capture of that larva or egg.

Movement was simulated by randomly reassigning all prey and predator individuals to a new layer each day based upon specified proportional densities by layer and the value of the DO in the bottom layer (Figure 2.4). The proportional densities were compiled from laboratory experiments done in vertical chamber that allowed for DO to be varied from top to bottom (Breitburg et al. 1999, 2003A). The probability that a prey or predator would move to a layer (surface, pycnocline, or bottom) was computed as the proportional density expected in that layer (from bottom DO) times the fraction of the water column volume in that layer divided by the sum of the proportional densities times fractional volumes of all three layers. A cumulative distribution of the three probabilities was then formed and a random number was generated and used to determine the layer to which the individual moved.

In addition to movement, DO also affected larval growth, predator capture success of larvae, and egg mortality rate. The DO concentration within each layer affected larval growth rates, predator capture success and egg mortality rates. Larval growth rates were slower when DO concentrations were less than 4 mg liter^{-1} (Figure 2.5). Sea nettle capture success was increased at low levels of DO while ctenophore capture success was unaffected by DO (Figure 2.6). The probability of eggs dying due to low DO concentration was based upon the results of

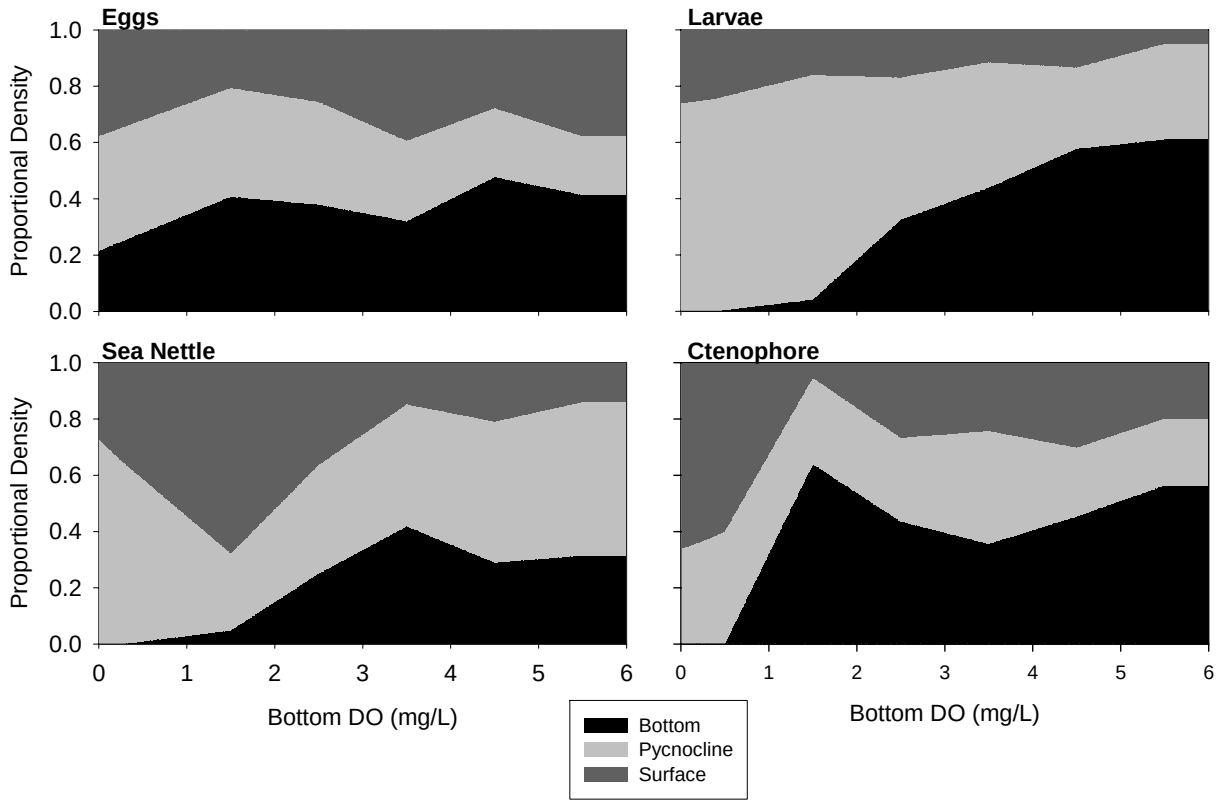

Figure 2.4 Proportional densities of eggs, larvae, sea nettles and ctenophores. Proportional densities are calculated as the proportion of individuals that would be in surface, pycnocline and bottom water layers if all layers of the water column were equal in volume. Data points were linearly interpolated to adjust vertical distributions for continuous bottom DO concentrations.

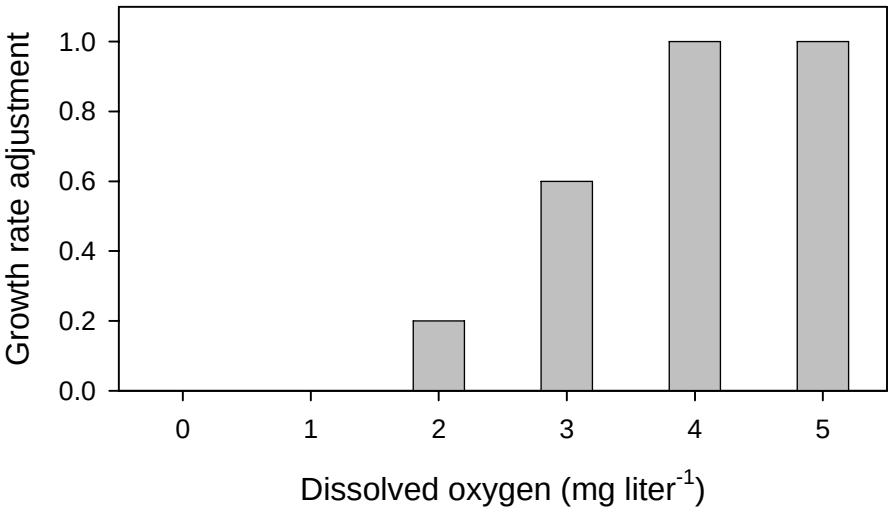

Figure 2.5 Adjustment for dissolved oxygen effects on larval bay anchovy growth rates (Breitburg et al. 1999).

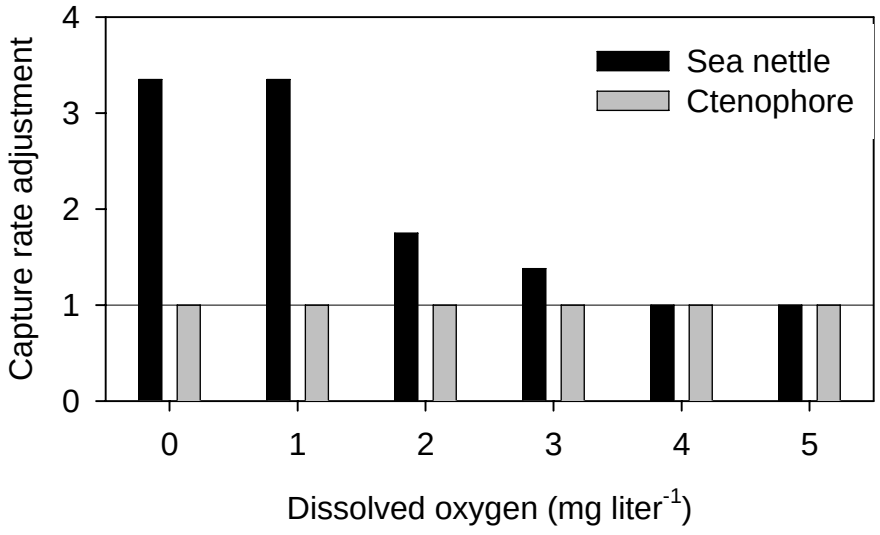

Figure 2.6 Adjustment for dissolved oxygen effects on sea nettle and ctenophore capture success. Sea nettle data was from Breitburg et al. (1999); ctenophore data from Breitburg et al. (2003A).

Chesney and Houde (1989), and was applied using a piece-wise linear function in which the proportion dying decreased from 0 at 3 mg liter^{-1} and higher DO concentration, to 0.5 at 2.8 mg liter^{-1}, and to 1.0 at 1 mg liter^{-1} or lower DO concentration.

2.2.5 Simulations

The individual-based model predicted daily egg mortality and 7-day larval mortality rates for each of the 18 combinations of the 3 land use scenarios, 3 Chesapeake Bay boundary conditions, and 2 water year types. Separate sets of 18 simulations were performed for eggs in June, larvae in June, eggs in July, and larvae in July, in each of the river segments 30, 32, 34, and 36 (Figure 2.1). These segments corresponded to the mesohaline portion of the Patuxent River from Broomes Island to below St. Leonard Creek, an area with a history of hypoxia, and where anchovy are abundant (Keister et al. 2000, Breitburg et al. 2003). The egg simulations in each month and segment were 30 one-day simulations using the conditions on each day; with new initial anchovy and predator conditions restarted each day. The larvae simulations were 7-days in duration, beginning on each day of the month, resulting in 30 values of 7-day mortality rates that overlap with shared days. For example, larval mortality rate for day 4 was computed over days 4-9, for day 5 over days 5-10, etc. July had only 25 predictions (not 30) because the last 7 days of July were not simulated as the needed values from the water quality model for the first week of August were not available.

I reported the daily DO concentrations in each layer, predicted daily mortality rates of eggs, and the predicted 7-day mortality rates of larvae that began on each day for the 18 conditions in June and in July for each of the four segments. To illustrate model results, I showed the DO, water layer thicknesses, and predicted mortality rates as time series for segment

34 in the wet year. Model results were summarized by combining the 30 values for each month and then displaying them in box plots.

All results shown were from single simulations of the individual-based model. The model is stochastic and random numbers are generated that affect the individual initial sizes of predators, the daily redistribution of prey and predators among the three layers, and determine the outcome of encounters between prey and predators. Replicate simulations that differed in their random number sequences generated similar predicted egg mortality and larval mortality rates. Differences in egg mortality rates were less than 3% d^{-1} among replicate simulations, and less than 5% $week^{-1}$ during June and 0.6% $week^{-1}$ during July for larval mortality rates.

2.3 Results

2.3.1 Water Column Structure and DO Concentrations

The estimated water column structure varied among days (Figure 2.7A), and showed consistent differences between June and July, across river segments, and between dry and wet years (Figure 2.8). Daily differences in water column structure were due to daily variations in river flow, which were reflected in the hydrodynamics module predictions of daily salinity and temperature with depth. Monthly averaged water column structure showed that pycnocline thickness increased and bottom layer thickness thinned between dry and wet years (left column versus right column in Figure 2.8), and that the bottom layer thickness increased moving down river (segments 30 to 36 in Figure 2.8). The difference between June and July was smaller in magnitude than the dry versus wet and river segment effects, and depended on whether it was the dry or wet year. For each segment, the dry year resulted in a thinner pycnocline and thicker surface layer between June and July, while the wet year resulted in a thicker pycnocline and thinner bottom layer between June and July. Using segment 34 as an example (Figure 2.8), in

Figure 2.7 Daily water column structure, bottom-layer DO concentrations, percentage of the eggs in the bottom layer, 1-day egg mortality rates and 7-day larval mortality rates for the three land-use and three Chesapeake Bay boundary condition scenarios for segment 34 during June and July of the wet year. (A) Bars: fraction of the water column in each layer. Top clear stack is surface layer, grey middle stack is pycnocline layer, and clear bottom stack is bottom layer. Lines: bottom-layer DO concentrations. Water quality scenario line colors and schemes are shown in the legend in Panel D. Horizontal lines at DO concentrations of 3, 2.8 and 1.0 mg liter^{-1} indicate the dissolved oxygen concentrations at which 0%, 50% and 100% egg mortality occur. (B) Percentage of all eggs in the bottom layer for the current land-use, 1.0× boundary condition scenario. Bar color shows the fraction of all eggs in the bottom layer that are alive, dead due to predation or dead due to hypoxia (C) 1-day egg mortality rates. (D) 7-day larval mortality rates.

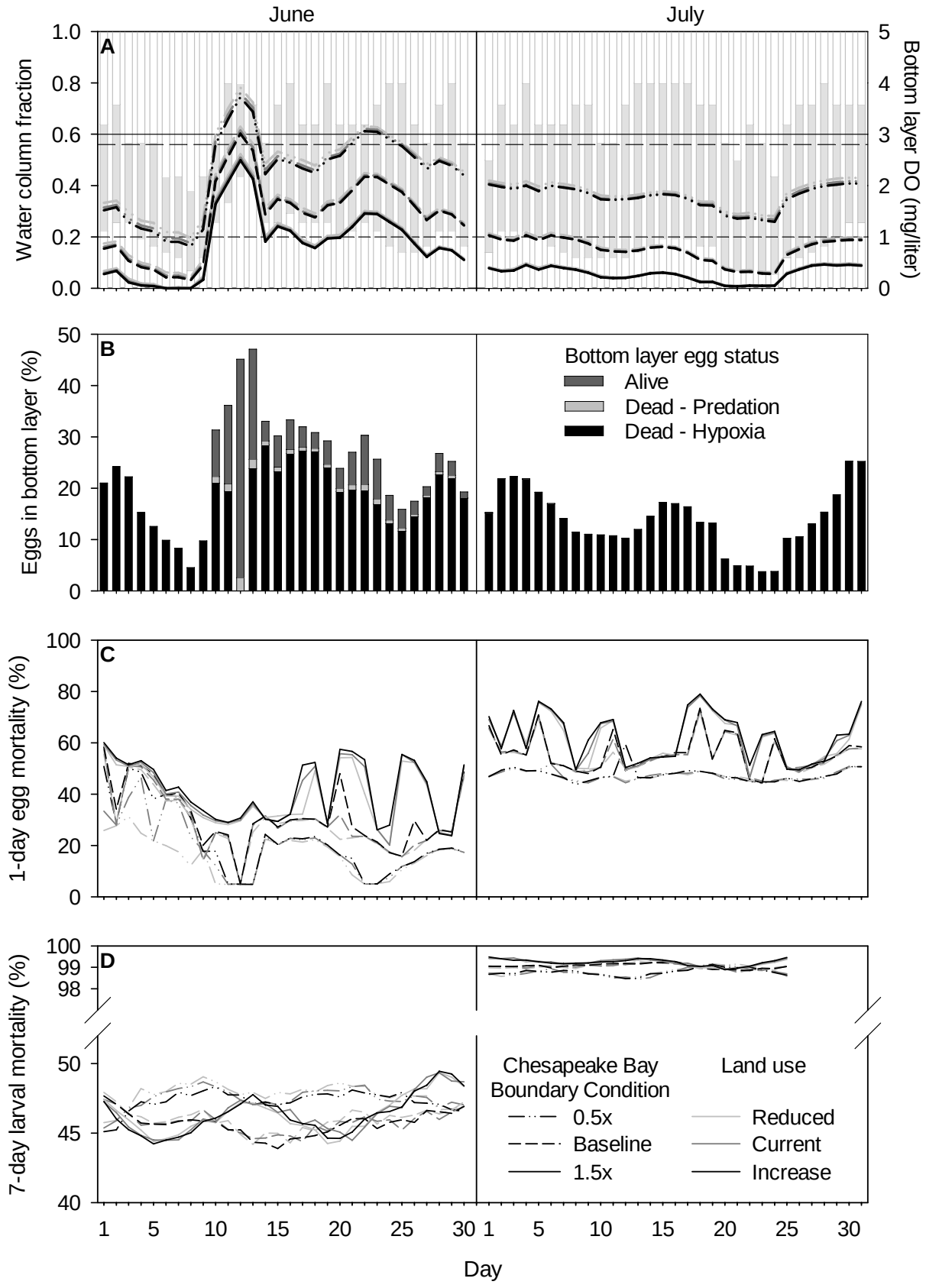
June
July
A
Water column fraction
Bottom layer DO (mg/liter)
B
Eggs in bottom layer (%)
Bottom layer egg status
Alive
Dead - Predation
Dead - Hypoxia
C
1-day egg mortality (%)
D
7-day larval mortality (%)
Chesapeake Bay Boundary Condition
0.5x
Baseline
1.5x
Land use
Reduced
Current
Increase
Day

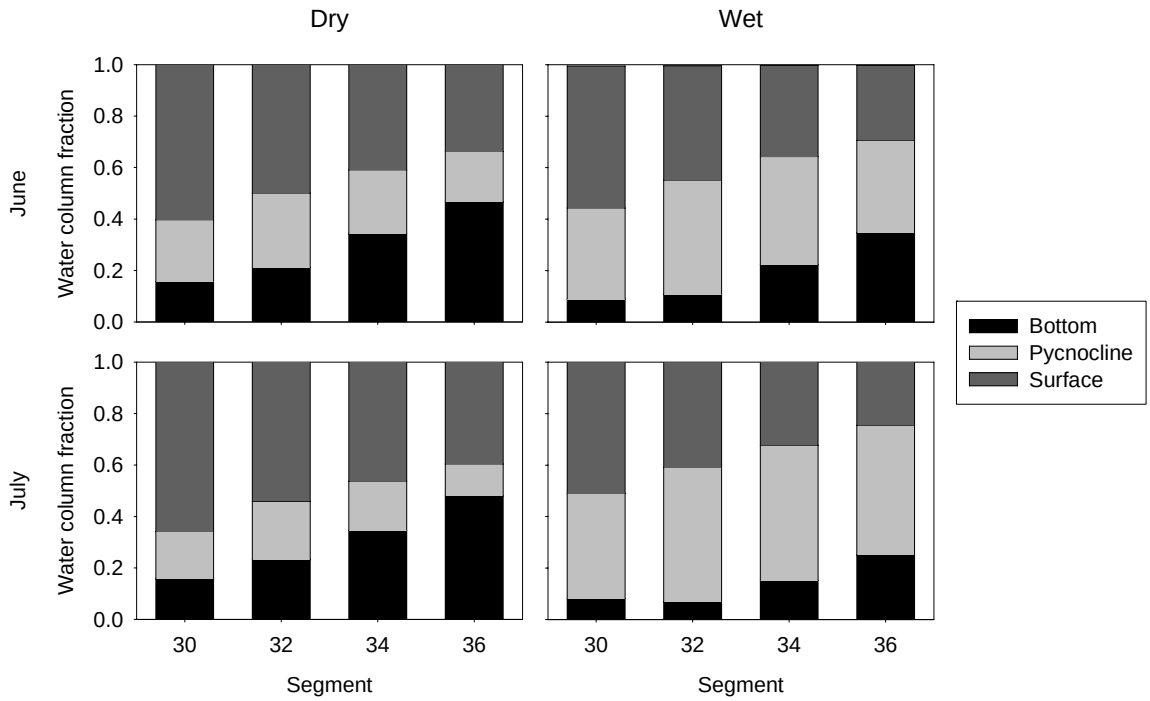

Figure 2.8 Mean water column fractions for wet and dry years during June and July. Proportions are the mean of the daily water column fractions for each month and water year type.

the dry year, the pycnocline was 25% of the water column in June versus 19% in July, while the surface layer increased from 40% of the water column in June to 46% in July. In the wet year, the pycnocline increased from 19% of the water column in June to 56% in July, while the bottom thinned from 48% of the water column to 15%.

Bottom DO concentrations also, at times, showed wide daily fluctuations (Figure 2.7A), with the Chesapeake Bay boundary conditions having the largest effect on monthly summarized values (Figure 2.9). Bottom layer DO concentrations decreased with increasing boundary condition nutrient loadings. During both wet and dry years, bottom layer DO concentrations for the 0.5× Chesapeake boundary condition was ~1 mg liter^{-1} higher than bottom layer DO concentrations for the baseline boundary condition scenario, which in turn, were about ~0.5 mg liter^{-1} higher than the 1.5x boundary condition. Pycnocline layer DO concentrations (not shown) were usually about 2 mg liter^{-1} higher than bottom layer DO concentrations, and roughly paralleled bottom layer DO concentration trends. Dissolved oxygen concentrations in the pycnocline layer frequently dipped below 3 mg liter^{-1}, the level at which egg mortality due to hypoxia began, when bottom-layer DO concentrations approached 1 mg liter^{-1}. Surface layer DO concentrations (not shown) were consistently above 5 mg liter^{-1}.

Bottom layer DO concentrations also showed a strong difference between dry and wet years, and smaller magnitude differences between months and across river segments. Across water years, the wet year generally had lower bottom DO concentrations than the dry year, and daily DO concentrations in the bottom layer in the wet year tended to be less variable during July than June (Figure 2.7A). Bottom DO tended to be lower in July than in June and to increase as one moved down River (segments 30 to 36).

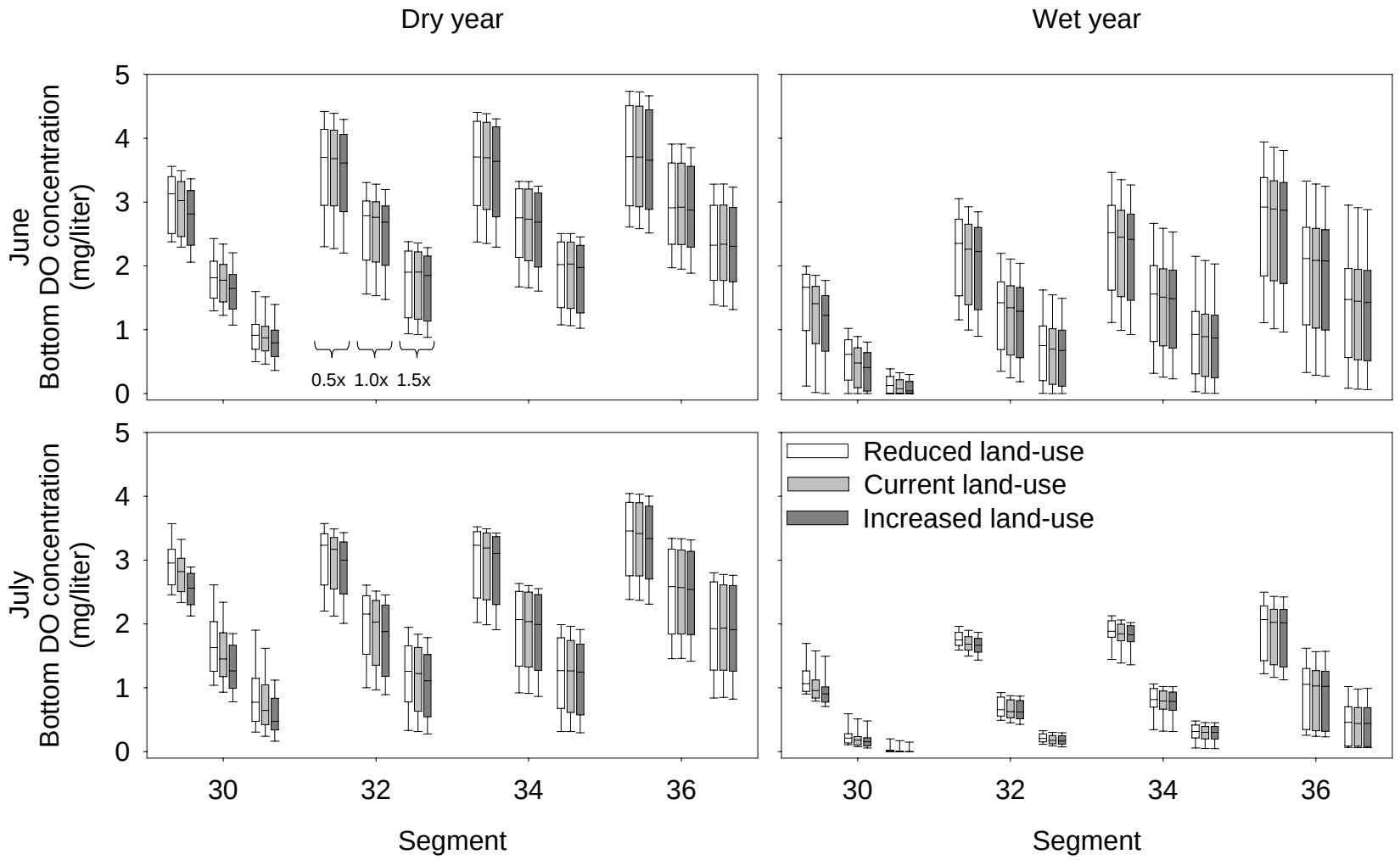

Figure 2.9 Boxplots showing monthly bottom-layer DO concentrations for wet and dry years during June and July. Whiskers show the 10^{th} and 90^{th} percentiles of the distribution. Box shows the 25^{th} and 75^{th} percentiles and the solid line in the box shows the median. Boundary condition scenarios are indicated in June-Dry year panel.

Land-use scenarios had very small effects on DO, relative to the effects of downstream boundary condition and dry versus wet years. There were brief sequences of a few days during which the small differences in DO concentrations had significant effects on egg mortality because the small differences resulted in pycnocline DO being just above or just below the threshold for DO affecting mortality. For example, during June 2 to 9 in segment 34 in the wet year, bottom DO under the 0.5x boundary condition varied slightly around 1 mg liter^{-1} between the reduced and increased land-use simulations (Figure 2.7A). Pycnocline DO concentrations (not shown) were approximately 2 mg liter^{-1} higher, varying around 3 mg liter^{-1}, the DO concentration at which direct mortality due to hypoxia began. This resulted in a difference in predicted egg mortality rates (Figure 2.7C). However, differences in bottom DO attributable to land-use scenarios were episodic, and effects were dampened in the monthly summaries.

2.3.2 Egg Mortality Rates

Mimicking bottom DO, egg mortality rates also showed daily variability (Figure 2.7B,C), and were most affected by the Chesapeake Bay boundary condition (Figure 2.10). Mortality rates varied from about 10% d^{-1} in June under the 0.5x boundary condition to about 30% to 40% d^{-1} under the 1.5x boundary condition, and mortality rates in July increased from about 40 to 50% d^{-1} under the 0.5x to about 60% d^{-1} under the 1.5x boundary condition. Most of the mortality of eggs in the bottom layer was due to hypoxia (Figure 2.7B).

Higher egg mortality rates in July compared to June were due to lower DO (Figure 2.9) and more and larger predators in July (Table 2.1). Bottom DO concentrations were consistently about 0.5 mg liter^{-1} lower in July than in June, which was often the difference between the pycnocline being above or below the 3 mg liter^{-1} threshold for direct mortality. While small-sized ctenophore density decreased between June and July (3.7 m^{-3} to 2.5 m^{-3}), the density of

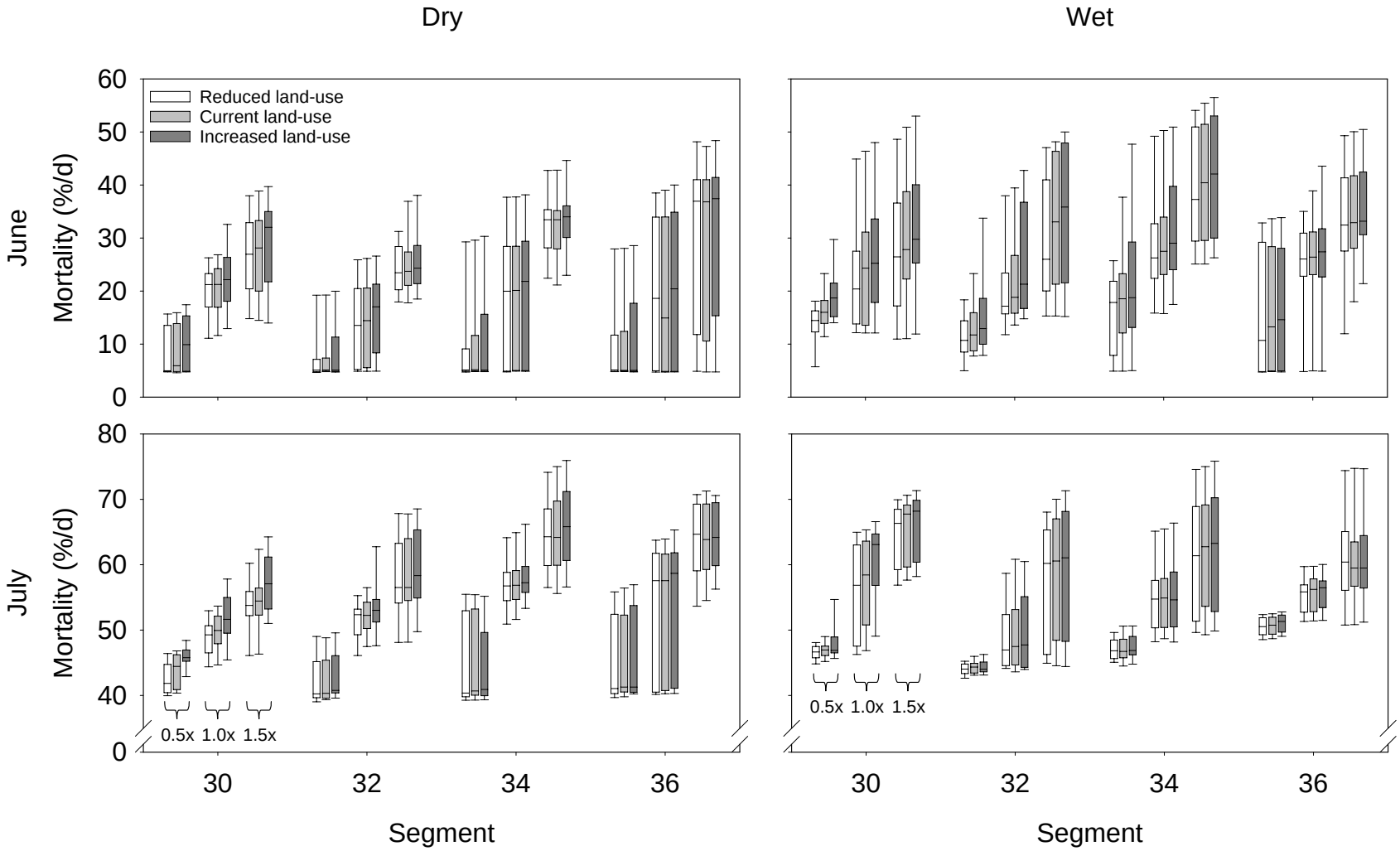

Figure 2.10 Boxplots showing monthly 1-day egg mortality rates for wet and dry years during June and July. Whiskers show the 10th and 90th percentiles of the distribution. Box shows the 25th and 75th percentiles and the solid line in the box shows the median. Land-use scenarios are shown in panel for the June-Dry year panel; boundary condition scenarios are indicated in the July panels.

large ctenophores increased (1 m^{-3} to 2.5 m^{-3}), and sea nettles were absent in June but present at 0.05 m^{-3} in July (Table 2.1).

The effects of water year type and river segment on egg mortality rates were inconsistent and relatively small in magnitude (Figure 2.10). During June, egg mortality rates for a segment were generally higher for the wet year than the dry year. For example in segment 36 for the baseline boundary condition, the median mortality for eggs was ~18% d^{-1} for the dry year and ~25% d^{-1} for the wet year. During July, egg mortality rates for a segment were sometimes higher in the dry year and sometimes higher in the wet year, depending upon the river segment. Egg mortality rates were lower in the dry year than the wet year in all segments for the 0.5x baseline boundary condition scenario. The baseline boundary condition had lower mortality rates in the dry year than the wet year for segment 30, but higher mortality rates in the dry year in segments 32, 34, and 36. The 1.5x boundary condition had lower mortality rates during the dry year in segments 30 and 32, but higher mortality rates in segments 34 and 36.

Egg mortality rates for the three land-use scenarios paired with each boundary condition were similar, but occasionally diverged when bottom layer DO varied slightly around 1 mg $liter^{-1}$ and pycnocline DO varied around 3 mg $liter^{-1}$. For example, during June 2 to 9 in segment 34 in a wet year, bottom DO concentrations for the reduced land-use under 0.5x baseline boundary condition were just slightly higher than under the baseline and increased land-use scenarios (Figure 2.7A). Yet, this resulted in significantly lower egg mortality rates under the reduced land-use scenario (Figure 2.7C). This divergence in mortality rates between land-use scenarios was because the pycnocline DO concentrations were also near the 3 mg $liter^{-1}$ value that induced DO-related egg mortality.

2.3.3 Larval Mortality Rates

Daily and monthly summarized larval mortality rates were dampened compared to egg mortality rates (Figure 2.7D versus 2.7C; Figure 2.11 versus 2.10). This was especially true in July, when larval mortality rates were very high and varied little among segments, and between wet and dry years. Reduced variability in predicted mortality rates was partly due to rates being computed for 7 day periods, and thereby smoothing over day-to-day variability in DO concentrations. Additionally, larvae from overlapping cohorts experienced similar mortality rates on days that were in common.

Focusing on the June rates, larval mortality rates, like egg rates, were most affected by the Chesapeake Bay boundary conditions, but unlike egg mortality rates, larval mortality rates decreased with increasing boundary conditions (Figure 2.11). Larval mortality rates were highest for the 0.5x boundary condition, while the rates for baseline and 1.5x boundary conditions were lower and sometimes overlapped with each other.

Larval mortality rates decreased under worsening DO conditions because of changes in the vertical positions of the larvae and their predators that resulted in different degrees of spatial overlap. Using the results for the 7 day period starting on day 530 (June 14) under the wet year and current land-use, the 0.5x boundary condition resulted in bottom DO concentrations that kept larvae in the bottom layer with their ctenophore predators (Figure 2.12A). About 20% of the larvae and 20-40% of the ctenophores were in the bottom layer. Under baseline boundary conditions, 40-50% of the ctenophores were in the bottom layer, while less then 2% of the larvae were because bottom DO was low enough to trigger avoidance by the larvae (Figure 2.12B). Under the 1.5x boundary condition, the bottom DO got low enough for larvae to completely

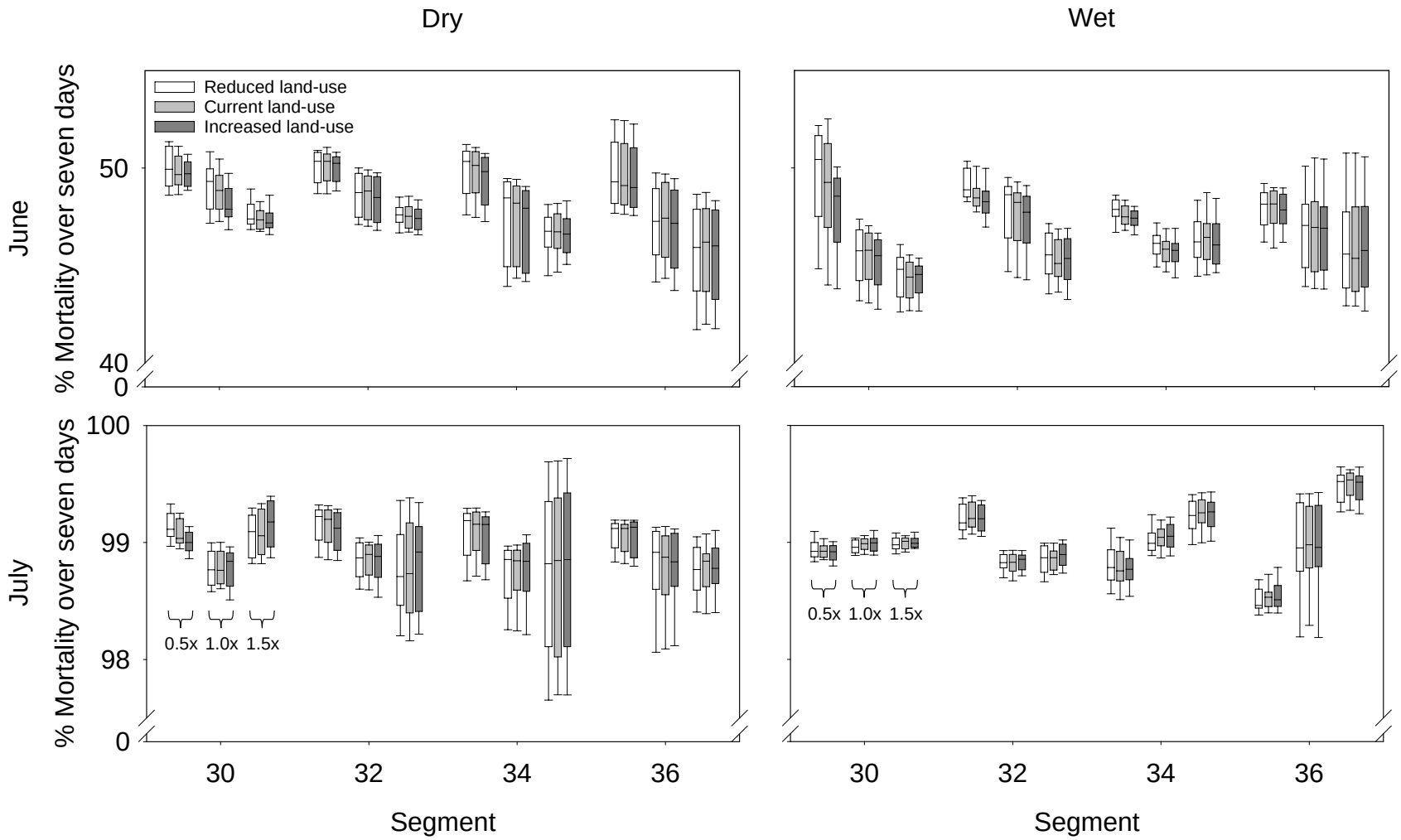

Figure 2.11 Boxplots showing monthly 7-day larval mortality rates for wet and dry years during June and July. Whiskers show the 10th and 90th percentiles of the distribution. Box shows the 25th and 75th percentiles and the solid line in the box shows the median. Land-use scenarios are shown in the June-Dry year panel; boundary condition scenarios are indicated in the July panels.

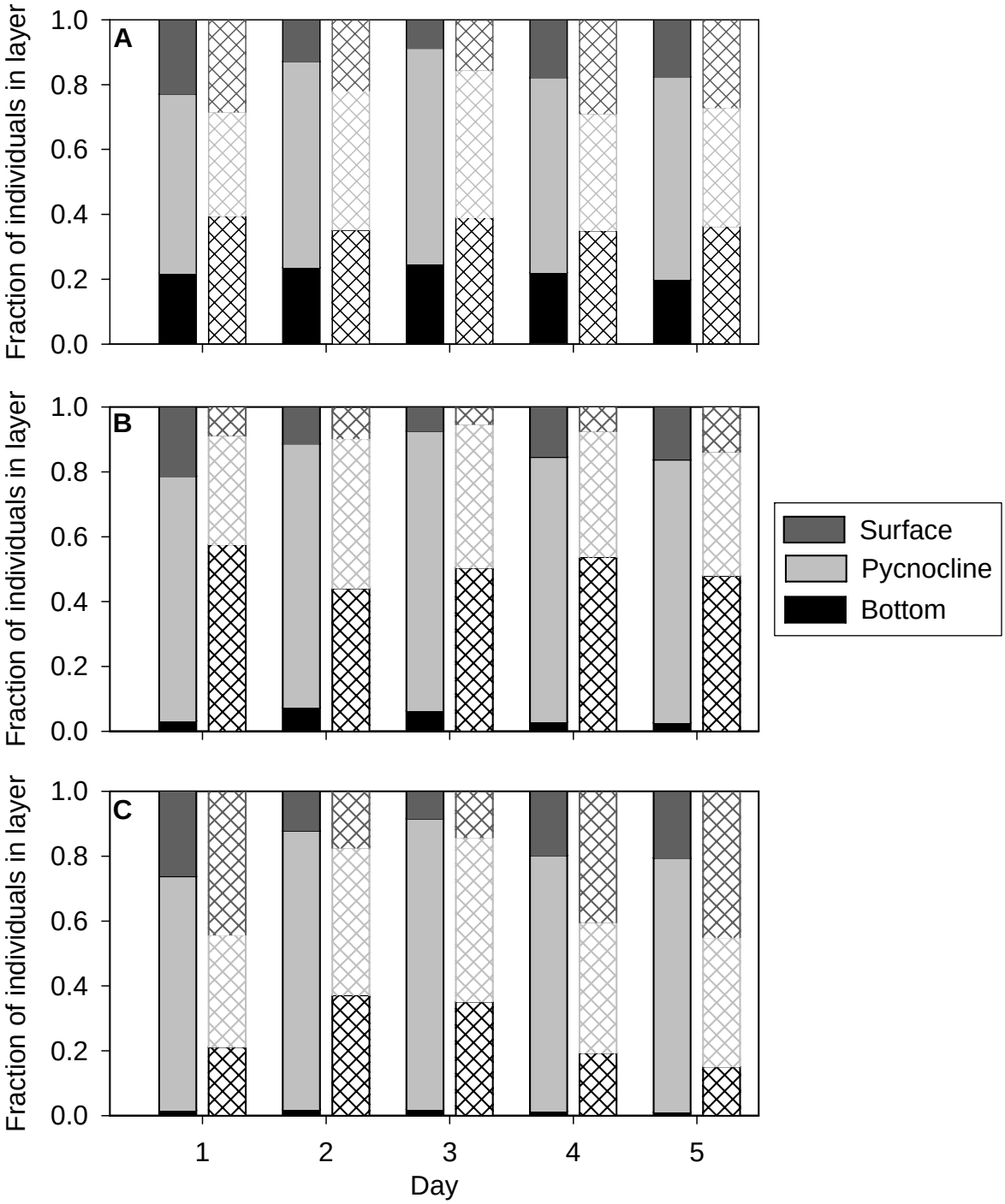

Figure 2.12 Vertical distributions of larvae and ctenophores in segment 34 for a wet year starting on Julian day 530. (A) 0.5× boundary condition (B) 1.0× boundary condition (C) 1.5× boundary condition. The top stack on each column is the fraction of all individuals in the surface layer, middle stack is fraction in the pycnocline and the bottom stack is fraction in the bottom. Anchovy distributions are shown in the solid columns and ctenophore distributions are shown in the cross-hatched columns.

avoid the bottom layer, while 15-35% of the ctenophores still remained in the bottom layer (Figure 2.12C).

2.4 Discussion

Chesapeake Bay water quality had a much bigger effect on egg and larval mortality rates than Patuxent River watershed land-use (Figure 2.10, 2.11). This was consistent with the predicted bottom-layer DO concentrations from the water quality model that were used as inputs to the individual-based model simulations (Figure 2.9). In a sensitivity analysis of the water quality model, Nice (2006) found that the effects of changing the downstream boundary conditions were felt up to 60 km from the mouth of the estuary, and heavily affected the river segments that were simulated. Examination of the effects of increasing and decreasing land-use in the Patuxent River watershed showed that changes in land-use caused a substantial difference in phytoplankton growth in both the upper and lower portions of the estuary and differences in DO concentrations in the upper estuary, but caused little or no difference in DO concentrations in the lower estuary. Nice (2006) suggested that the Chesapeake Bay boundary condition had a larger effect on DO concentrations than the local Patuxent River watershed because the Chesapeake Bay boundary contributed approximately 10 times more water to the lower Patuxent River estuary than the combined total of the point and non point source stream flow inputs.

Water column structure varied across days, segments, months, and water years (Figures 2.7A, 2.8). Daily changes in water column structure were the result of the time varying inputs into the hydrodynamics module and day-to-day variation in the biological processes of the water quality module. Pycnocline thickness increased and bottom layer thickness thinned between dry and wet years, and the bottom layer thickness increased moving downriver (Figure 2.8). Water discharge to the Patuxent River from its watershed was 3.4 times higher in the wet year than in

the dry year (Jordan et al. 2003). The increased water flows lead to stronger stratification (indicated by the thicker pycnocline) of the water column and lower bottom layer dissolved oxygen concentrations in the bottom layer (Hagy et al. 2004). The fraction of the water column in the bottom layer progressively increased moving from segment 30 to segment 36 as the depth of the water column increased from ~17 m in segment 30 to ~ 36 m in segment 36 (Nice 2006). Additionally, the river channel is roughly V-shaped, thus shallower vertical segments had larger volumes than deeper vertical segments. The difference in water column structure between June and July was smaller in magnitude than the dry versus wet and river segment effects (Figure 2.8).

Water column structure, combined with the nutrient boundary conditions and internal biological processes simulated by the water quality module, affected bottom layer DO concentrations. Daily bottom DO concentrations, at times, showed wide fluctuations (Figure 2.7A), with the Chesapeake Bay boundary conditions having the largest effect (Figure 2.9). Bottom layer DO concentrations decreased with increasing boundary condition nutrient loadings, were lower during wet years than dry years, and showed small but consistently lower concentrations as one moved upriver and during July compared to June. Variation in July was also lower than in June. Higher spring flow resulted in stronger stratification during the summer (Kemp et al. 1992, Turner et al. 1987, Seliger and Boggs 1988), and resulted in a doubling of the flow-weighted mean concentrations of total suspended sediments, organic carbon, and some forms of P entering the Patuxent from its watershed, but did not significantly affect the mean concentrations of silicon and several forms of nitrogen (Jordan et al. 2003). Increased nutrient concentrations during the wet year enhanced phytoplankton production that sank into the bottom layer, which with the thinner bottom layer, resulted in increased and concentrated benthic respiration consuming DO. Warmer water temperatures during July further increased production

and benthic demands (Kemp et al. 1992). The pattern of lower DO in upstream segments and in July was consistent with the historical summertime spatial pattern of bottom DO concentrations in the Patuxent River reported by D'Elia et al. (2003).

Bay anchovy egg mortality rates were strongly linked to water quality, with better water quality (i.e., 0.5× boundary and reduced land-use) resulting in lower mortality rates (Figure 2.10). Across segments and water years, bottom-layer DO concentrations (Figure 2.9) were sufficiently hypoxic on at least some of the days simulated for each of the three Chesapeake Bay boundary condition scenarios to cause egg mortality rates of 50% or more on most days in the bottom layer of the water column (Figure 2.7B). This was because bay anchovy eggs have a low tolerance for hypoxic conditions, having a 12 hour LC_{50} of 2.8 mg liter^{-1} (Chesney and Houde 1989). This intolerance for hypoxia frequently made the bottom-layer of the water column lethal to anchovy eggs. On days when the bottom-layer DO concentrations approached 1 mg liter^{-1}, hypoxic conditions also extended into the pycnocline layer, thereby causing additional egg mortality due to hypoxia.

Egg mortality rates due to hypoxia were also affected by the water column structure. For example, conditions in the bottom-layer on June 3-8, with the exception of the fraction of the water column in the bottom-layer, were stable (Figure 2.7A). Dissolved oxygen concentrations in the bottom-layer on these days was consistently below the 1 mg liter^{-1} threshold below which bay anchovy eggs suffered 100% mortality due to hypoxia. Additionally, the bottom-layer DO concentrations were below 0.5 mg liter^{-1}, the concentration below which ctenophores avoided the bottom-layer of the water column. Bay anchovy eggs were unable to respond to DO concentrations, thus the only factor affecting the number of eggs dying because of hypoxic conditions in the bottom-layer was the fraction of the water column in the bottom-layer. The

fraction of the water column in the bottom layer decreased from 0.26 on June 3 to 0.07 on June 8th (Figure 2.7A). Over that same time interval, the percentage of eggs in the bottom layer declined from 23% on June 3 to 5% on June 8 because of the decrease in the fraction of the water column in the bottom layer (Figure 2.7B). Thus, changes in water column structure alone were able to cause an 18% reduction in overall egg mortality rates between June 3rd and June 8th. However, it should be noted, that if DO concentrations in the pycnocline are also hypoxic, reductions in egg mortality rates in the bottom-layer may be counteracted by increased egg mortality in the pycnocline layer.

Due to indirect effects, the effect of the Chesapeake Bay boundary condition on larval mortality rates during June was opposite to that predicted for egg mortality rates. Predicted larval mortality rates during July were uniformly very high, and thus made determining the effects of boundary conditions, land-use, and water years very difficult. During June, the 1.5x baseline boundary conditions scenario generally had the lowest larval mortality rates during both the wet year and the dry year (Figure 2.11). Mortality rates for the baseline boundary condition scenarios were generally about the same as the 1.5x baseline boundary condition scenario or slightly higher, while the 0.5x baseline boundary condition scenario always had the highest mortality rates. Mortality rates for the 1.5x and baseline boundary condition scenarios were low because hypoxic conditions (DO < 1 mg liter^{-1}) in the bottom layer (Figure 2.8) caused larvae to move from the bottom layer to the pycnocline, while ctenophores were generally able to remain in the bottom layer (Figure 2.12C), creating a spatial refuge from predation for the larvae. In contrast, larvae and ctenophores in the 0.5x baseline boundary condition scenario tended to be more evenly distributed among the three layers of the water column which resulted in a significant fraction of the larvae being exposed to predation (Figure 2.12A).

Predicted bay anchovy egg and larval mortality rates were comparable to the mortality rates reported in the literature. June and July egg mortality rates (0.06 to 0.96 d^{-1} and 0.61 to 1.7 d^{-1}) were within the range of the stage-specific mortality rates reported for eggs in July in Chesapeake Bay (0.02 to 4.69 d^{-1}, Dorsey et al. 1996). However, the vast majority of simulated mortality rates of eggs for June and July were below Dorsey's average mortality rate (1.6 d^{-1}). Larval mortality rates for June (0.08 to 0.10 d^{-1}) and for July (0.53 to 0.76 d^{-1}) were within the range of rates (0.08 to 1.20 d^{-1}) reported for Chesapeake Bay by Cowan and Houde (1990) and MacGregor (1994). However, in contrast to Rilling and Houde (1999), larval mortality rates were predicted to increase between June and July rather than decrease. The predicted June larval mortality rates were more typical of the rates reported for mesocosm studies (e.g. 0.08 to 0.23 d^{-1}, Cowan and Houde 1990)) than for field studies (e.g., 0.23 to 1.20 d^{-1} MacGregor 1994), suggesting that the mix of predator types and sizes used in the June simulations should be adjusted. Simulated larval mortality rates for July were towards the high end of the reported mortality rates (e.g. 0.30 to 0.45, Leak and Houde 1987; 0.32 to 0.89 d^{-1}, Castro and Cowen 1991; and 0.23 to 1.20 d^{-1} MacGregor 1994), suggesting that ctenophores and sea nettles may indeed be the major predators on anchovy larvae during July.

Differences in egg and larval mortality rates between my simulated rates and the rates reported in the literature are likely due to differences in the predator fields. Simulations only included ctenophores and sea nettles as predators. Houde et al. (1994) compared the predicted mortality rates of anchovy eggs and larvae due to predation by gelatinous predators with observed mortality rates and found that gelatinous predators were likely responsible for 22% and 40.0% of total egg and larval mortality rates, respectively. The current set of simulations ignored the potential effects of other invertebrate predators and fish on anchovy egg and larval mortality

rates. Additionally, planktonic invertebrate predators such as amphipods, isopods, and predatory copepods may be important, as Cowan and Houde (1990) reported larval mortality rates of (~15% d^{-1}) in mesocosms with ambient microzooplankton levels and no predators (e.g. ctenophores, sea nettles and fish).

I highlight four main improvements to this analysis that would likely increase the realism of model predictions. Future modeling efforts should attempt to include the effects of wet and dry years on sea nettle and ctenophore abundances and spatial distribution. Jung and Houde (2004) found that larval mortality rates in the mainstem of the Chesapeake Bay were lower in years with high salinity (dry years), potentially because of the effects of salinity on predator abundance and spatial distribution (Purcell and Decker 2005, Breitburg and Fulford 2006). During wet years, the initiation of asexual production of sea nettles by benthic polyps may be delayed due to low salinity. If production of sea nettles is delayed, then ctenophore numbers may be higher than usual as sea nettles consume ctenophores. Additionally, water years may affect the spatial distribution of sea nettles (Decker et al. 2007), as they are found in a relatively narrow range of temperature (26 to 30°C) and salinity (10 to 16). Sea nettles may be more abundant in Chesapeake Bay tributaries during dry years than wet years due to increased salinity and temperature in dry years. It may also be useful to consider the long term effects of hypoxia and anoxia on the benthic polyps of sea nettles and the production of sea nettle medusae. Persistent hypoxic or anoxic conditions over a period of several years may reduce the polyp population and subsequently reduce the number of medusae that are produced (Purcell and Decker 2005, Breitburg and Fulford 2006).

The second improvement to the model should be to link water quality model predictions of chlorophyll *a* production to the assigned larval growth rates in the IBM. While the water

quality model predicted that DO concentrations in the lower Patuxent estuary would be relatively insensitive to changes in Patuxent watershed land-use, chlorophyll *a* concentrations in the lower estuary were sensitive to changes in land-use (Nice 2006). Differences in chlorophyll *a* concentrations between scenarios could affect the availability of micro- and meso-zooplankton prey for larval bay anchovy which would affect larval growth rates (e.g. Saksena and Houde 1972). This may affect larval mortality rates as faster growing larvae may have lower overall mortality rates than slower growing larvae (Houde 1987).

The third improvement to the model would be to allow the Chesapeake Bay boundary DO concentrations to vary in response to changes in Chesapeake Bay nutrient loads. Dissolved oxygen concentrations at the mouth of the Patuxent River were predicted by the CE-QUAL-ICM water quality model for Chesapeake Bay (Chapter 3) to change by about 1 mg liter^{-1} when Chesapeake Bay nutrient loads were increased or decreased by 50%. If these changes in boundary condition DO concentration affect upstream DO concentrations, they could result in the DO concentrations in the segments of the Patuxent River that were simulated being overestimated for increased nutrient loads and underestimated for decreased nutrient loads. Small differences in DO concentrations could have potentially large effects on egg and larval survival (e.g. eggs during June 1 to 10 and larvae for the 7-day period starting on June 14).

The fourth suggested improvement for future modeling studies would be to do simulations that were continuous from the eggs through the first week of life of larvae or longer. The counter-acting dependence of egg mortality and larvae mortality on nutrient loadings makes their separate analyses difficult to combine. Simulations that go from egg through larvae would integrate these counter-acting effects of water quality, thereby giving a clearer overall view of water quality effects on early life stage survival.

Future application of the linked model approach used here should involve a consistency check between the interval vertical mixing assumed in the CE-QUAL-W2 (water quality) model and the three layers identified by application of the pycnocline detection algorithm to CE-QUAL-W2 model output. In my analysis, the thicknesses of the surface, pycnocline, and bottom layers greatly affected the predicted responses of anchovy mortality to hypoxia. These layers were identified by post-processing of the vertical temperature and salinity predicted by the water quality model. However, within the water quality model assumptions were made about how the vertical mixing changed with depth (i.e., layering was implicitly represented). Consistency between the implicit layering assumed in the vertical mixing of the water quality model and the three layers identified from the water quality model output would increase our confidence in the linked model approach.

My analysis focused on only one aspect of the effects of water quality (i.e., anchovy egg and larval mortality), and should not be interpreted as suggesting that reduced nutrient loadings from the local Patuxent watershed would have no beneficial effects. Predicted egg morality rates and larval mortality rates in the lower estuary were insensitive to changes in Patuxent land-use. There were episodes (a few days) during which land-use caused differences in egg mortality rates (e.g., June 2-9, Figure 2.7C), but these were relatively rare. Examination of surface and bottom layer DO concentrations farther upriver showed much larger differences among the three land-use scenarios. Reduced land-use caused 1-2 mg liter^{-1} higher DO concentrations in the surface layer and 2-3 mg liter^{-1} higher DO concentrations in the bottom layer for days at a time during June and July. These changes in primary production and higher DO concentrations would provide benefits. However, from the perspective of bay anchovy, these large differences in surface and bottom DO concentrations rarely resulted in DO values below 3 mg liter^{-1}, which is

above the threshold for anchovy mortality effects. Furthermore, anchovy spawning is concentrated in the lower portion of the estuary where water is more saline (Dovel 1971). Land-use scenarios caused large differences in productivity and DO, but these differences were not in locations of prime bay anchovy spawning and rarely would have triggered significant mortality anyway.

Changes in Patuxent River watershed land-use would contribute to regional (Chesapeake Bay) water quality, as the Patuxent River is a tributary of the Chesapeake Bay (Boynton et al. 1995, Fisher et al. 2006). The Patuxent River has been shown to export organic nitrogen to the Chesapeake Bay (Boynton et al. 1995), which contributes to eutrophication. Nice (2006) noted that his simulations showed that "the large impact of downstream boundary conditions on DO concentrations in the lower estuary coupled with the lack of sensitivity to nutrient loadings from upstream tributaries implies that water quality at Broomes Island and the lower portions of the estuary will not improve without Bay wide reductions in nutrient loadings". In order to benefit anchovy spawning in the Patuxent River, land-use planning and nutrient loading reduction strategies should consider both local (specific watershed) and regional (Bay-wide) conditions.

2.5 References

Bailey, K. M. and R. S. Batty. 1983. A laboratory study of predation by *Aurelia aurita* on larval herring (*Clupea harengus*): experimental observations compared with model predictions. Marine Biology 72: 295-301

Bockstael, N. E. and E. G. Irwin. 2003. Public policy and the changing landscape. Estuaries 26: 210-225

Boesch, D. F., R. B. Brinsfield and R. E. Magnien. 2001. Chesapeake Bay eutrophication: Scientific understanding, ecosystem restoration, and challenges for agriculture. Journal of Environmental Quality 30: 303-320

Boynton, W. R., J. H. Garber, R. Summers, and W. M. Kemp. 1995. Inputs, transformations, and transport of nitrogen and phosphorus in Chesapeake Bay and selected tributaries. Estuaries 18: 285-314

Breitburg, D. L. 1994. Behavioral response of fish larvae to low dissolved oxygen concentrations in a stratified water column. Marine Biology 120: 615-625

Breitburg, D.L., K. A. Rose, and J. H. Cowan, Jr. 1999. Linking water quality to larval survival: Predation mortality of fish larvae in an oxygen-stratified water column. Marine Ecology Progress Series 178: 39-54

Breitburg, D. L., A. Adamack, K. A. Rose, S. E. Kolesar, M. B. Decker, J. E. Purcell, J. E. Keister, and J. H. Cowan, Jr. 2003A. The pattern and influence of low dissolved oxygen in the Patuxent River, a seasonally hypoxic estuary. Estuaries 26: 280-297

Breitburg, D. L., T. E. Jordan, D. Lipton. 2003B. Preface – from ecology to economics: Tracing human influence in the Patuxent River estuary and its watershed. Estuaries 26: 167-170

Breitburg, D. L. and R. S. Fulford. 2006. Oyster-sea nettle interdependence and altered control within the Chesapeake Bay ecosystem. Estuaries and Coasts 29: 776-784

Castro, L. R. and R. K. Cowen. 1991. Environmental factors affecting the early life history of bay anchovy *Anchoa mitchilli* in Great South Bay, New York. Marine Ecology Progress Series 76: 235-247

Chesney, E. J. and E. D. Houde. 1989. Laboratory studies on the effect of hypoxic waters on the survival of eggs and yolk-sac larvae of the bay anchovy, *Anchoa mitchilli*. P. 184-191. *In* E. D. Houde, E. J. Chesney, T. A. Newberger, A. V. Vasquez, C. E. Zastrow, L. G. Morin, H. R. Harvey, and J. W. Gooch, (eds.), Population Biology of Bay Anchovy in mid-Chesapeake Bay. Final Report to Maryland Sea Grant Ref. No. (UM-CEES) CBL 89-141. Solomons, Maryland.

Cole, T. M. and S. A. Wells. 2000. CE-QUAL-W2: A two-dimensional, laterally averaged, hydrodynamic and water quality model, Version 3.0, U.S. Army Corps of Engineers, Washington, D.C.

Correll, D. L., T. E. Jordan, and D. E. Weller. 1999. Effects of interannual variation of precipitation on stream discharge Rhode River subwatersheds. Journal of the American Water Resources Association 35: 73-82

Cowan, J. H. Jr. and E. D. Houde. 1990. Growth and survival of bay anchovy (*Anchoa mitchilli*) larvae in mesocosm enclosures. Marine Ecology Progress Series 68: 47-57

Cowan, J. H. Jr. and E. D. Houde. 1992. Size-dependent predation on marine fish larvae by ctenophores, scyphomedusae and planktivorous fish. Fisheries Oceanography 1: 113-126

Cronin, T. M. and C. D. Vann. 2003. The sedimentary record of climatic and anthropogenic influence on the Patuxent Estuary and Chesapeake Bay Ecosystems. Estuaries 26: 196-209

Decker, M. B., C. W. Brown, R. R. Hood, J. E. Purcell, T. F. Gross, J. C. Matanoski, R. O. Bannon, E. M. Setzler Hamilton. 2007. Predicting the distribution of the scyphomedusa *Chrysaora quinquecirrha* in Chesapeake Bay. Marine Ecology Progress Series 329: 99-113

D'Elia, C. F., W. R. Boynton, and J. G. Sanders. 2003. A watershed perspective on nutrient enrichment, science and policy in the Patuxent River, Maryland: 1960-2000. Estuaries 26: 171-185

Dorsey, S. E., E. D. Houde, and J. C. Gamble. 1995. Cohort abundances and daily variability in mortality of eggs and yolk-sac larvae of bay anchovy, *Anchoa mitchilli* in Chesapeake Bay. Fishery Bulletin 94: 257-267

Dovel, W. L. 1971. Fish eggs and larvae of the upper Chesapeake Bay. Natural Resource Institute, University of Maryland, Special Report No. 4. 71 pgs.

EPA. 2003. Technical support document for identification of Chesapeake Bay designated uses and attainability. U.S. Environmental Protection Agency Region III Chesapeake Bay Program Office, Annapolis, MD

Fisher, T. R., J. D. Hagy III, W. R. Boynton, and M. R. Williams. 2006. Cultural eutrophication in the Choptank and Patuxent estuaries of Chesapeake Bay. Limnology and Oceanography 51(1, part 2): 435-447.

Gerritsen, J., and J. R. Strickler. 1977. Encounter probabilities and community structure in zooplankton: a mathematical model. Journal of the Fisheries Research Board of Canada 34: 77-82

Hagy, J. D., W. R. Boynton, C. W. Keefe, K. V. Wood. 2004. Hypoxia in Chesapeake Bay, 1950-2001: Long-term change in relation to nutrient loading and river flow. Estuaries 27:634-658

Houde, E. D. 1987. Fish early life dynamics and recruitment variability. American Fisheries Society Symposium 2: 17-29

Houde, E. D., J. C. Gamble, S. E. Dorsey, and J. H. Cowan, Jr. 2004. ICES Journal of Marine Science. 51: 383-394

Jordan, T. E., E. Weller, and D. L. Correll. 2003. Sources of nutrient inputs to the Patuxent River estuary. Estuaries. 26: 226-243

Jung, S. and E. D. Houde. 2004. Production of bay anchovy *Anchoa mitchilli* in Chesapeake Bay: application of size-based theory. Marine Ecology Progress Series 281: 217-232

Keister, J. E., E. D. Houde, and D. L. Breitburg. 2000. Effects of bottom-layer hypoxia on abundances and depth distributions of organisms in Patuxent River, Chesapeake Bay. Marine Ecology Progress Series 205: 43-59

Kemp, W. M., P. A. Sampou, J. Garber, J. Tuttle, W. R. Boynton. 1992. Seasonal depletion of oxygen from bottom waters of Chesapeake Bay: roles of benthic and planktonic respiration and physical exchange processes. Marine Ecology Progress Series 85: 137-152

Kemp, W. M., W. R. Boynton, J. E. Adolf, D. F. Boesch, W. C. Boicourt, G. Brush, J. C. Cornwell, T. R. Fisher, P. M. Glibert, J. D. Hagy, L. W. Harding, E. D. Houde, D. G. Kimmel, W. D. Miller, R. I. E. Newell, M. R. Roman, E. M. Smith, J. C. Stevenson. 2005. Eutrophication of Chesapeake Bay: historical trends and ecological interactions. Marine Ecology Progress Series 303: 1-29

Leak, J. C. and E. D. Houde. 1987. Cohort growth and survival of bay anchovy *Anchoa mitchilli* larvae in Biscayne Bay, Florida. Marine Ecology Progress Series 37: 109-122

Lung, W. S. and S. Bai. 2003. A water quality model for the Patuxent estuary: Current conditions and predictions under changing land-use scenarios. Estuaries 26: 267-279

MacGregor, J. M. 1994. Offshore-onshore pattern and variability in abundance and distribution of bay anchovy, *Anchoa mitchilli*, eggs and larvae in Chesapeake Bay. M.S. thesis. University of Maryland, College Park 138 pp.

Nice, A. J. 2006. Developing a fate and transport model for arsenic in estuaries. Ph.D. Dissertation, University of Virginia, Charlottesville, Virginia

NOAA 2003. Water level data collected at the Center for Operational Oceanographic Products and Services (CO-OPS) Station 8577330, Solomons Island, MD, from November 1937 through present. http://www.coops.nos.noaa.gov/.

Powledge, F. 2005. Chesapeake Bay restoration: A model of what?. BioScience. 55: 1032-1038
Purcell, J. E. and M. B. Decker. 2005. Effects of climate on relative predation by scyphomedusae and ctenophores on copepods in Chesapeake Bay during 1987-2000. Limnology and Oceanography 50: 376-387

Rilling, G. C. and E. D. Houde. 1999. Regional and temporal variability in growth and mortality of bay anchovy, *Anchoa mitchilli*, larvae in Chesapeake Bay. Fishery Bulletin 97: 555-569

Saksena, V. P. and E. D. Houde. 1972. Effect of food level on the growth and survival of laboratory-reared larvae of bay anchovy (*Anchoa mitchilli* Valenciennes) and scaled sardine (*Harengula pensacolae* Goode & Bean). Journal of Experimental Marine Biology and Ecology 8: 249-258

Seliger, H. H. and J. A. Boggs. 1988. Long-term pattern of anoxia in the Chesapeake Bay, p. 570-583. *In* M. P. Lynch and E. C. Krome (eds.), Advances in Chesapeake Bay Research. Proceedings of a Conference (Baltimore, Maryland. March 29-31, 1988). Chesapeake Research Consortium, Solomons, Maryland

Turner, R. E., W. W. Schroeder, W. J. Wiseman. 1987. The role of stratification in the deoxygenation of Mobile Bay and adjacent shelf bottom waters. Estuaries 10: 13-19

Weller, D. E., T. E. Jordan, D. L. Correll, and Z.-J. Liu. 2003. Effects of land-use change on nutrient discharges from the Patuxent River watershed. Estuaries 26: 244-266

CHAPTER 3: COUPLING HYDRODYNAMIC, WATER QUALITY, AND INDIVIDUAL–BASED MODELS TO SIMULATE THE EFFECTS OF CHANGES IN NUTRIENT LOADINGS ON BAY ANCHOVY IN CHESAPEAKE BAY

3.1 Introduction

There is a growing need to link fish growth (bioenergetics) and population dynamics models with physical and biogeochemical models as a part of the need for ecosystem-based management approaches (deYoung et al. 2004, Runge et al. 2004). Understanding the link between water quality and fish population dynamics is especially important with the widespread efforts to reduce eutrophication in coastal waters (e.g. Cloern 2001, Rabalais et al. 2002; Breitburg et al. 2003). Changes in how an ecosystem is managed, such as altering the level of nutrient loading, can have large and complex impacts on the ecosystem (Rabalais et al. 2002), and can cause changes in the timing and spacing of ecosystem production dynamics. Most water quality models that are used to simulate the effects of different levels of nutrient loading on an estuary do not make ecological predictions at trophic levels higher than zooplankton (Brandt and Mason 2003, Runge et al. 2004, Lett et al. submitted). Many fish growth and population models focus on fish dynamics, and do not include water quality and trophic levels lower than zooplankton (e.g. Luo and Brandt 1993, Rose et al. 1999, Adamack 2003, Lett et al. submitted). Two earlier studies (Brandt and Mason 2003, Breitburg et al. 2003) that linked the output of a water quality model of the Patuxent River to fish bioenergetics models have shown that the responses of fish to changes in nutrient loading levels can be complex and variable across life stages.

The need to link fish bioenergetics and population models with water quality is particularly important in the Chesapeake Bay (Bay) ecosystem, as the Bay watershed is undergoing a large restoration effort (~$18.7 billion; Chesapeake Bay Program 2007).

Historically, the Bay has had episodic hypoxic and anoxic conditions in the deeper portions of the water column (Cooper and Brush 1991, Cronin and Vann 2003, Hagy et al. 2004). Since the time of European settlement, the extent and intensity of hypoxic and anoxic conditions has increased due to increased nitrogen, phosphorous, and sediment loading to the Bay (Boesch et al. 2001, Hagy et al. 2004, Kemp et al. 2005, Fisher et al. 2006). Nutrient and sediment loadings have increased because of increases in the human population size, changes in land use, and the increasing use of agricultural fertilizers.

High nutrient flows into the Bay leads to the production of excess phytoplankton which eventually leads to hypoxia and anoxia. Phytoplankton that goes ungrazed, dies then sinks to the bottom layer where it is broken down by microbial processes that consume oxygen (Kemp et al. 1992). During late spring and summer, the bottom layer of the water column becomes isolated from the surface layer because of density stratification, which limits re-aeration of the bottom layer. The combination of increased biological oxygen demand and limited re-aeration of the bottom layer results in hypoxic or anoxic conditions in large portions of the bottom layer of the Chesapeake Bay.

Since the signing of the first Chesapeake Bay Agreement in 1983 (Boesch et al. 2001, Powledge 2005, Chesapeake Bay Program 2007), the Bay and its tributaries have been undergoing a coordinated restoration program that has the goal of improving and protecting the water quality and living resources of the Bay ecosystem. The Chesapeake Bay initiative led to the banning of phosphate in laundry detergents in Maryland in 1984, and later the removal of phosphorus at wastewater treatment plants (Lung and Bai 2003). Biological nitrogen removal began at the eight major wastewater treatment plants around the Patuxent River in 1991 (Fisher et al. 2006), and has been added or is planned for additional wastewater treatment plants located

throughout the Chesapeake Bay watershed (Randall et al. 1999). Recently, the Chesapeake 2000 agreement was signed, outlining restoration plans for the Bay that include an on-going effort to reduce nitrogen and phosphorus loadings and a new initiative to reduce sediment loading (Chesapeake Bay Program 2007). By 2010, the objective of the restoration program is to "Correct the nutrient- and sediment-related problems in the Chesapeake Bay and its tidal tributaries sufficiently to remove the Bay and the tidal portions of its tributaries from the list of impaired waters under the Clean Water Act". It is not clear what achieving this goal will mean for fish growth, population dynamics, and food web interactions (Kemp 2004).

Bay anchovy (*Anchoa mitchilli*) is a good candidate species for linking water quality to fish growth and population dynamics. Bay anchovy is one of the dominant fish species in the Bay in terms of both abundance and biomass (Baird and Ulanowicz 1989, Houde et al. 1989, Jung and Houde 2003), and is a major trophic link between the zooplankton and the piscivores (Baird and Ulanowicz 1989, Hartman and Brandt 1995). Baird and Ulanowicz (1989) reported that bay anchovy consumed about 15-18% of zooplankton production during the summer and fall, which represented about 70-90% of all the zooplankton consumed by planktivorous fish. In turn, bay anchovy were the source of 60-90% of the energy intake of piscivorous fish that fed upon bay anchovy during the summer, fall, and spring seasons. Bay anchovy in Chesapeake Bay have also been the focus of detailed, and long-term study (e.g., Houde et al. 1989, Houde and Zastrow 1991, Jung and Houde 2004A).

The need for quantitative linkage between water quality and fish, coupled with increasing computing power, have lead to recent efforts to link water quality and fish dynamics models (Runge et al. 2004). Hermann et al. (2001) statically coupled a 3-dimensional hydrodynamic model and a nitrogen-phytoplankton-zooplankton model with an individual-based model of

larval walleye pollock (*Theragra chalcogramma*). The coupled models were used to simulate the growth and transport of larval walleye pollock in the western Gulf of Alaska. Brandt and Mason (2003) coupled a 2-dimensional water quality model with an Atlantic menhaden (*Brevoortia tyrannus*) bioenergetics model to predict the effects of land use changes on menhaden growth rate potential in the Patuxent River. Luo et al. (2001) coupled a 3-dimensional water quality model with an Atlantic menhaden bioenergetics model to estimate the carrying capacity of menhaden in the Chesapeake Bay. In all of these examples, links between water quality and fish models have been static (i.e., fish dynamics do not affect the dynamics of the water quality model). A static link was used in some cases (e.g., larval pollack analysis) because the physical models required many hours of computing time (e.g. 125 CPU hours on a Cray Y-MP) and large amounts of memory (Hermann et al. 2001).

More recently, there has been a move towards the development of spatially-explicit, full life cycle models that include all life stages of fish, how they move in space, and the use of computed dynamics to determine the number of new young entering the population each year (Lett et al. submitted). Continued development of spatially-explicit, full life cycle models are expected to provide a platform to more fully address issues related to how natural and human induced environmental changes will affect fish populations and fisheries. By including spatial heterogeneity and simulating multiple generations, it becomes possible to predict how changes in the environment will affect both the spatial distribution of fish and their long-term population dynamics.

In this chapter, I dynamically couple the 3-dimensional water quality model of the Chesapeake Bay with a spatially-explicit individual-based population dynamics model for bay anchovy. The individual-based anchovy model simulates the growth, mortality, and spatial

distribution of anchovy on the same grid as the water quality model. The coupled models are used to predict the effects of increasing or decreasing the nutrient loading to Chesapeake Bay on bay anchovy growth, biomass, and spatial distribution. Wet, normal, and dry years are simulated in the sequence they occurred during the years 1984 to 1993. Recruitment of new juveniles each year is specified as low or high and is imposed every year, and reduced, baseline, and increased nutrient loadings are simulated. The analysis demonstrates that we have the knowledge and computing power to dynamically couple complicated water quality models with fish growth and population dynamics models, and also sheds some light on the possible effects of how changes in nutrient loadings can affect bay anchovy via changes in hypoxia and zooplankton production.

3.2 Methods

3.2.1 Chesapeake Bay Water Quality Model

The Chesapeake Bay Environmental Modeling Package (CBEMP) was developed to assist in the management of eutrophication in the Chesapeake Bay ecosystem. The CBEMP is a package of three models: a three-dimensional hydrodynamics (CH3D-WES) model (Johnson et al. 1993), an eutrophication (CE-QUAL-ICM) model (Cerco and Cole 1993, Cerco and Meyers 2000, Cerco and Noel 2004), and a sediment diagenesis model (DiToro 2001). The modeling package used a 4,073 cell grid to represent Chesapeake Bay. The model grid divided the surface of Chesapeake Bay into a horizontal grid of 729 cells that were roughly 5 × 10 km each (Figure 3.1). Vertically, each column of cells was 2 to 15 cell layers deep, with each cell having a depth of ~1.5 m. The hydrodynamics model was run first and stored output was used as inputs to the eutrophication and diagenesis models, which were then run simultaneously.

The hydrodynamics model used curvilinear hydrodynamics in three dimensions to produce three-dimensional predictions of velocity, diffusion, surface elevation, salinity, and

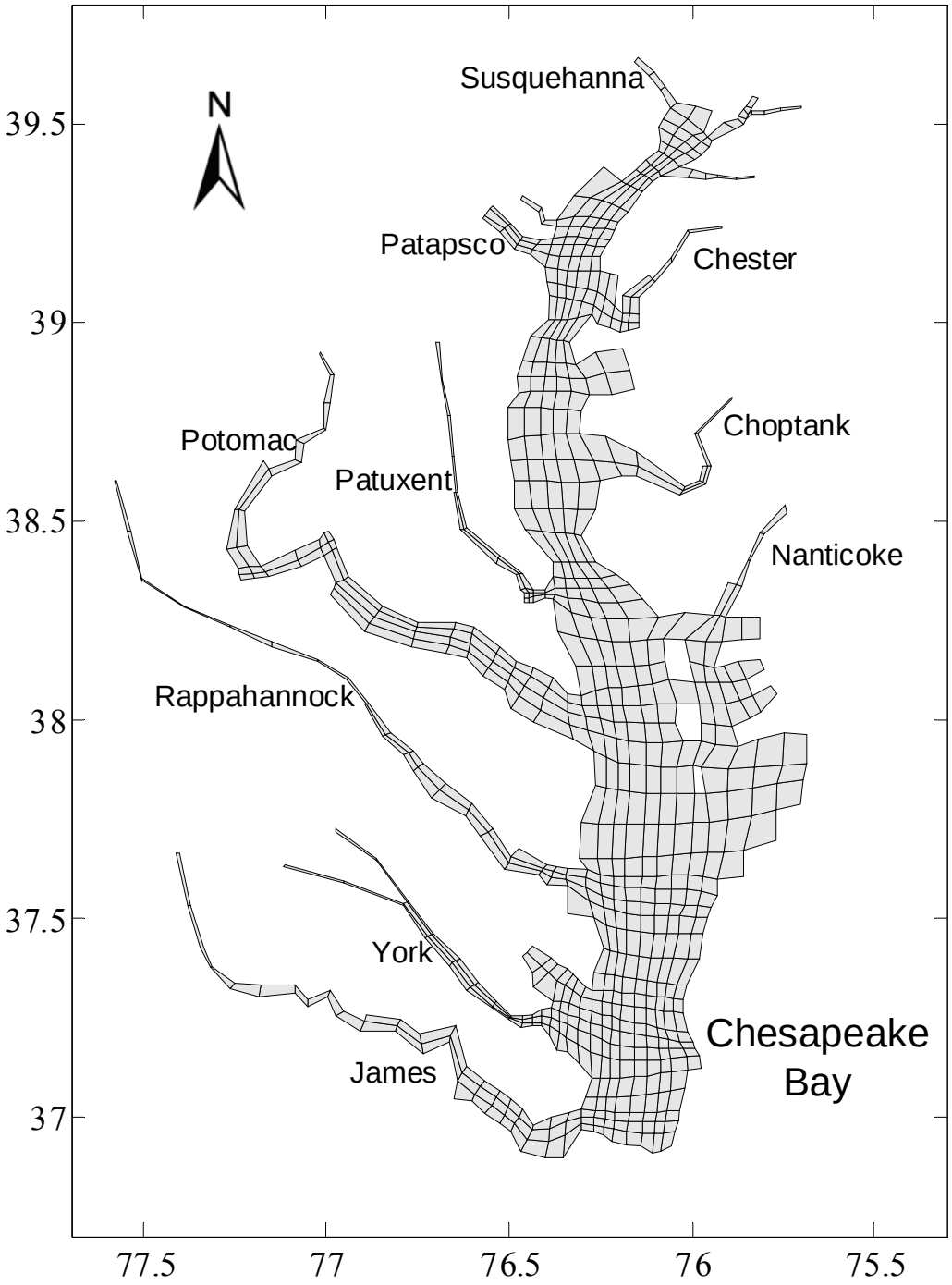

Figure 3.1 Chesapeake Bay water quality model grid and the location of some key tributaries.

temperature for each cell on an intratidal (≈ 5 min) time scale (Cerco and Cole 1993). A Lagrangian processor was then used to filter out intratidal details from the hydrodynamic output; while maintaining intertidal scale (≈ 12 h) transport (Dortch et al. 1992). Inputs to the hydrodynamics model included wind speed, air temperature, tributary freshwater inflows, surface heat exchange, tides, and the time-varying vertical distributions of temperature and salinity at the open boundary (Johnson et al. 1993). The hydrodynamic model was validated using 3 one-month simulations and 3 one-year simulations for 1984, 1985, and 1986 (Johnson et al. 1993). Validation of the model consisted of comparing recorded and computed water levels, flow velocities, salinities and temperatures. Comparisons were made through the analysis of time series plots and computed difference measures between predicted and observed data. An overall comparison of model results with field data indicated that the hydrodynamics model behaved well and was a good representation of the intertidal hydrodynamics of the Chesapeake Bay (Johnson et al. 1993).

The eutrophication model simulated nutrient, phytoplankton, and zooplankton dynamics in Chesapeake Bay on the same three dimensional model grid as the hydrodynamics model (Cerco and Cole 1993, Cerco and Noel 2004). The eutrophication model tracked the concentration of 23 constituents, including temperature, several forms of carbon, nitrogen, and phosphorous, spring and winter phytoplankton groups, micro-zooplankton, and meso-zooplankton (Table 3.1). The primary forcing functions for the eutrophication model were hydrodynamic output from the hydrodynamics model, fall-line nutrient loads from the Susquehanna River and other major tributaries, non-point-source loads from below the fall line, point-source loads from municipal and industrial sources, atmospheric loads, open-mouth boundary conditions, solar radiation, and temperature (Cerco and Cole 1993, Cerco 1995).

Table 3.1 Eutrophication model state variables (Cerco and Cole 1993, Cerco and Noel 2004).

Group	Forms tracked
Temperature	
Salinity	
Dissolved oxygen	
Inorganic suspended solids	
Zooplankton	Micro-zooplankton Meso-zooplankton
Algae	Summer group Winter group
Carbon	Dissolved organic carbon Labile particulate organic carbon Refractory particulate organic carbon
Nitrogen	Ammonium Nitrate + nitrite Dissolved organic nitrogen Labile particulate organic nitrogen Refractory particulate organic nitrogen
Phosphorus	Total phosphate Dissolved organic phosphorus Labile particulate organic phosphorus Refractory particulate organic phosphorus
Silica	Dissolved silica Particulate biogenic silica
Chemical oxygen demand	

Nutrient-related constituents were tracked as g nutrient m^{-3}, while phytoplankton and zooplankton were tracked as g C m^{-3}. This model has been extensively calibrated through comparison with Chesapeake Bay water quality data (e.g. temperature, chlorophyll *a*, dissolved oxygen (DO) concentrations, nutrient concentrations, zooplankton concentrations) on multiple spatial and temporal scales (Cerco and Cole 1993; Cerco and Noel 2004). Two specific examples of model to data comparison done for model calibration were a comparison of three-years of model data to observations of nutrient and chlorophyll *a* concentrations at a mid-Bay sampling station (CB5.2) and a comparison of predicted nutrient, chlorophyll *a*, DO concentrations, temperature, and salinity to data along the main axis of the Bay during the summer (Cerco and Cole 1993).

Constituent dynamics were updated approximately every 15 minutes for each model cell using a three dimensional mass-conservation equation which was solved using the finite-difference method (Cerco and Cole 1993). The mass-conservation equation was used to determine horizontal and vertical advection and diffusion for each constituent, in each cell, each time step. The rate of change of each constituent due to biological processes was expressed as the sum of the process rates that affected that constituent. Phytoplankton biomass was affected by production (photosynthesis), respiration, predation, and settling. Photosynthetic rates were affected by temperature, light intensity, and nutrient concentrations. Respiration was dependent on temperature. Zooplankton biomass was increased through consumption of phytoplankton, dissolved organic carbon (DOC) and, in the case of meso-zooplankton, the consumption of micro-zooplankton (Cerco 2004). Zooplankton biomass was decreased by respiration, mortality, and predation. Zooplankton grazing, metabolism, and respiration were affected by temperature, and grazing depended on prey densities. Exposure to hypoxia or anoxia increased zooplankton

mortality rates. Nutrient concentrations were decreased by photosynthetic uptake, consumption by zooplankton (DOC only), and by uptake by the sediments. Nutrient concentrations were increased by nutrient recycling following the death of algae and zooplankton, and by nutrients being recycled from the sediments (via the sediment diagnesis model). Nutrient concentrations were also increased by nutrient inflows from the Bay's tributaries and point sources.

3.2.2 Bay Anchovy Model

The bay anchovy model was a spatially-explicit individual-based population model that tracked the growth, death, and movement of individual bay anchovy in the same 3-dimensional grid as the eutrophication model. The anchovy model was dynamically coupled to the eutrophication model. Anchovy growth and mortality rates were affected by temperature, zooplankton, and DO concentrations predicted by the eutrophication model. To grow, anchovy consumed micro- and meso-zooplankton in their cell, which acted as a predation mortality term on the zooplankton concentrations in the eutrophication model. Zooplankton biomass consumed by the anchovy was returned to the eutrophication model in the form of particulate and dissolved nutrients. Anchovy consumption was dependent on anchovy body weight, zooplankton densities, and temperature. Low DO concentrations affected anchovy via vertical movement (via avoidance), slowed growth, and increased mortality rate.

In order to conveniently track anchovy movement, the grid coordinates were converted from the latitude and longitude coordinates used in the eutrophication model to Universal Transverse Mercator (UTM) coordinates, which are given in terms of meters (m). The conversion was done using the equations of Snyder (1987), and assumed that the shape of the Earth conformed to the dimensions assumed by the 1980 Geodetic Reference System/World Geodetic System 1984 ellipsoid. To confirm that model cell sizes were consistent for the two

grids, I compared the side lengths of the anchovy model grid cells to the eutrophication model grid cells. Differences in side lengths for the two grids were less than 0.1 m per side.

3.2.2.1 Annual recruitment

Bay anchovy were added to simulations as weekly cohorts of 23-mm long, 30-day-old juveniles. Based upon the spawning pattern of bay anchovy observed in previous studies (Luo and Musick 1991, Zastrow et al. 1991, Jung and Houde 2004A), anchovy cohorts of juveniles were added to the model between early June and mid October. Total number added in each year was specified as a fixed number (low, median, or high, see below). These total numbers were then divided up into weekly cohorts. The numbers of individuals in each of the weekly cohorts were fewest in early June and mid-October, and peaked during mid-August (Figure 3.2). Model individuals were generated from each of the introduced weekly cohorts, and their growth, survival, and movement was followed. This was repeated for each year of the simulation.

The initial positions of the newly generated juvenile individuals were randomly selected from the cells in the model grid in proportion to the volume of each cell. If an individual was placed within a cell that had a DO concentration less than 3.0 mg liter^{-1} or a zooplankton concentration of less than 0.005 g C m^{-3} then the individual was randomly placed in a different cell until a cell was found with sufficient dissolved oxygen and zooplankton. The initial position of an anchovy in terms of continuous x, y, and z co-ordinates was set to the centroid of the cell in which the anchovy was initially placed.

3.2.2.2 Growth and Bioenergetics

Growth was based upon the bay anchovy bioenergetics model that was developed by Luo and Brandt (1993). Each eutrophication model time step (~ 15 minutes), the growth of each model individual was determined using the equation:

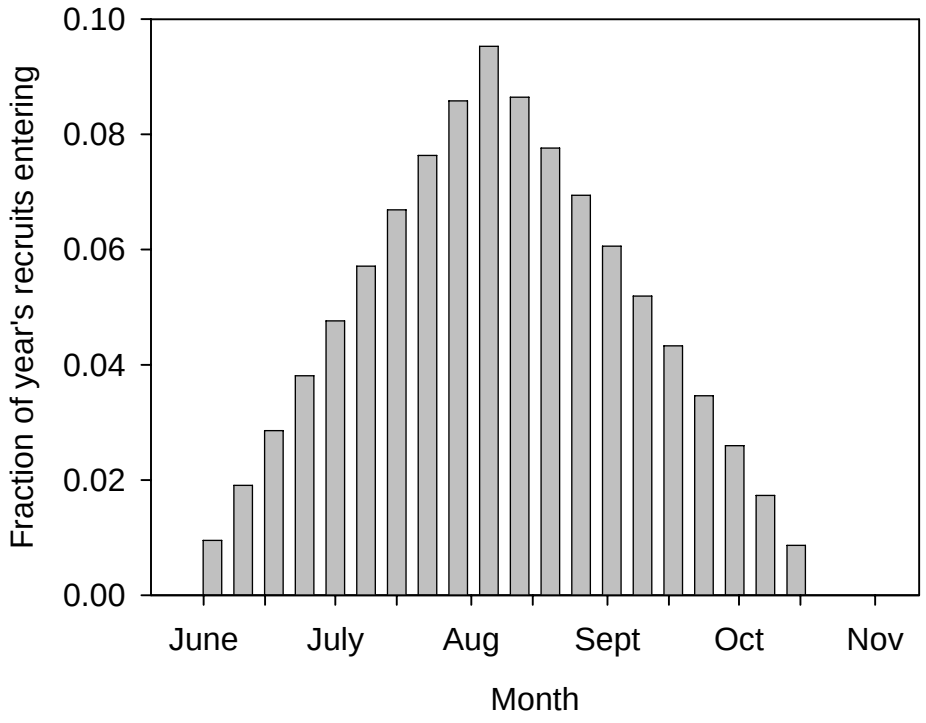

Figure 3.2 Fraction of the year's total number of juvenile recruits added as a part of weekly cohorts. Ticks labeled with months are the first of the month while unlabeled ticks are the 15th.

$$\frac{dW_i}{dt} = [CON_i - (R_i + SDA_i + F_i + E_i + REP_i)] \cdot \frac{Cal_z}{Cal_f} \cdot W_i \quad (3.1)$$

where i = individual number; W_i = wet weight of an anchovy (g wet weight); CON_i = amount of prey consumed; R_i = respiration; SDA_i = specific dynamic action; F_i = excretion; E_i = egestion; REP_i = reproduction; Cal_z = caloric density of prey (cal (g prey)$^{-1}$); Cal_f = caloric density of fish (cal (g wet weight)$^{-1}$). Consumption and the loss terms were all in units of g prey (g wet weight)$^{-1}$ d^{-1}. The ratio of the caloric densities converts g prey to g anchovy. All parameter values are given in Table 3.2. Each model individual was exposed to the temperature and zooplankton densities in its current cell, as predicted by the eutrophication model, to compute growth.

The energy loss terms were respiration, specific dynamic action, excretion, egestion, and reproduction (Table 3.2). Respiration was modeled as a power function of weight and then adjusted for temperature using a Q_{10} function. Egestion was modeled as a fraction of consumption, while excretion and specific dynamic were modeled as fractions of assimilated energy (consumption minus egestion). Energy related to reproduction was expended during days 115 to 246 of each year by anchovy that were at least 43 mm long and that had a positive net energy intake for the time step. The energy used for reproduction was set to half of the net energy intake, and reproduction costs were applied to all individuals (males and females).

Consumption was the amount of food that was consumed by an anchovy during each time step, and depended on a maximum possible consumption and micro- and meso-zooplankton densities. The anchovy's maximum consumption for a time step was determined using the standard bioenergetics equation (Luo and Brandt 1993):

$$CON_{\max} = a_c W_i^{b_c} f(T) \quad (3.2)$$

where a_c = maximum consumption rate of a 1 g bay anchovy at the optimal temperature for consumption (g prey (g wet weight)$^{-1}$ d^{-1}); b_c = exponent for the weight dependence of the

Table 3.2 Parameter values used in the model equations for bay anchovy growth and consumption from Luo and Brandt (1993). Values of the eight K feeding efficiency parameters were determined during calibration of the model. Values of the vulnerability parameters (v) were all set to one and so did not affect the proportion of micro- versus meso-zooplankton consumed.

Symbol	Parameter description	Parameter value
Consumption		
a_c	Intercept for maximum consumption (g prey (g wet weight)$^{-1}$ d^{-1}	0.41
b_c	Exponent for maximum consumption	-0.33
Q	Slope for temperature dependence on consumption	2.22
T_0	Optimum temperature for consumption	27°C
T_m	Maximum temperature for consumption	33°C
K_{11}	Half saturation constant for micro-zooplankton to anchovy < 43 mm (g wet weight m^{-3})	4.8
K_{12}	Half saturation constant for meso-zooplankton to anchovy < 43 mm (g wet weight m^{-3})	0.04
K_{21}	Half saturation constant for micro-zooplankton to anchovy 43-60 mm (g wet weight m^{-3})	10.0
K_{22}	Half saturation constant for meso-zooplankton to anchovy 43-60 mm (g wet weight m^{-3})	2.0
K_{31}	Half saturation constant for micro-zooplankton to anchovy 60-90 mm (g wet weight m^{-3})	20.0
K_{32}	Half saturation constant for meso-zooplankton to anchovy 60-90 mm (g wet weight m^{-3})	5.0
K_{41}	Half saturation constant for micro-zooplankton to anchovy >90 mm (g wet weight m^{-3})	80.0
K_{42}	Half saturation constant for meso-zooplankton to anchovy >90 mm (g wet weight m^{-3})	20.0
v_1	Vulnerability of micro-zooplankton to anchovy	1.0
v_2	Vulnerability of meso-zooplankton to anchovy	1.0
Respiration		
a_r	Intercept for maximum standard respiration (g O_2 (g wet weight)$^{-1}$ d^{-1})	0.0115
b_r	Exponent for maximum standard respiration	-0.346
Q	Slope for temperature dependence of standard respiration	2.25
T_{0r}	Temperature for standard respiration	30°C
T_{mr}	Maximum temperature for standard respiration	36°C
S	Specific dynamic action coefficient	0.10
A	Activity parameter	2.0

Table 3.2 continued

Egestion and excretion		
A	Intercept for temperature dependence of egestion	0.77
B	Exponent for temperature dependence of egestion	-0.40
a_u	Proportion of assimilated food excreted	0.15
Caloric density		
Cal_z	Caloric density of micro- and meso-zooplankton (calorie (g prey)$^{-1}$)	610
Cal_F	Caloric density of bay anchovy (calorie (g wet weight)$^{-1}$)	1000

consumption; and $f(T)$ = a temperature dependent function to adjust CON_{max} (Hewett and Johnson 1987). The function $f(T)$ had a range of 0 to 1, and its shape was determined by three parameters: optimal temperature T_o (27 °C), Θ (2.2) that mimics a Q_{10} relationship, and the maximum temperature (33 °C; Luo and Brandt 1993). At low water temperatures (~0 °C), the value of the function was at or near zero. As water temperature increased, the value of the function slowly increased reaching 1.0 at the optimal temperature for anchovy (27 °C; Luo and Brandt 1993). The value of the function decreased rapidly at temperatures warmer than the optimal temperature, and eventually dropped to zero at the maximum temperature (37 °C).

Bay anchovy consumed micro- and meso-zooplankton in their present cell, as generated from the eutrophication model. During each time step, the amount of zooplankton consumed by each anchovy was determined using a type II functional response for multiple prey types that depended upon the maximum consumption rate (Rose et al. 1999). The total amount of zooplankton consumed by each anchovy was determined by summing over the two prey types:

$$C_{ij} = \frac{CON_{\max}(PD_{ij}v_j / K_{cj})}{1 + \sum_{k=1}^{2}(PD_{ik}v_k / K_{ck})} \quad (3.3)$$

$$CON_i = \sum_{k=1}^{2} C_{ij} \quad (3.4)$$

where C_{ij} = the amount of prey type *j* consumed by the *i*th anchovy (g prey type *j* (g wet weight)$^{-1}$ d^{-1}); PD_{ij} = the density of the *j*th prey type available to the *i*th anchovy; v_j = the vulnerability of the *j*th prey type to the *i*th anchovy (dimensionless); K_{cj} = the half saturation constant for anchovy in length class *c* feeding on the *j*th prey type (g prey m^{-3}); and CON_i = the total amount of prey consumed by the *i*th anchovy (g prey type *j* (g wet weight)$^{-1}$ d^{-1}). Micro- and meso-zooplankton were assumed to be equally vulnerable to predation (all v_j were set to one). Densities of micro- and meso-zooplankton were converted from g C m^{-3} in the eutrophication

model to g wet weight m^{-3} for use in the anchovy model by multiplying by 12.5 (dry weight was 20% of wet weight and carbon weight was 40% of dry weight; Mauchline 1998). Values of the K parameters were specified by length class of anchovy (<43 mm, 43 – 60 mm, 60 – 90 mm, and >90 mm), and were determined via calibration under baseline conditions based upon agreement of predicted and target young-of-year (YOY) anchovy lengths in October and length at age 3.

A logistic sigmoidal function (Figure 3.3) was used to simulate the physiological effects of exposure to low dissolved oxygen on anchovy growth rate:

$$f(DO_{cell}) = 1/(1 + e^{(-2.1972 DO_{cell} + 6.5916)}) \quad (3.5)$$

where DO_{cell} is the dissolved oxygen concentration in the cell currently occupied by the anchovy. The change in weight for a timestep was multiplied by $f(DO_i)$ to simulate slowed growth under hypoxic conditions. The function began to reduce anchovy growth at a DO concentration of ~6 mg $liter^{-1}$. Growth was reduced to 50% of normal growth at a DO concentration of 3 mg $liter^{-1}$, and growth approached zero at DO concentrations less than 1 mg $liter^{-1}$.This function was previously developed by Luo et al. (2001) for Atlantic menhaden, and was later used by Ludsin et al. (in review) for bay anchovy.

3.2.2.3 Mortality

Bay anchovy mortality was determined each timestep using an overall instantaneous mortality rate M (d^{-1}). There were four sources of mortality for bay anchovy in the model: general mortality (M_G), starvation mortality (M_{starv}), mortality due to exposure to hypoxia or anoxia (M_{DO}), and mortality due to old age. General, starvation, and hypoxia mortality rates were summed to obtain the overall instantaneous mortality rate for each individual each time step.

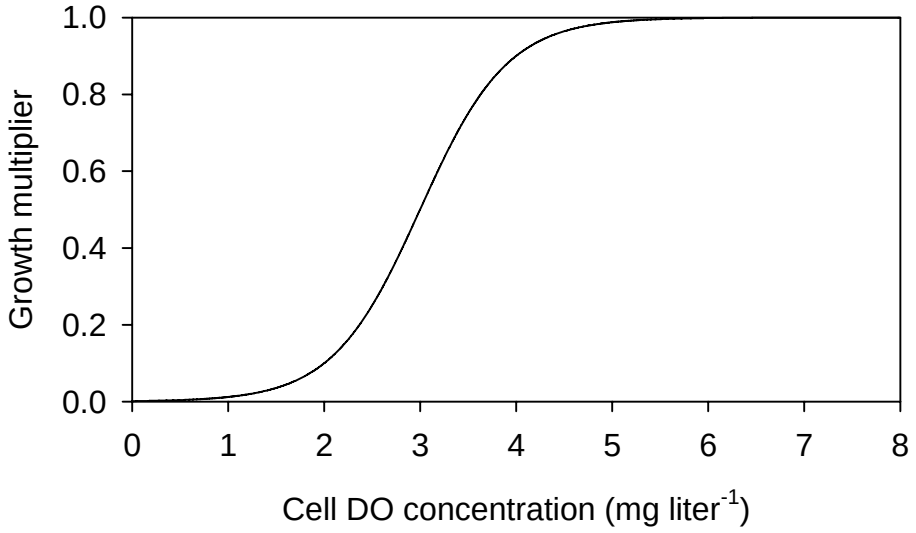

Figure 3.3 A logistic sigmoidal function used to represent the physiological stress of exposure to low DO concentration on anchovy growth rate.

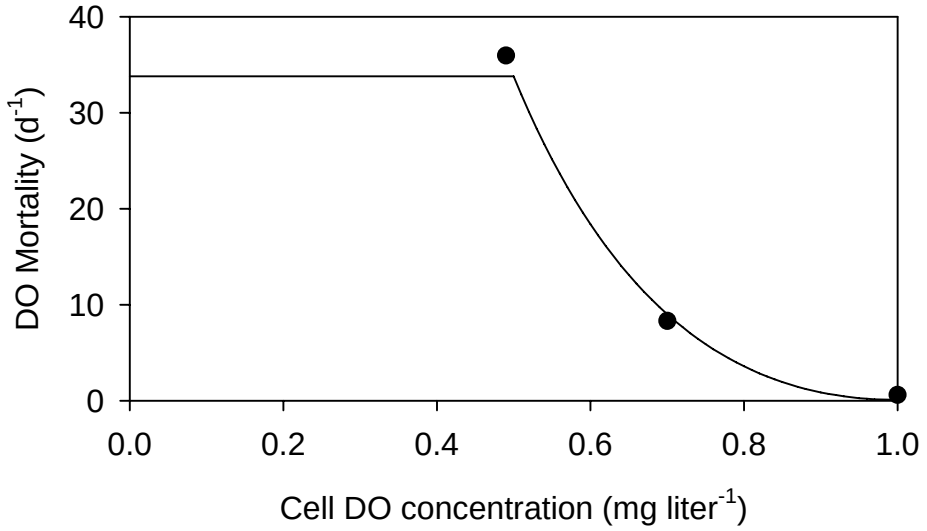

Figure 3.4 Anchovy instantaneous mortality rate due to exposure to hypoxic conditions. Circle symbols indicate the instantaneous mortality rates of Atlantic menhaden exposed in a laboratory experiment to various DO concentrations for two hours (Burton et al. 1980).

The general mortality rate represented all causes of mortality that anchovy may have experienced in Chesapeake Bay, except for hypoxia, starvation, and old age, which were explicitly accounted for with separate terms in model simulations. The general mortality rate was assumed to be constant during the winter (October through March) at 0.005 d^{-1}, and decreased with anchovy length during the summer (April through September):

$$M_G = q \cdot L^{-1} \quad (3.6)$$

where q = the length-specific mortality coefficient (1.17 mm^{-1}). Jung and Houde (2004A) estimated winter-time and length-dependent summer mortality rates based upon six years (1995-2000) of field-data. Because I separated out hypoxia, starvation, and old age mortality, I used the lowest observed summer and winter mortality rates estimated by Jung and Houde for general mortality.

Mortality rate due to exposure to hypoxia depended on the DO in the cell presently occupied by the anchovy:

$$M_{DO} = 0.093487 + 70.11894 \cdot (\ln[\mathrm{DO}_{\mathrm{cell}}])^2 \quad (3.7)$$

where M_{DO} = the instantaneous mortality rate due to exposure to low DO; and DO_{cell} = dissolved oxygen concentration (mg $liter^{-1}$). I fit this function to experimental data on menhaden (*Brevoortia tyrannus*) reported by Burton et al. (1980). Groups of menhaden were exposed to one of three DO concentrations for a period of two hours. A mortality probability for each group was determined based on the proportion of the group that survived the two hour exposure period. I converted the mortality probabilities for each group to instantaneous mortality rates, and fit a regression model to the mortality rates versus DO concentration data (Figure 3.4). As mortality rates became extremely high at low DO concentrations (Figure 3.4) and anchovy were only able

to move vertically once every ~4 time steps, I set the maximum mortality rate due to exposure to low DO to 33.78 d^{-1}, the rate for a bottom DO concentration of 0.5 mg $liter^{-1}$.

Starvation mortality was applied to anchovy whose weight was 70% or less of the expected weight given their length. Each time step that an anchovy was under 70% of its expected weight, a starvation mortality rate (M_{Starv}) of 0.1 d^{-1} was applied to the modeled individual.

The fourth source of anchovy mortality, which was not included in the instantaneous mortality term, was mortality due to old age. Newberger et al. (1989) found that bay anchovy generally did not live past three years of age. All anchovy in the model that were still alive upon reaching an age of 1095 days (3 years) were removed from the simulation due to old age.

3.2.2.4 Movement

I used a kinesis model for horizontal and vertical movement of each individual anchovy. The model was originally proposed by Humston (Humston et al. 2000; Humston 2001). The position of each anchovy was tracked in continuous x, y, and z space, in which x and y corresponded to the anchovy's UTM coordinates and z was the distance from the water surface. Horizontal movement in the x, horizontal movement in the y, and vertical movement in the z were evaluated separately (x and y twice per day; z every hour).

The movement model added an inertia component and a random component resulting in a net velocity for each of the x, y, and z dimensions. The net velocities were multiplied by the time since last evaluation to determine changes in distance for x, y, and z, which then were added to the current location to get a new x, y, and z location. Inertial movement was based on the velocity during the previous time step. The net velocity (V_t, m s^{-1}) was computed as the sum of inertial and random components:

$$V_t = f(V_{t-1}) + g(\varepsilon) \quad (3.8)$$

where $f(V_{t-1})$ = a function that was based upon the anchovy's velocity during the previous movement step, the inertia component; and g(ε) = a function of a random deviate, the random component.

The functions $f(V_{t-1})$ and g(ε) defined the relative contributions of the inertia and random components to the anchovy's velocity during the current movement time step. The relative contribution of each component was dependent on how close a movement cue was to its optimum level. When conditions in a cell were close to the optimum, the inertial component dominated movement. When conditions in a cell were far from the optimum, the random component dominated movement. Both functions were described using Gaussian functions:

$$f(V_{t-1}) = V_{t-1} \times H_1\left[e^{(-0.5)[(Q_M - Q_{M0})/\sigma]^2}\right]$$
$$g(\varepsilon) = \varepsilon \times H_2\left[e^{(-0.5)[(Q_M - Q_{M0})/\sigma]^2}\right] \quad (3.9)$$

where H_1 and H_2 control the height of the function and were restricted to the range 0 to 1.0; σ = variance and controlled the width of the Gaussian function; ε = a random number drawn from a normal distribution; Q_M = the actual value of the movement cue; and Q_{M0} = the optimum value of the movement cue. The random deviate ε was drawn from a normal distribution with a mean:

$$|\bar{\varepsilon}| = \sqrt{(\Phi^2/2)} \quad (3.10)$$

where Φ = the maximum sustained swimming velocity of an individual. The standard deviation was set to half of the maximum swimming speed. ε also had an equal probability of being positive or negative. Values for movement-related parameters are given in Table 3.3.

Horizontal (x and y) movement depended on the cues from water temperature and zooplankton density, while vertical (z) movement depended on water temperature and DO. The

densities of the micro- and meso-zooplankton were combined into a single measure of overall prey availability by using the functional response portion of consumption, expressing consumption as the proportion of maximum consumption realized. Water temperature and prey availability were selected for the cues as they were the key factors affecting anchovy growth. The optimal temperature for anchovy was set to 27°C, the optimal temperature for consumption (Luo and Brandt 1993). To ensure that anchovy tried to maximize consumption, the optimum value for prey availability was set to 80% of CON_{MAX}. Dissolved oxygen concentration was selected to control vertical movement, as a major potential source of mortality for anchovy was exposure to hypoxia when they entered the bottom layers. To avoid mortality due to hypoxia, while at the same time preventing anchovy from aggregating at the surface of the water column, I set the optimum DO concentration to 5.0 mg $liter^{-1}$.

Deviates from optimal were computed separately for each cue, and the smaller of the water temperature and prey availability was used to determine the net velocities for x and y movement, while the product of water temperature and DO was used for vertical movement. Vertical movement was restricted to a maximum change of 3 m per vertical movement step in order to simplify the tracking of anchovy movement. This was done as anchovy can potentially swim many times the depth of the water column between the one-hour movement time steps.

Once the distances that an anchovy moved along x, y and z had been determined, a two part process was used to update the anchovy's position. In the first part of the process, the anchovy's horizontal position was updated. The anchovy's new x and y values were determined by adding the distances moved along x and y to the anchovy's previous position. A point-in-polygon subroutine (Geometry – Geometric Calculations 2007) was used to determine if the anchovy's new position was outside the cell in which it started. If the anchovy finished in the

Table 3.3 Description and values of parameters for the kinesis movement model.

Symbol	Description	Value
Common parameters		
H_1	Height parameter for the inertia component of movement	0.75
H_1	Height parameter for the random component of movement	0.9
Φ	maximum swimming velocity	1 body length s^{-1}
Horizontal movement		
Q_{M0}, temperature	optimum temperature	27°C
σ, temperature	standard deviation for temperature	2°C
Q_{M0}, prey availability	prey availability	0.8 C_{MAX}
σ, prey availability	standard deviation for prey availability	0.05
Vertical movement		
Q_{M0}, temperature	optimum temperature	27°C
σ, temperature	standard deviation for temperature	4°C
Q_{M0}, dissolved oxygen	optimum dissolved oxygen	5.0 mg $liter^{-1}$
σ, dissolved oxygen	standard deviation for dissolved oxygen	1.5 mg $liter^{-1}$

same cell that it started in, the anchovy's horizontal movement was complete for the current movement step. If the anchovy was no longer in the cell that it started in, the algorithm checked to see if the anchovy was in one of the cells that were immediately adjacent to the starting cell. If the anchovy was not in one of the immediately adjacent cells, the algorithm checked to see if the anchovy was in any of the other cells in the same vertical layer. If the new horizontal position was not in any of the cells in the current layer, then it was known that the anchovy had moved off of the model grid. Vertical position had not yet been evaluated; therefore, if the individual was not in the same vertical layer as when it started the time step, the individual had to be off the model grid. The point at which the anchovy crossed onto land was determined, and the distance moved from the grid edge to the anchovy's stopping point was reflected back onto the model grid and the anchovy's final horizontal position was recalculated. The process was repeated until the anchovy's horizontal position finished on a cell within the model grid.

The second part of the process was to update the individual's vertical position. Updating vertical position was simpler because the z value was constrained to the interval between the surface and bottom of the water column and all cells in the vertical dimension were the same shape and thickness. If the z value was above the surface or below the bottom, the z value was reset to place the anchovy just below the surface or just above the bottom. Once the anchovy's final position was determined, its velocities along the x- and y-axes for the current movement step were recalculated using the anchovy's starting and final positions. The recalculated velocities were used to set V_{t-1} for the next movement step.

3.2.2.5 Numerical Considerations

As the total number of bay anchovy in Chesapeake Bay is on the order of 10^9 to 10^{14} (Jung and Houde 2004A), I used super-individuals (Scheffer et al. 1995) to simulate the bay

anchovy population. By using super-individuals, it was possible to simulate extremely large numbers of fish at the population-level with a reasonable number of model individuals. When using super-individuals, each model individual being simulated was given an initial worth, which was the number of identical population individuals that the model individual represented. All simulations introduced ~100,000 model individuals per year. The initial worth of each model individual within a recruitment scenario was set to a constant value that was determined as the total number of recruits (low recruitment = $\sim 3.6 \cdot 10^{11}$ individuals; median recruitment = $\sim 1.2 \cdot 10^{12}$ individuals; high recruitment = $\sim 1.58 \cdot 10^{12}$ individuals) divided by the number of model individuals. The initial worth of each model individual was $3.6 \cdot 10^{6}$ individuals for the low recruitment scenario, $1.2 \cdot 10^{7}$ individuals for the median recruitment scenario, and $1.584 \cdot 10^{7}$ individuals for the high recruitment scenario.

To determine the amount of prey consumed, the prey consumed by a model individual was multiplied by that individual's worth. Mortality of anchovy was simulated by decrementing the individual's worth by the total mortality rate (M, d^{-1}):

$$Worth_{i,t+1} = Worth_{i,t} e^{-M(\Delta t)} \quad (3.11)$$

where Δt = the length of the time step (d). If a model individual reached old age (1095 days) or its worth dropped below 0.001, then it was removed from the simulation. Model predictions of densities, lengths, weights, and other outputs were adjusted by the worth of the individual model anchovy.

3.2.3 Modifications to the Eutrophication Model to Accommodate Bay Anchovy

The eutrophication model was calibrated previously without anchovy predation on zooplankton. Because I added explicit mortality by anchovy, I adjusted the summer algal biomass mortality rate and the two zooplankton mortality rates to allow for consumption by

anchovy and yet still result in reasonable predictions of zooplankton densities. The overall equation governing zooplankton biomass dynamics in the eutrophication model was (Cerco 2004):

$$\frac{dZ}{dt} = \left[Gz - BMz - Mz\right] \cdot Z - PRz \quad (3.12)$$

where Z = zooplankton biomass (g C m^{-3}); Gz = growth rate of zooplankton group z (d^{-1}); BMz = basal metabolic rate of zooplankton group z (d^{-1}); Mz = mortality (d^{-1}); and PRz = predation on zooplankton group z (g C m^{-3} d^{-1}). The mortality term on zooplankton without explicit mortality due to anchovy was:

$$PRz = BPRz \cdot Z^2 \cdot f(T) \quad (3.13)$$

where BPRz = the baseline predation rate on zooplankton (d^{-1}); and f(temp) = a functional response to temperature. Based upon calibration results, the predation term was modified by multiplying the original equation by 0.3, thereby reducing the original predation mortality rate on zooplankton, and adding in the summed consumption rate of the modeled anchovy. To provide sufficient prey for bay anchovy to survive and grow, I also reduced the mortality rate of the summer algal group from 1.00 d^{-1} to 0.15 d^{-1}. Reducing the mortality rate of the summer algal group increased algal biomass, which lead to an increase in zooplankton biomass. Increasing zooplankton biomass increased the amount of zooplankton prey available for anchovy to consume. The effects of these changes were assessed as a part of the calibration of the anchovy model.

3.2.4 Simulations

Three sets of model simulations were performed: calibration and baseline, effects of increased and decreased nutrient loadings, and effects of kinesis versus random movement (Table 3.4). Single model simulations were reported, as runs that used different random number

seeds generated very similar model predictions of growth, densities, and spatial distributions. The calibration simulations were based on short 5-year runs, while the baseline, nutrient loadings, and movement comparison simulations involved a spin-up period for the eutrophication and anchovy models, followed by 10 years of actual anchovy simulation. All simulations used various combinations of wet, normal, and dry water years from the hydrodynamics, low, median, and high annual anchovy recruitments that were repeated every year, and reduced, baseline or increased nutrient loadings to the eutrophication model (Table 3.4).

3.2.4.1 Water Years

I had eutrophication model input files and hydrodynamics output for the years 1984, 1985, and 1986. The USGS (http://md.water.usgs.gov/monthly/bay.html) has developed a water year classification method for Chesapeake Bay. Water years were classified by comparing a year's mean stream inflow to a 69 year record of mean inflow to Chesapeake Bay (1937 to present). Water years with stream inflows in the middle 50 percent were classified as normal water years. Water years with stream inflows in the highest 25 percent were classified as wet water years, while years with stream inflows in the lowest 25 percent were classified as dry water years. Based upon the USGS classification system, the year 1984 was a dry water year, 1985 was a wet year, and 1986 was a normal year. Calibration used a sequence of 1986 conditions (normal years). For all other simulations, I strung together 1984 (dry), 1985 (wet), and 1986 (normal) water years in order to match the sequence of wet, normal, and dry years observed between 1984 and 1993.

3.2.4.2 Bay Anchovy Recruitment

The total annual recruitment used for low and high recruitment levels in model simulations was based on estimates provided by Jung and Houde (2004A). As a part of the

Table 3.4 Summary of model runs, including those used as spin-up simulations that provided initial starting values for the baseline and nutrient loadings simulations.

Run	Simulation	Nutrient load	Recruitment level	Water years	Details
Calibration, baseline, and effects of water year and recruitment level					
1	Initial calibration runs	Baseline	Median	5 normal years	Multiple runs ran to calibrate zooplankton and algal mortality rates, and determine K values for anchovy growth
2	Pre-run – baseline	Baseline	No anchovy	10 normal years	10 year pre-run ran to allow changes in nutrient loads to reach a new equilibrium level
3	Baseline – low	Baseline	Low	3 normal years + 1984-1993	Initial conditions were set to the output from run 2. Used to compare micro- and meso-zooplankton densities to densities from the originally-calibrated (without anchovy) eutrophication model runs. Anchovy lengths, abundance, and biomass were compared to field data. Used to assess the effects of water year and recruitment level.
4	Baseline – high	Baseline	High	3 normal years + 1984-1993	Initial conditions were set to the output from run 2. Used to compare micro- and meso-zooplankton densities to densities from originally-calibrated (without anchovy) eutrophication model runs. Anchovy lengths, abundance and biomass are compared to field data. Used to assess the effects of water year and recruitment level.

Table 3.4 continued

Effects of increased and decreased nutrient loadings					
5	Pre-run – decreased	Decreased	No anchovy	10 normal years	10 year pre-run ran to allow changed nutrient loads to reach a new equilibrium level
6	Pre-run - increased	Increased	No anchovy	10 normal years	10 year pre-run ran to allow changed nutrient loads to reach a new equilibrium level
7	Decreased loads – low	Decreased	low	3 normal years + 1984-1993	Initial conditions were set to the output from run 5. Used to assess the effects of water year and recruitment level
8	Increased loads – low	Increased	low	3 normal years + 1984-1993	Initial conditions were set to the output from run 6. Used to assess the effects of water year and recruitment level
9	Decreased loads – high	Decreased	high	3 normal years + 1984-1993	Initial conditions were set to the output from run 5 Used to assess the effects of water year and recruitment level.
10	Increased – high	Increased	high	3 normal years + 1984-1993	Initial conditions were set to the output from run 6. Used to assess the effects of water year and recruitment level
Effects of kinesis versus random movement					
11	Random movement – low	baseline	low	3 normal years + 1984-1993	Initial conditions were set to the output from run 2; vertical distribution; biomass; compared to run 2
12	Random movement – high	baseline	high	3 normal years + 1984-1993	Initial conditions were set to the output from run 2; vertical distribution; biomass; compared to run 3

Trophic Interactions in Estuarine Systems (TIES) project, Jung and Houde estimated the total number of eggs produced each year by bay anchovy between 1995 and 2000. I used these egg production values, and age dependent growth and size dependent mortality rates reported by Jung and Houde from the same study, and estimated the number of 23-mm long bay anchovy produced each year (Table 3.5). Low recruitment ($3.6 \cdot 10^{11}$ individuals) was set to the year with the lowest of the five annual estimates (Table 3.5, 1996), and high recruitment ($1.58 \cdot 10^{12}$ individuals) was set to the year with the highest of the five annual estimates (Table 3.5, 2000). My low recruitment condition is probably truly low as data from the Maryland Department of Natural Resources Bay-wide index (Durrell and Weedon 2005) indicated that age-0 bay anchovy CPUE (catch per unit seine haul) has declined since 1959. Additionally, there is some evidence that suggests anchovy may be experiencing excessive predation due to a recent increase in striped bass abundance (Griffin and Margraf 2003, Ludsin et al. submitted). My high recruitment condition, while high for the 1995 to 2000 period, may be closer to average recruitment relative to the long-term record for anchovy.

3.2.4.3 Nutrient Loading Scenarios

Three nutrient loadings were used: baseline, decreased, and increased. The baseline nutrient loading scenario used the nutrient loads observed during the years 1984, 1985, and 1986. The decreased scenario reduced nutrient loads by 50%. A 50% reduction in nutrient loadings is roughly equivalent to that required under the Chesapeake 2000 Agreement, which requires reductions of 48% and 53% (based on 1985 levels) for total nitrogen and phosphorus inputs (Kemp et al. 2005; Chesapeake Bay Program 2007). The increased scenario increased baseline nutrient loads by 50%. The increased loading scenario provided a contrasting scenario to the

Table 3.5 Estimated number of eggs and October recruits from Jung and Houde (2004A) and the calculated number of 23-mm juvenile bay anchovy. The highest, median, and lowest values of 23-mm juveniles were used to start each year-class in the individual-based model.

Year	Total egg production ($\times 10^{14}$)	Calculated number of 23 mm juveniles ($\times 10^{11}$)	Number of recruits in October ($\times 10^{9}$)
1995	0.6	4.4	44.5
1996	1.5	3.6	29.2
1997	3.4	11.9	97.0
1998	1.0	11.5	273.8
1999	1.8	12.0	99.4
2000	2.1	15.8	182.7

decreased loading scenario. The increased nutrient loading scenario may reflect future conditions if no action is taken, but no such land-use and loadings projections have been made.

3.2.4.4 Initial Conditions from Spin-Up

The full-blown simulations (i.e., all except calibration) used spin-up periods to allow for changes in nutrients loadings to reach their full effect and to reduce the effects of initial anchovy conditions. Cerco (1995) reported that it took approximately 10-years for the eutrophication model to show a near-complete response to nutrient load reductions, mostly due to the relatively slow rate of processes in the sediments. Before each simulation was started, the eutrophication model was run for 10 years using normal water years under the same nutrient loading scenario (i.e. baseline, increased, or reduced) as the planned simulation (Table 3.4, Run 2). The pre-run did not include bay anchovy. The final conditions from the 10-year pre-run were then used to set the initial conditions for the eutrophication model in the actual simulations with anchovy.

To initialize the bay anchovy population, each 10-year simulation was preceded by a three-year string of normal water years. During the three year start-up period, anchovy were added to the simulation as a part of the weekly cohorts, using the same level of recruitment as the planned simulation. By the end of the third start-up year, a complete three age-class population of anchovy was present in the model.

3.2.4.5 Calibration Simulations

The water quality model was calibrated using 5-year runs with normal water years repeated every year (Table 3.4, Run 1). Anchovy recruitment each year was set to the median level of recruitment expected for 23 mm long juvenile anchovy (Table 3.5) based upon field data from Jung and Houde (2004A). I adjusted the K values, and the reductions in zooplankton and algal mortality terms, in repeated model simulations until: (1) realistically-sized anchovy were

generated (45 mm in October; maximum size of 110 mm after 3 years, Houde and Zastrow 1991), and (2) zooplankton densities were roughly similar to the values generated from the originally calibrated (without anchovy and without adjusted mortality rates) eutrophication model.

3.2.4.6 Baseline Simulations

After calibration I performed two baseline simulations (Table 3.4, Runs 3 and 4) to confirm the realism of the calibration and to interpret the effects of water year and anchovy recruitment level on predicted dynamics. I first compared the predicted daily densities of micro- and meso-zooplankton over the ten year baseline simulations at a key mid-Bay location (station CB5.2) with those from the previously calibrated eutrophication model. Station CB5.2 corresponded to the location of a long-term water quality monitoring station (Chesapeake Bay Program 2007), and was an area of focus during the calibration of the eutrophication model (Cerco and Cole 1993). I then compared predicted mean lengths of YOY anchovy in October, growth rate of YOY from recruitment to October, and October and May abundances and biomasses, to reported values using the last three years of the two baseline simulations. The last three years were used as they included a wet, normal, and dry year, and they were representative of the dynamics during the different water year types. To further compare predicted growth rates to observed data, I plotted the mean lengths of anchovy from early, middle, and late recruited cohorts by water year and recruitment level.

To compare the effect of water year and recruitment level on predicted dynamics, I used the same growth by cohort, biomasses, and abundances output from the comparison to data, plus spatial maps of model outputs averaged for the water column during July. Spatial maps of salinity, temperature, bottom layer DO, and meso-zooplankton densities from the high

recruitment baseline simulation (Table 3.4, Run 4) were compared for the wet, normal, and dry water years. Only the high recruitment baseline results were compared because anchovy did not greatly affect these output variables. Spatial maps of anchovy densities for the high and low recruitment simulations were compared among the wet, normal, and dry years. Finally, the effect of wet, normal, and dry years were also examined by comparing the mean latitude of age-1 and older anchovy for April through August among water years and recruitment levels, and the mean latitude of age-1 and older anchovy in July by length class versus reported values for 2001-2005 from the CHESFIMS Project (Miller *personal communication*[1]). The five years of field data were assigned to wet, normal, and dry water years based on the USGS classification method described previously (2001 and 2002 – dry; 2005 – normal; 2003 and 2004 – wet).

3.2.4.7 Nutrient Loadings Simulations

The 10-year baseline simulations (with low and high recruitment) were repeated but with reduced nutrient loadings (Table 3.4, Runs 7 and 9) and increased nutrient loadings (Table 3.4, Runs 8 and 10). To summarize the effects of nutrients loadings on hypoxia, the total volume of hypoxic water was plotted for the ten years plus the three spin-up years. The same spatial plots as reported for the baseline simulations were repeated for the decreased and increased nutrient loadings. Additionally, the anchovy lengths by cohort plot was repeated using the likely worst case scenario for anchovy growth; decreased nutrient loadings and high recruitment. Young-of-year anchovy lengths in October, survival from recruitment to late October, and YOY biomass in October were summarized for the wet, normal, and dry years under low and high recruitment and for the three nutrient loadings scenarios. Finally, to help interpret the effects of nutrient loadings on survival, the percent of all anchovy dying from hypoxia, starvation, old age, and general

[1] Miller, T. J. Chesapeake Bay Fishery-Independent Multispecies Survey. Sponsored by the NOAA-Chesapeake Bay Office. http://hjort.cbl.umces.edu/cfdata.htrml. Accessed on 7/5/07

mortality were computed by nutrient loading scenario using all deaths that occurred over the entire simulations.

3.2.4.8 Kinesis Versus Random Movement Simulations

The third set of simulations compared random movement (Table 3.4, Runs 11 and 12) with kinesis movement (Table 3.4, Runs 3 and 4) under baseline nutrient loading. Random movement in the horizontal direction (x and y) was simulated by randomly generating an angle between 0 and 360°, and then determining the distance moved as the product of the maximum distance swum times a random number between 0 and 1. Maximum distance swum was computed for each individual on each time step as the product of the anchovy's length, swimming speed (1 body length s^{-1}), and time step. Each vertical movement time step, a random direction was selected (up or down) and the distance moved was randomly generated from 0 to 3 m. The effect of kinesis versus random movement was assessed using a vertical snapshot of anchovy distributions in two cross-bay transects, and a time series plots of total anchovy biomass.

3.3 Results

3.3.1 Assessment of Calibration Using Baseline Simulations

Micro- and meso-zooplankton densities in baseline simulations that included anchovy (Table 3.4, Runs 3 and 4) were always within a factor of two to three of predicted densities without anchovy. Micro-zooplankton was underestimated under both high and low recruitment (blue and red lines in Figures 3.5A,B) compared to the simulation done without anchovy (black line). Micro-zooplankton densities for simulations with anchovy (red and blue lines) were close to the densities observed in the water quality model simulation without anchovy (black line) for the spring bloom. During the summer-fall bloom, micro-zooplankton densities for simulations

Figure 3.5 Micro- and meso-zooplankton densities at sampling station CB5.2, a station located in the mid-bay region of Chesapeake Bay. Micro- and meso-zooplankton densities are shown for baseline nutrient load simulations done with and without anchovy for the 3 year pre-run period of normal water years followed by the 1984 to 1993 sequence of water years. Simulations with anchovy were done with both low and high recruitment. Densities are shown for the 3 year spin-up period of normal water years followed by the 1984 to 1993 water years. Field measurements of zooplankton densities are provided for comparison. (A) Micro-zooplankton densities in the bottom layer at station CB5.2 (B) Micro-zooplankton densities in the top layer at station CB5.2 (C) Meso-zooplankton densities at station CB5.2. The symbol legend for all three panels is shown in Panel A.

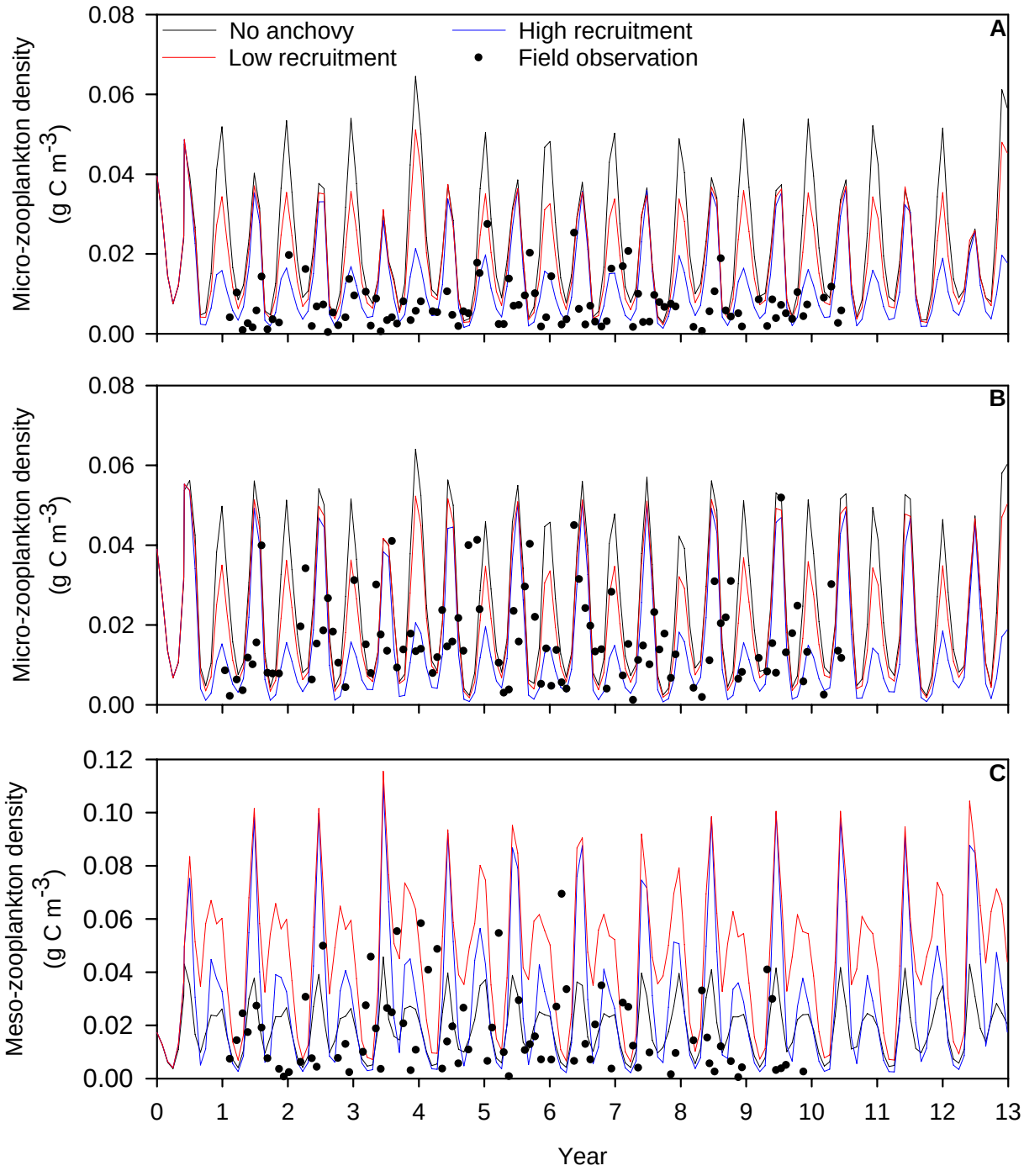
No anchovy
Low recruitment
High recruitment
Field observation
A
B
C
Micro-zooplankton density
(g C m-3)
Meso-zooplankton density
(g C m-3)
0.00
0.02
0.04
0.06
0.08
0.10
0.12
0
1
2
3
4
5
6
7
8
9
10
11
12
13
Year

with anchovy were 2-3-fold lower than the densities predicted by simulations without anchovy. Meso-zooplankton densities for simulations with anchovy were generally 2-3-fold higher than the densities predicted by the eutrophication model without anchovy under both low and high recruitment (red and blue lines versus black line in Figure 3.5C). Meso-zooplankton had higher densities when anchovy were included in simulations because their non-specific mortality rate was decreased by 70%. Micro-zooplankton densities were lower when anchovy were included in simulations, as micro-zooplankton experienced increased predation from meso-zooplankton due to their higher densities when anchovy were included. Nitrate and phosphate concentrations were almost identical between simulations without and with anchovy, while chlorophyll-a concentrations were generally within 50 to 80% of each other (results not shown).

Micro- and meso- zooplankton densities were generally higher when anchovy recruitment was low than when recruitment was high. The peak micro-zooplankton densities for low and high recruitment consistently exceeded the field data; this was also true for the originally calibrated eutrophication model without anchovy. Predicted meso-zooplankton densities for low and high recruitment were within the range of the field data for most of each year. The exception was during the spring bloom when meso-zooplankton populations spiked.

Model predictions of anchovy lengths and growth rates for YOY individuals that survived to the end of October for baseline simulations were generally comparable with the October field observations of Jung and Houde (2004A, their Table 2). The mean lengths of anchovy when recruitment was low (~43 mm, Table 3.6) were slightly lower than the range of mean lengths (46.7 – 55.6 mm) reported by Jung and Houde (2004A). Lengths under high recruitment (~31 mm) were 14 to 16 mm shorter than the shortest mean lengths observed. The mean lengths of early, peak, and late cohorts under both low and high recruitment (Figure 3.6)

Table 3.6 Predicted mean length in October, growth rate of survivors, abundance, and biomass of anchovy in dry, normal, and wet years of the baseline simulation under low and high anchovy recruitment compared to observed values from Jung and Houde (2004A) for the field data years with the lowest, median, and highest number of 23-mm long anchovy recruits (Table 3.5). N/A denotes data not available.

Year type	Mean length (mm)	Growth rate (mm d^{-1})	Abundance ($\times 10^9$)	Biomass (metric tonnes)
		Low Recruitment		
Dry	41.7	0.35	52.6	36,294
Normal	42.9	0.36	56.6	42,487
Wet	43.3	0.37	54.2	40,572
		High Recruitment		
Dry	30.4	0.17	184.9	44,033
Normal	31.3	0.19	201.9	52,651
Wet	32.8	0.22	203.9	62,781
		Jung and Houde		
Low	49.1	N/A	29.2	25,000
Median	48.8	N/A	185.4	138,500
High	49.8	N/A	182.7	150,000

Table 3.7 Predicted May abundances and biomass of anchovy in dry, normal, and wet years of the baseline simulations with low and high anchovy recruitment compared to observed values reported by Jung and Houde (2004A) for the field data years with the lowest, median, and highest number of 23-mm long anchovy recruits (Table 3.5).

Year type	Low Recruitment	
	Abundance ($\times 10^9$)	Biomass (metric tonnes)
Dry	0.876	9,183
Normal	0.833	8,606
Wet	0.783	8,411
	High Recruitment	
Dry	2.27	7,407
Normal	2.18	6,941
Wet	2.07	7,722
	Jung and Houde	
Low	4.9	3,000
Median	7.7	10,000
High	6.2	20,000

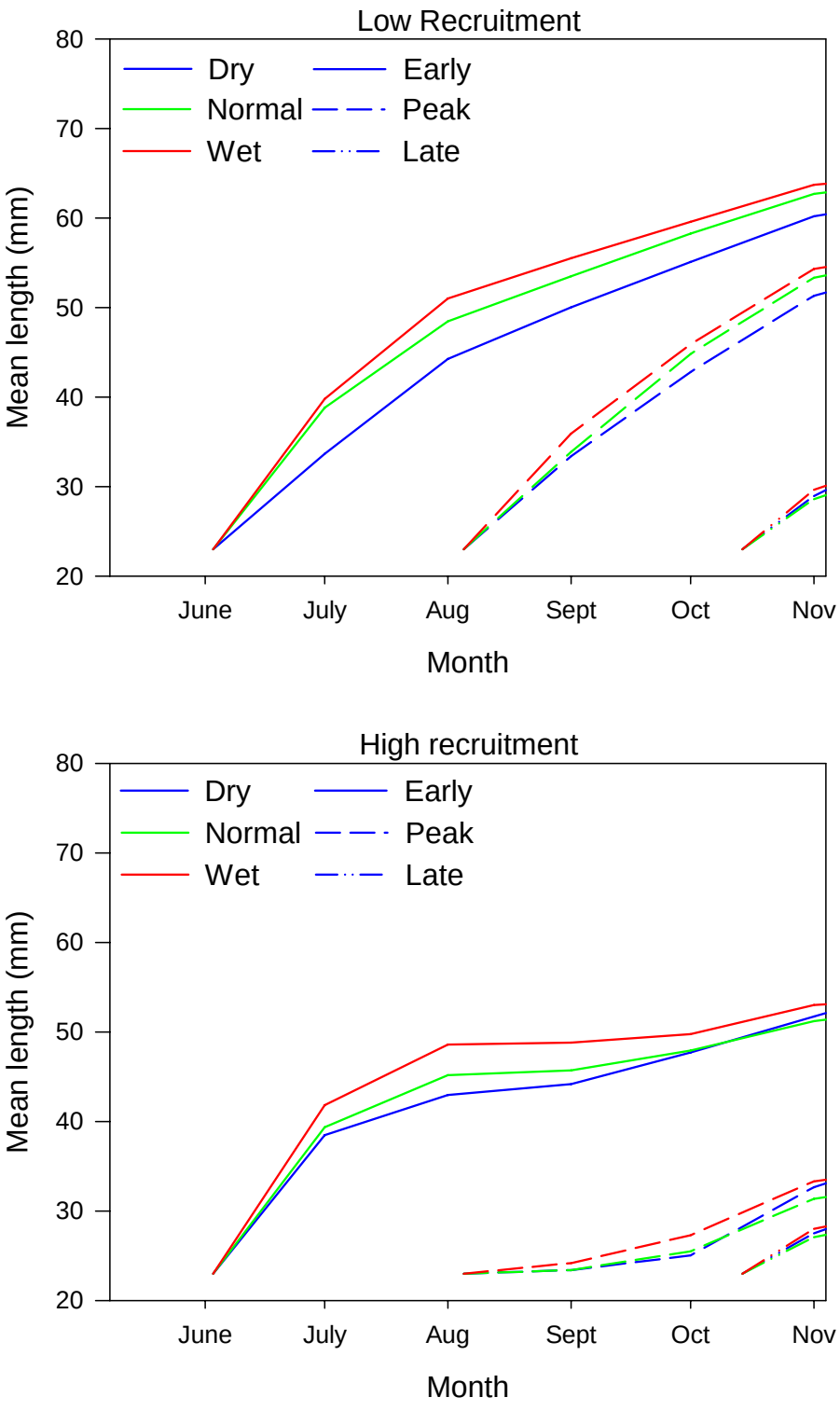

Figure 3.6 Mean growth trajectories of anchovy under low and high recruitment. Trajectories are shown from recruitment in early, peak and late cohorts to late October during dry, normal and wet water years with baseline nutrient load.

were within the range of mean lengths for individual cohorts (24.0 – 69.0 mm) reported by Jung and Houde (2004A). Predicted YOY anchovy growth rates for both the low and high recruitment (~0.36 and ~0.2 mm d^{-1}, Table 3.6) were similar to the juvenile anchovy growth rates of 0.20 – 0.33 mm d^{-1} reported for mid-Chesapeake Bay (Morin and Houde 1989, Newberger 1989).

Predicted abundances of anchovy in late October were within the range of abundances observed by Jung and Houde (2004A). Predicted anchovy abundances under low recruitment (52.6 to 56.6 x 10^9, Table 3.6) were twice the estimated October abundance of 29.2×10^9 for1996, the year of field data with the lowest juvenile recruitment (Table 3.5). However, the abundance was close to the 47.7×10^9 observed during 1995, the year with the second lowest juvenile recruitment (0.8×10^{11} more recruits than 1996). Predicted abundances under the high recruitment year (184.9 to 203.9 $\times10^9$, Table 3.6) were also close to the October abundance of 182.7×10^9 estimated for 2000, the year of field data with highest number of 23 mm juveniles (Table 3.5).

October biomass of bay anchovy was under-predicted for the high recruitment scenario, and May abundance was under-predicted for both low and high recruitment scenarios. Anchovy biomasses predicted for low recruitment (36,294 to 42,487 metric tonnes, Table 3.6) were similar to the fall peak in biomasses observed during years with low estimated anchovy biomass (~25,000 to 50,000 metric tonnes; Jung and Houde 2004A, their Figure 4A). However, predicted biomasses for the high recruitment scenario (44,033 to 62,781 metric tonnes, Table 3.6) were less than half of the field-based estimates (~100,000 to 150,000 metric tonnes) during years with high anchovy biomass. Predicted May biomasses under low and high recruitment (Table 3.7) were similar to Jung and Houde's biomasses. The predicted range of biomasses was 6,491 to 9,183 metric tonnes versus Jung and Houde's estimates of ~3,000 to 12,000, with an extreme field-estimated value of 20,000 metric tonnes. However, predicted abundances in May (Table

3.7) were underestimated in the baseline simulations compared to field estimates (0.783×10^9 to 2.27×10^9 versus 2.1×10^9 to 11.8×10^9).

3.3.2 Effects of Water Year and Recruitment Level in Baseline Simulations

Examination of the effects of water years and recruitment level in baseline simulations focused on the last three years of each simulation as they included a wet, normal, and dry year, and they were representative of the dynamics during the different water year types. Water-column-averaged salinity, water temperature, and bottom layer DO concentrations for a snapshot in July varied across the three water years. Bay-wide salinity was highest during the dry year and lowest during the wet year (Figure 3.7). Water temperatures along the main channel were generally cooler during the wet year than during the dry and normal years (Figure 3.8); temperatures were warmer in the wet year in the northernmost area and the eastern edge of the Bay. Temperatures in the dry year were generally cooler along the main channel of the northern bay than in the normal year, but warmer in other areas. Hypoxic conditions were present in the bottom-layer for all three water years (middle row in Figure 3.9). The extent of hypoxic conditions was similar for the dry and normal years, but was more extensive for the wet year. During the wet year, the extent of hypoxia along the main channel extended further southward than during the dry and normal water years. Additionally, areas of hypoxic conditions in the bottom-layer were more prevalent along the eastern side of the Bay.

The spatial pattern of July meso-zooplankton densities was similar across the three water years, while densities increased from dry to normal to wet years (middle row of Figure 3.10). Meso-zooplankton had the highest densities along the main channel of the Bay in the upper and mid-bay regions, and along the main channels of the Patuxent and Potomac Rivers. Across water years, zooplankton densities were lowest during the dry year and highest during the wet year.

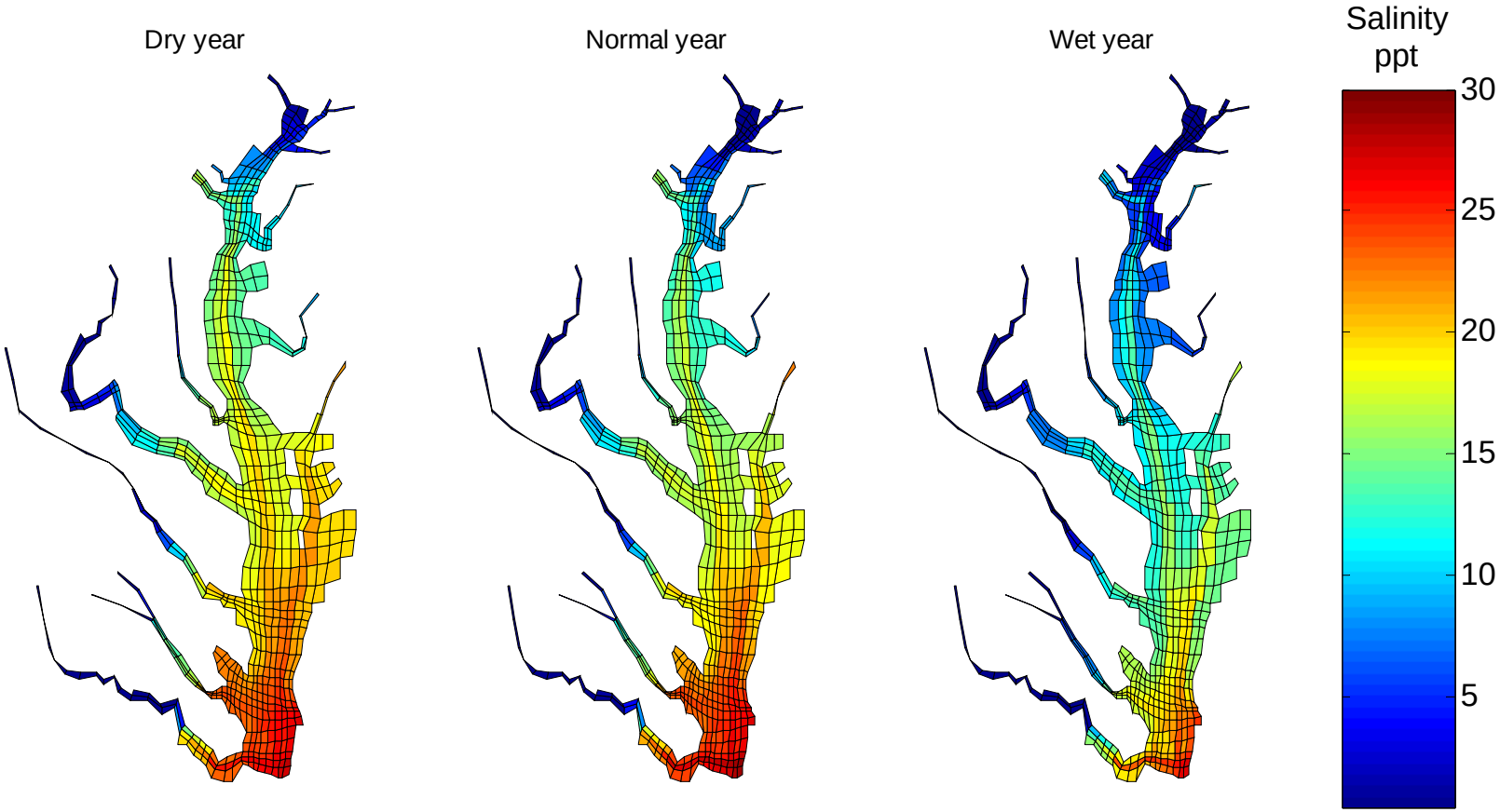

Figure 3.7 Water-column-averaged July salinity (ppt) for dry, normal, and wet years for all nutrient loads.

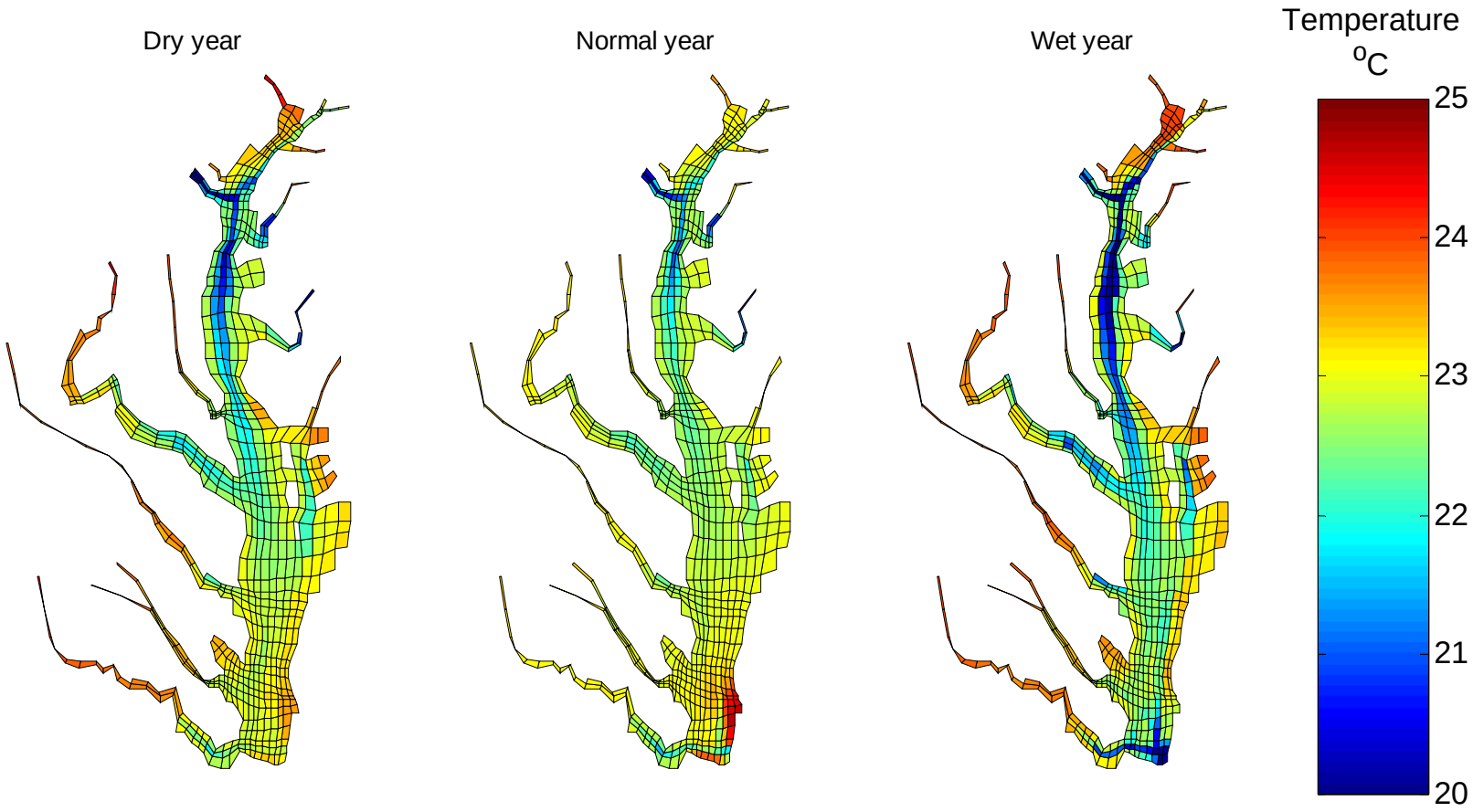

Figure 3.8 Water-column-averaged July temperature (°C) for dry, normal, and wet years for all nutrient loads.

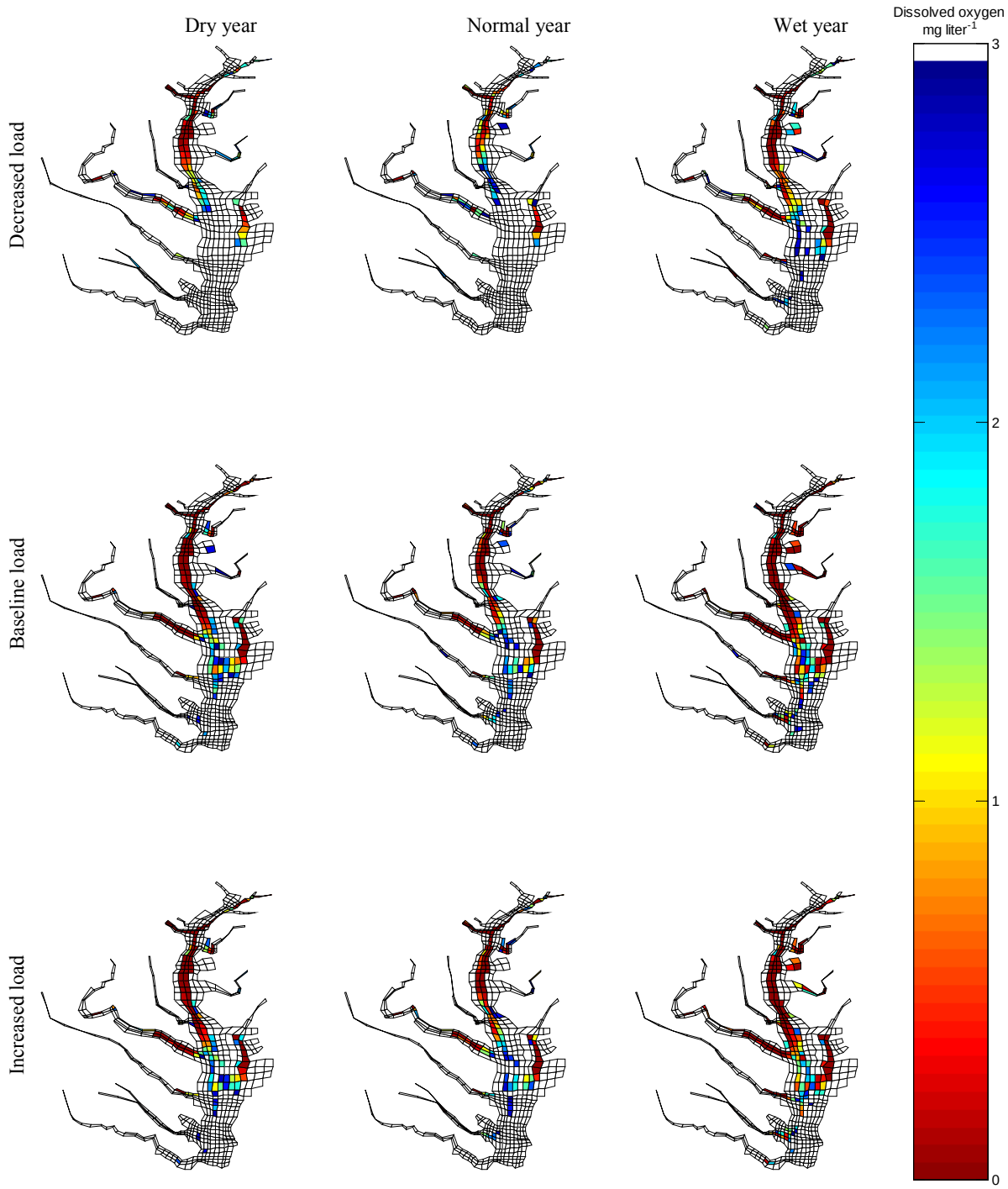

Figure 3.9 July bottom-layer dissolved oxygen concentrations for dry, normal and wet years under decreased, baseline and increase nutrient loads. DO concentrations are not shown for cells with concentrations greater than 3 mg liter^{-1}.

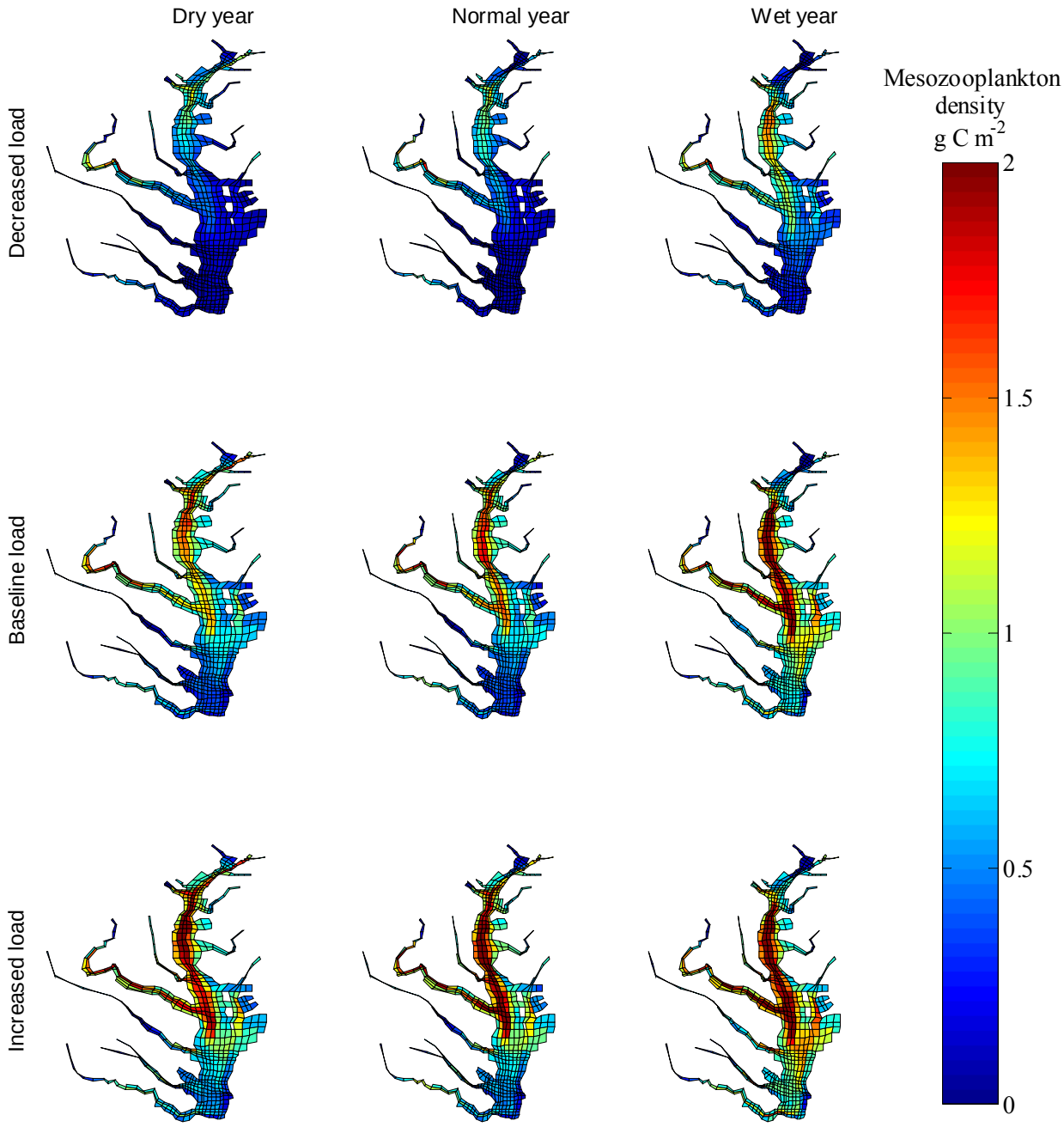

Figure 3.10 Water-column-averaged July meso-zooplankton densities (g C m^{-3}) for dry, normal and wet years under decreased, baseline and increased nutrient loads and high anchovy recruitment.

The spatial extent of high meso-zooplankton densities (>1 g C m^{-3}) was similar between the dry and normal years, while during wet years, high zooplankton densities were predicted throughout much of the Bay.

Recruitment level affected anchovy lengths more than water years (Figure 3.6). For a given level of recruitment, anchovy from the same cohort, but in different water years, had divergent growth trajectories over the summer, but grew to approximately the same length by October. Anchovy from cohorts under low recruitment generally grew longer than anchovy under high recruitment, especially during the summer period when the mean length trajectories of the early and peak cohorts under high recruitment were almost flat.

Recruitment level had a larger effect on October anchovy abundances and biomass than did water years. Predicted October abundances were almost 4-fold higher under high recruitment compared to under low recruitment (184.9×10^9 to 203.9×10^9 versus 52.6×10^9 to 56.6×10^9, Table 3.6), while October biomass was only 25 to 50% higher (44,033 to 62,781 metric tonnes versus 36,204 to 42,487 metric tonnes). Water year had little effect on October abundances and biomasses under low recruitment (52.6×10^9 to 56.6×10^9 and 36,294 to 42,487 metric tonnes), and a larger (but still small) effect under high recruitment (184.9×10^9 to 203.9×10^9 and 44,033 to 62,781 metric tonnes).

The diminished response in October biomass relative to abundance was due to density-dependent summertime growth, which was further amplified in the following May abundances and biomasses. Mean lengths and growth rates from recruitment to October were lower under high recruitment compared to low recruitment (Figure 3.6, Table 3.6). Predicted May abundances were about 3-fold higher under high recruitment versus low recruitment (2.07×10^9 to 2.27×10^9 versus 0.783×10^9 to 0.833×10^9, Table 3.7), while the smaller-sized individuals resulted

in predicted biomass actually being lower under the high recruitment (6,941 to 7,722 metric tonnes under high recruitment versus 8,606 to 9,183 metric tonnes under low recruitment).

Water year and recruitment level had roughly equal effects on anchovy spatial patterns. As would be expected, anchovy densities were generally higher under high recruitment than under low recruitment (note scale difference between Figures 3.11 and 3.12). For all three water years under both high and low recruitment, anchovy were primarily located along the main channel of the Bay, with the highest densities being found in the lower Bay (middle rows of Figures 3.11 and 3.12). During wet years, anchovy appeared to be more heavily concentrated lower down in the Bay than during dry and normal years.

The mean latitude of age-1 and older anchovy was influenced more by water year than by recruitment level (Figure 3.13). Mean latitudes in April were similar for all water years and recruitment levels, although the three northernmost values were for the high recruitment scenario and the three southernmost values were for the low recruitment scenario. The difference between the April latitude for the three high recruitment simulations and the three low recruitment simulations was only about a tenth of a degree (~11 km). The change in mean latitude from April to August (southward movement) was about the same for the high versus low recruitment simulations, but was much larger for the wet versus dry and normal year simulations. During dry and normal water years the southward shift between April and August was ~0.15 degrees, while the averaged southward shift during the wet year was ~0.30 degrees.

Model predictions of the mean latitude of age-1 and older anchovy by length category were generally comparable to field data from the CHESFIMS project (Figure 3.14). For all three water years, the predicted mean latitude of anchovy overlapped with the observed latitudes for the intermediates length classes. The predicted distributions of anchovy in the smallest size class

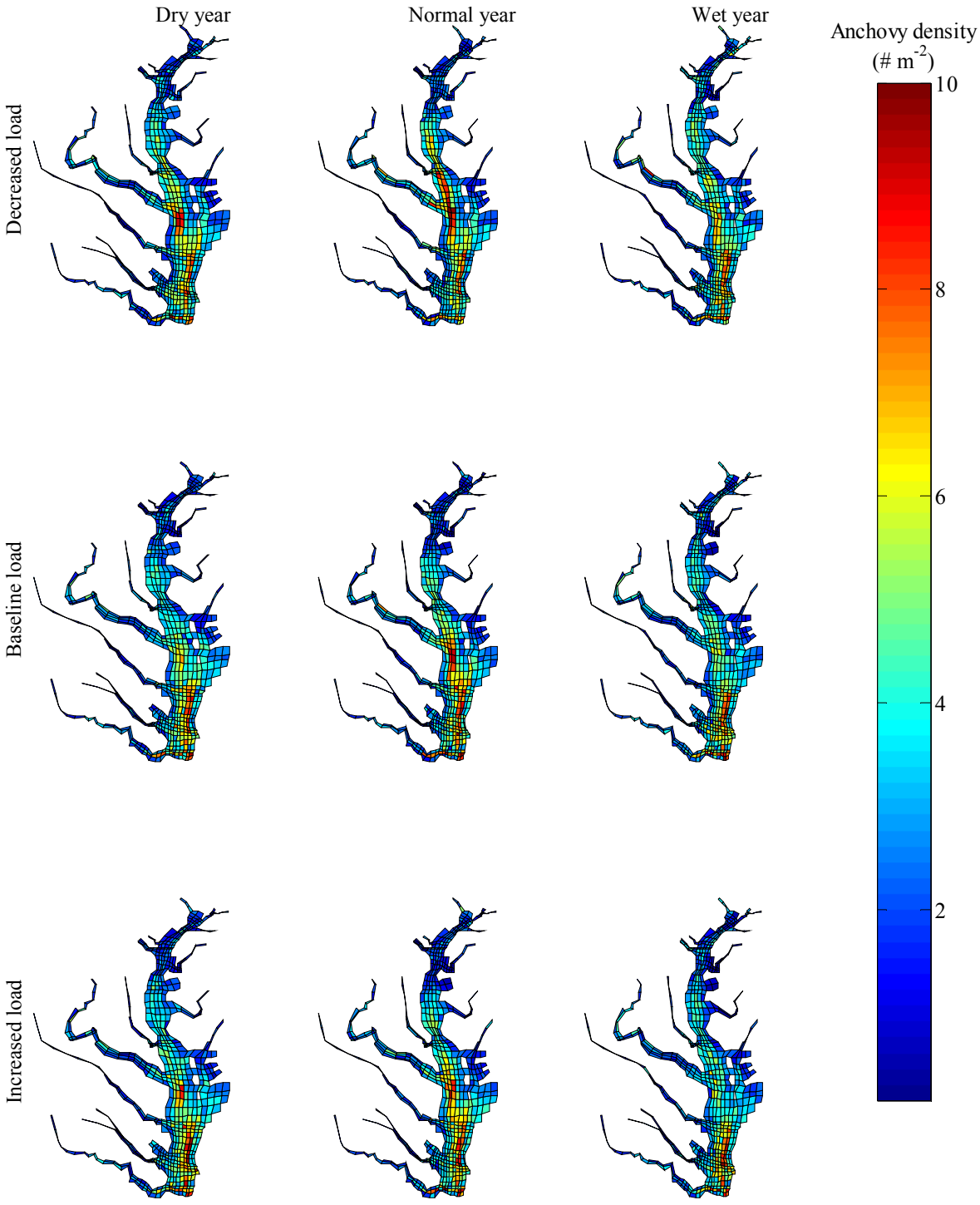

Figure 3.11 July depth-integrated (# m^{-2}) anchovy densities for dry, normal and wet years under decreased, baseline and increased nutrient loads and low anchovy recruitment.

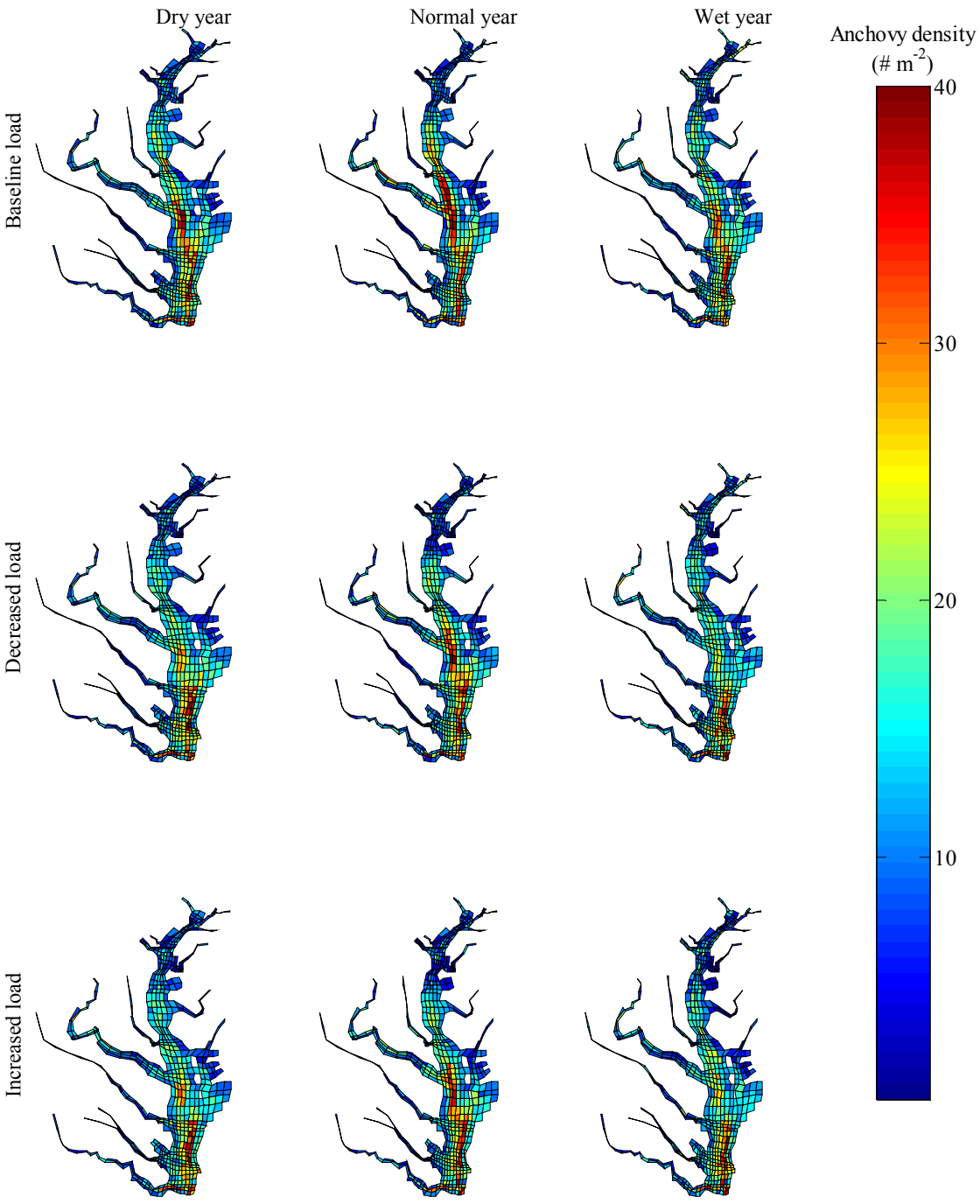

Figure 3.12 July depth-integrated (# m^{-2}) anchovy densities for dry, normal and wet years under decreased, baseline and increased nutrient loads and low anchovy recruitment.

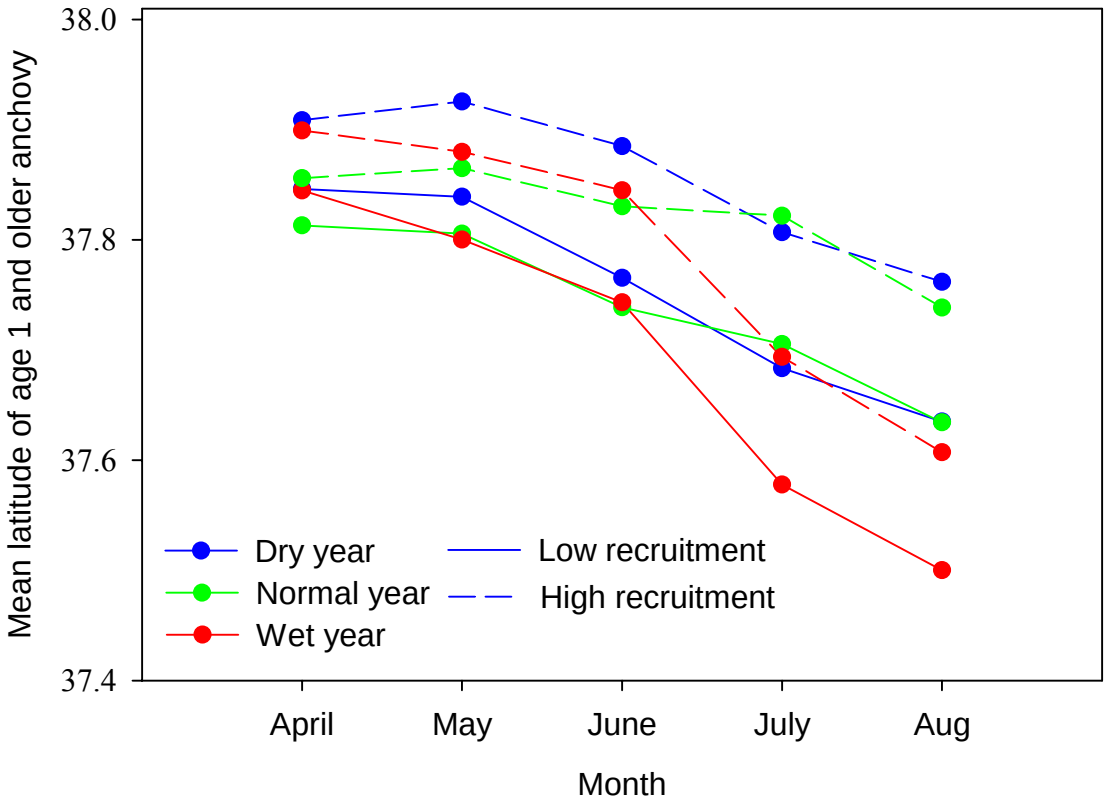

Figure 3.13 Change in mean latitude of age 1 and older anchovy between May and August for dry, normal and wet water years under baseline nutrient load.

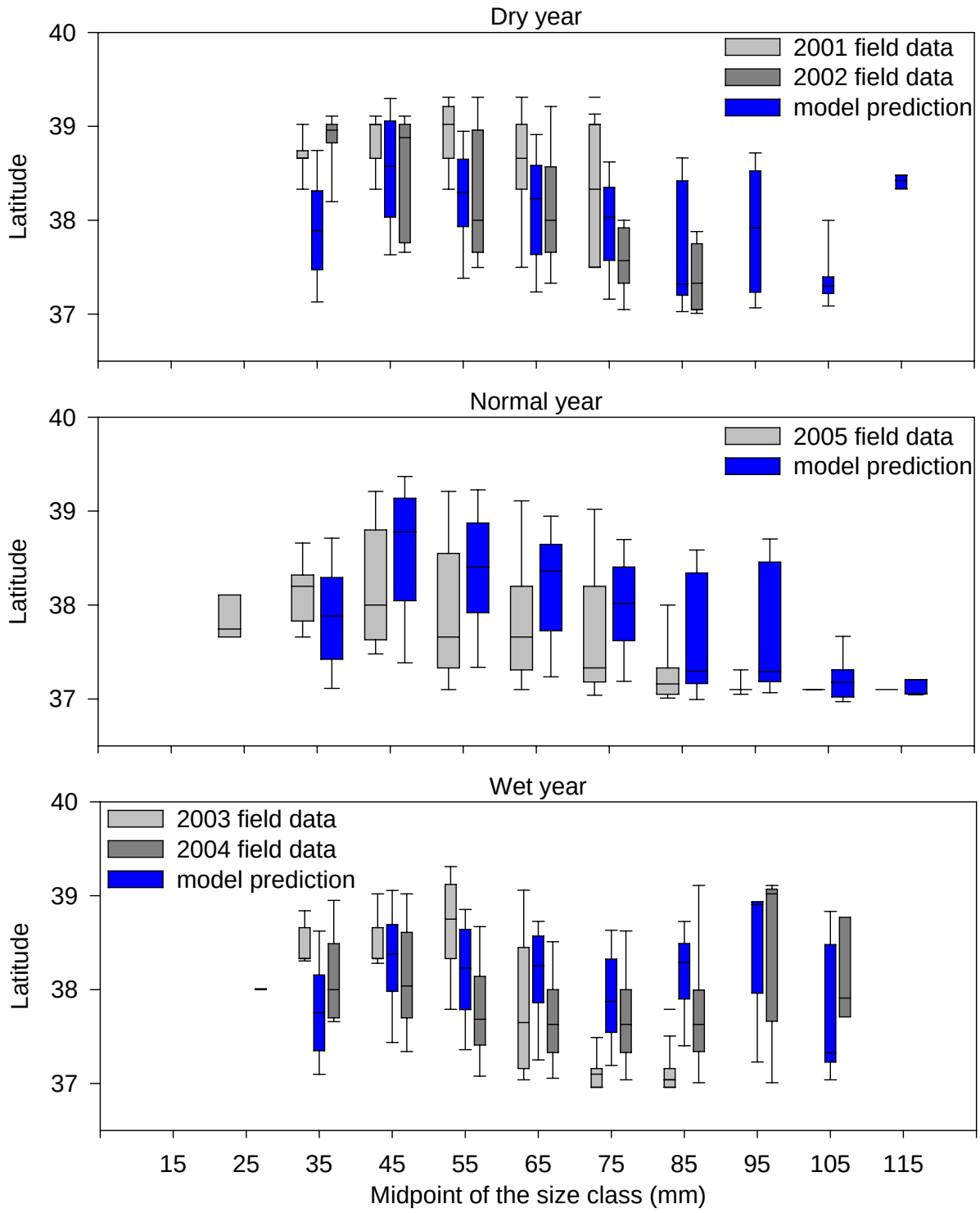

Figure 3.14 Predicted distributions of anchovy in October for dry, normal and wet water years under baseline nutrient load compared to field observations of the distributions of anchovy in the fall. Anchovy field distributions are from the CHESFIMS project (Miller *personal communication*).

(35 mm) were further south than observed, while the distributions of larger anchovy (≥85 mm) size classes tended to be further north than observed.

3.3.3 Effects of Nutrient Loadings

Dissolved oxygen concentrations and zooplankton densities were affected by changes in nutrient loading, but temperature and salinity were not. The major effect of increasing the nutrient load on bottom-layer DO concentration was to increase the intensity of hypoxia. For a given water year (column in Figure 3.9), decreased nutrient loadings eliminated hypoxia in the bottom layer for much of the Bay south of the Potomac River compared to the baseline loading. Increased nutrient loading showed a smaller effect, as spatial maps of DO under increased loadings looked roughly similar to maps under baseline nutrient loading. The larger effect of reduced nutrient loadings was also seen in the total volume of hypoxic water (Figure 3.15). A 50% increase in nutrient loadings resulted in only a small increase in the volume of hypoxic water compared to the baseline scenario, while reduced nutrient loadings decreased the volume of hypoxic water by ~20-40% depending on the water year.

Changing nutrient loadings affected both the density and the spatial extent of zooplankton (columns in Figure 3.10). Higher nutrient loads (from decreased load to baseline load to increased load) resulted in higher zooplankton densities throughout the Bay. Additionally, the area of higher zooplankton density (>1 g C m^{-3}) extended further south for all three water years, with the widest extent occurring during the wet year. The most dramatic increases in zooplankton densities and spatial extent were predicted between the decreased nutrient loadings in a dry year and increased nutrient loadings in a wet year (top left to bottom right in Figure 3.10).

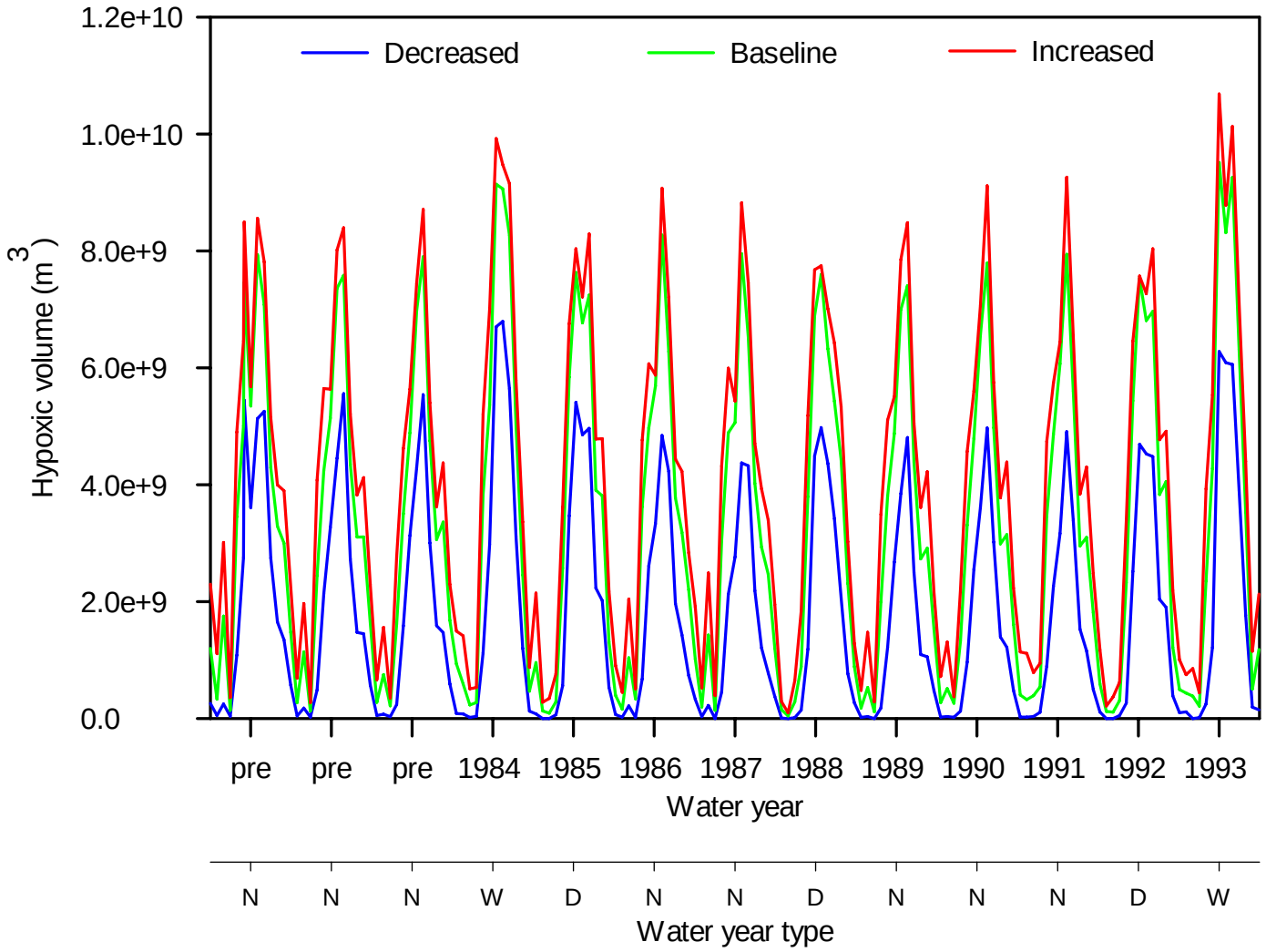

Figure 3.15 Volume of hypoxic water for decreased, baseline and increased nutrient loads during the three pre-run years and the water years from 1984 to 1993. Spin-up years are indicated by the label "pre". Water year type is indicated by the initials: D = dry year, W = wet year, and N = normal year. Water year types were obtained from the USGS (http://md.water.usgs.gov/monthly/bay.html).

Increased zooplankton with increasing nutrient loadings resulted in faster growth and larger anchovy. The benefits of higher zooplankton, however, were smaller under high recruitment due to density-dependent effects. Under both low and high recruitment, increasing the nutrient load resulted in an increase in the lengths of YOY anchovy in October (blue to green to red in Figure 3.16), however the increase in October lengths was dampened under high recruitment compared to low recruitment. Growth trajectories (Figure 3.17) of the early, peak, and late cohorts under decreased nutrient loadings (low food) and high recruitment (abundant anchovy) showed simulated anchovy grew, but the mean lengths of all three cohorts trailed behind baseline mean lengths for high recruitment. Peak and late cohorts grew only slightly before winter.

Anchovy survival from recruitment to October was only mildly affected by changes in the level of nutrient loading (Figure 3.18). While the effect of nutrient loadings on survival was consistent, the magnitude of the effect was small. The largest difference in survival rates was for the wet year under low recruitment (13.6% under decreased loadings to 11.9% under increased loadings). Anchovy survival was reduced when nutrient loading was increased due to an increase in the number of anchovy dying due to exposure to hypoxia (Figure 3.19).

The slight reduction in survival under increased nutrient loadings (Figure 3.18) was more than offset by faster growth rates (Figures 3.16 and 3.17), resulting in predicted October anchovy biomass increasing with increasing nutrient loadings (Figure 3.20). Anchovy biomass was lowest under both low and high recruitment when nutrient loads were decreased (blue bar), and was highest when nutrient loadings were increased (red bar).

Increasing nutrient loads caused a southward shift in the areas with the highest anchovy densities under both low and high recruitment (Figures 3.11 and 3.12). The southward shift in

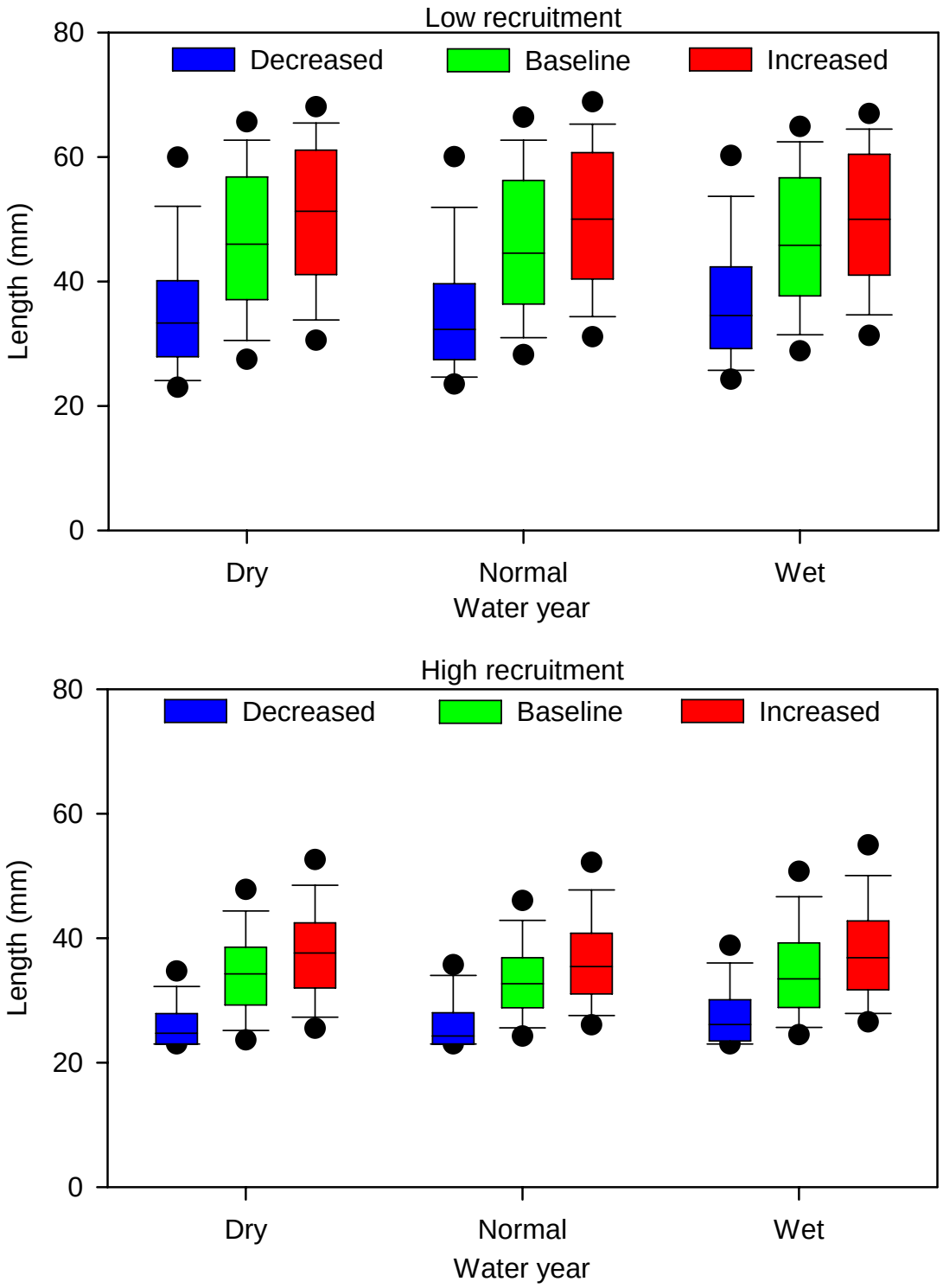

Figure 3.16 October length distributions of anchovy for dry, normal and wet years under decreased, baseline and increased nutrient loads for low and high recruitment. Circles show the 5th and 95th percentiles of the distributions. Whiskers show the 10th and 90th percentiles, the box shows the 25th and 75th percentiles and the solid line in the box shows the median.

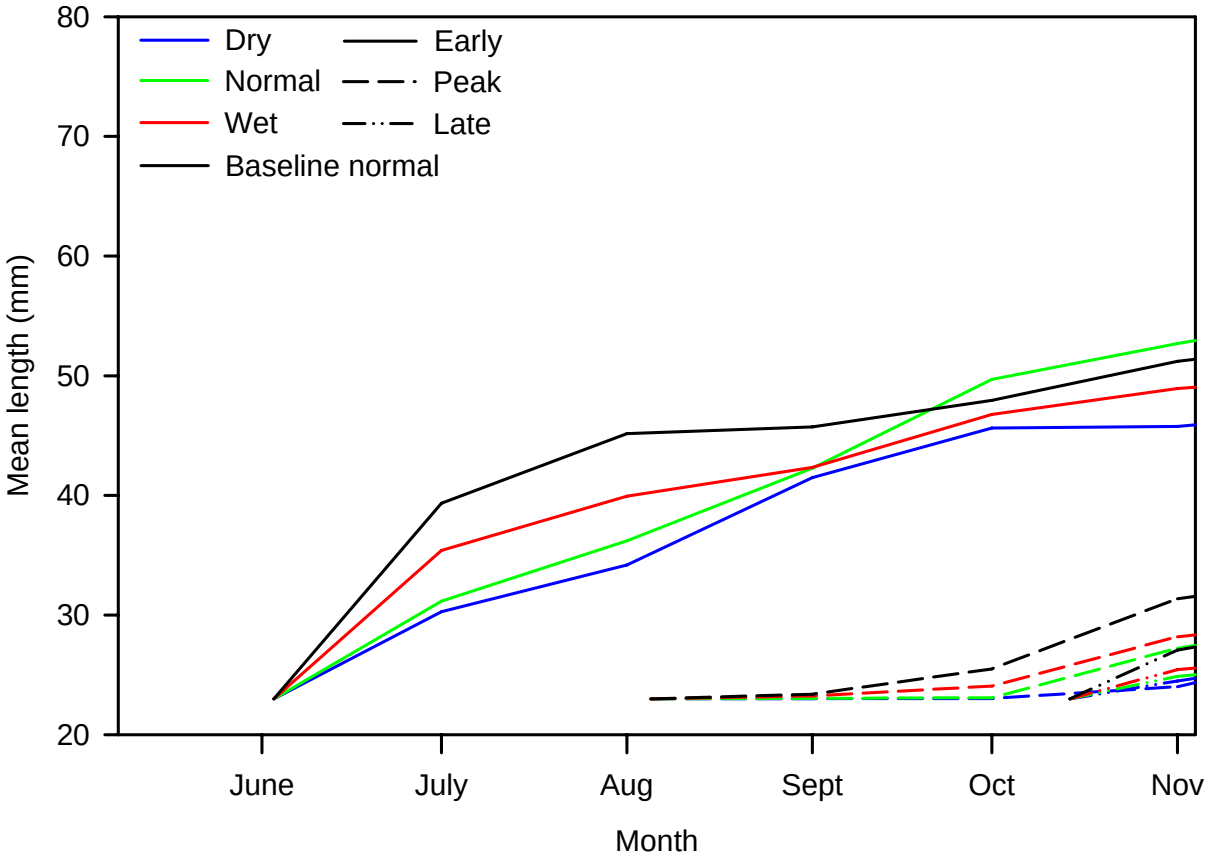

Figure 3.17 Mean growth trajectories of anchovy under high recruitment and decreased nutrient load for dry, normal and wet water years. Trajectories are shown from recruitment in early, peak and late cohorts to late October. Mean growth trajectories of anchovy under high recruitment and baseline nutrient load during a normal water year are shown from recruitment in early, peak and late cohorts to late October for comparison.

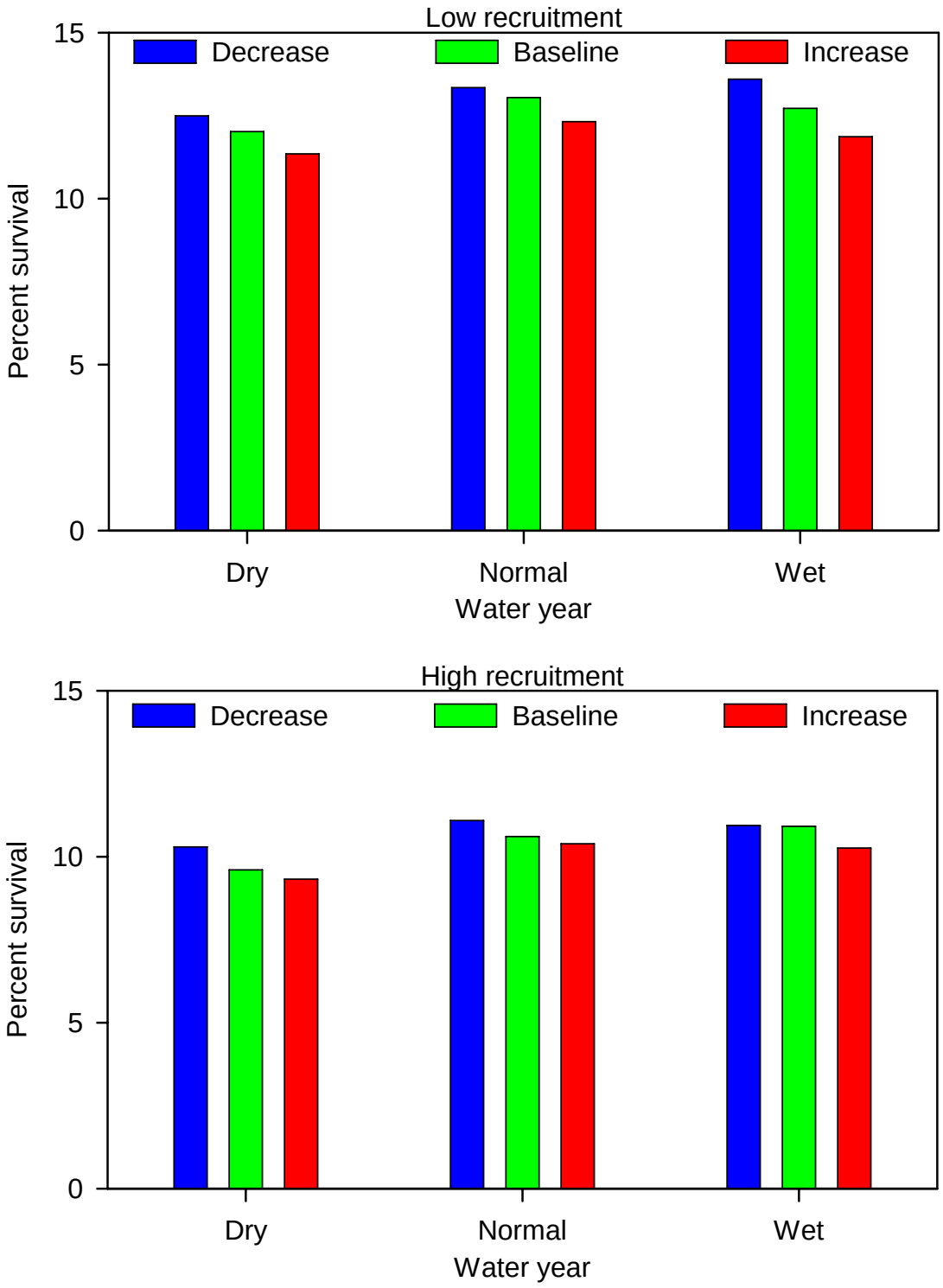

Figure 3.18 Percent survival of anchovy from recruitment to October for dry, normal and wet years under decreased, baseline and increased nutrient loads for low and high recruitment.

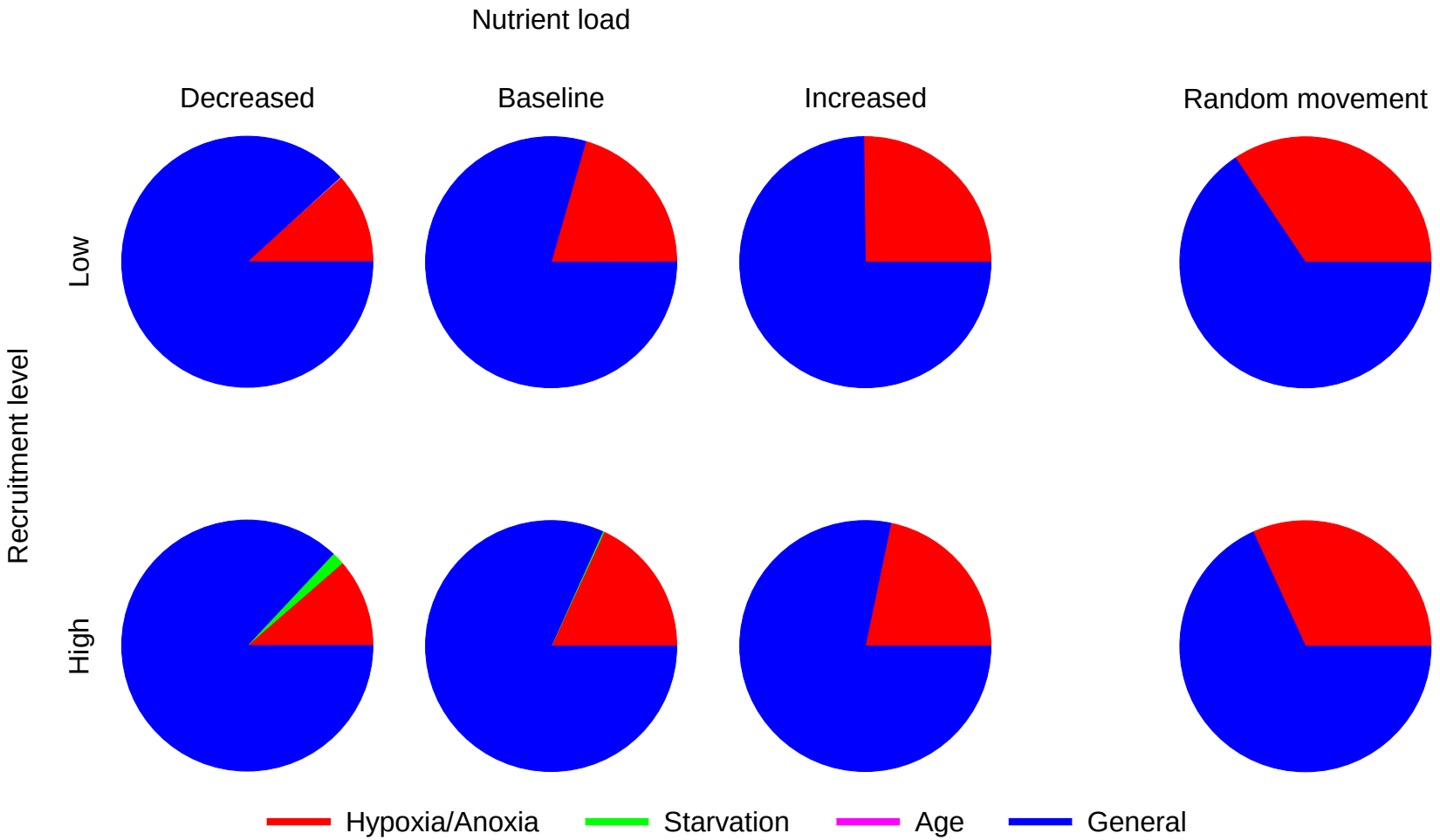

Figure 3.19 Causes of anchovy mortality for all anchovy dying over the course of the three pre-run years and the 10 water years from 1984 to 1993 for decreased, baseline and increased nutrient loads and low and high recruitment. Additionally, the sources of mortality for anchovy using random movement for baseline nutrient load with low and high recruitment is shown. Causes of mortality include exposure to hypoxia and anoxia, starvation, old age, and general, size dependent mortality.

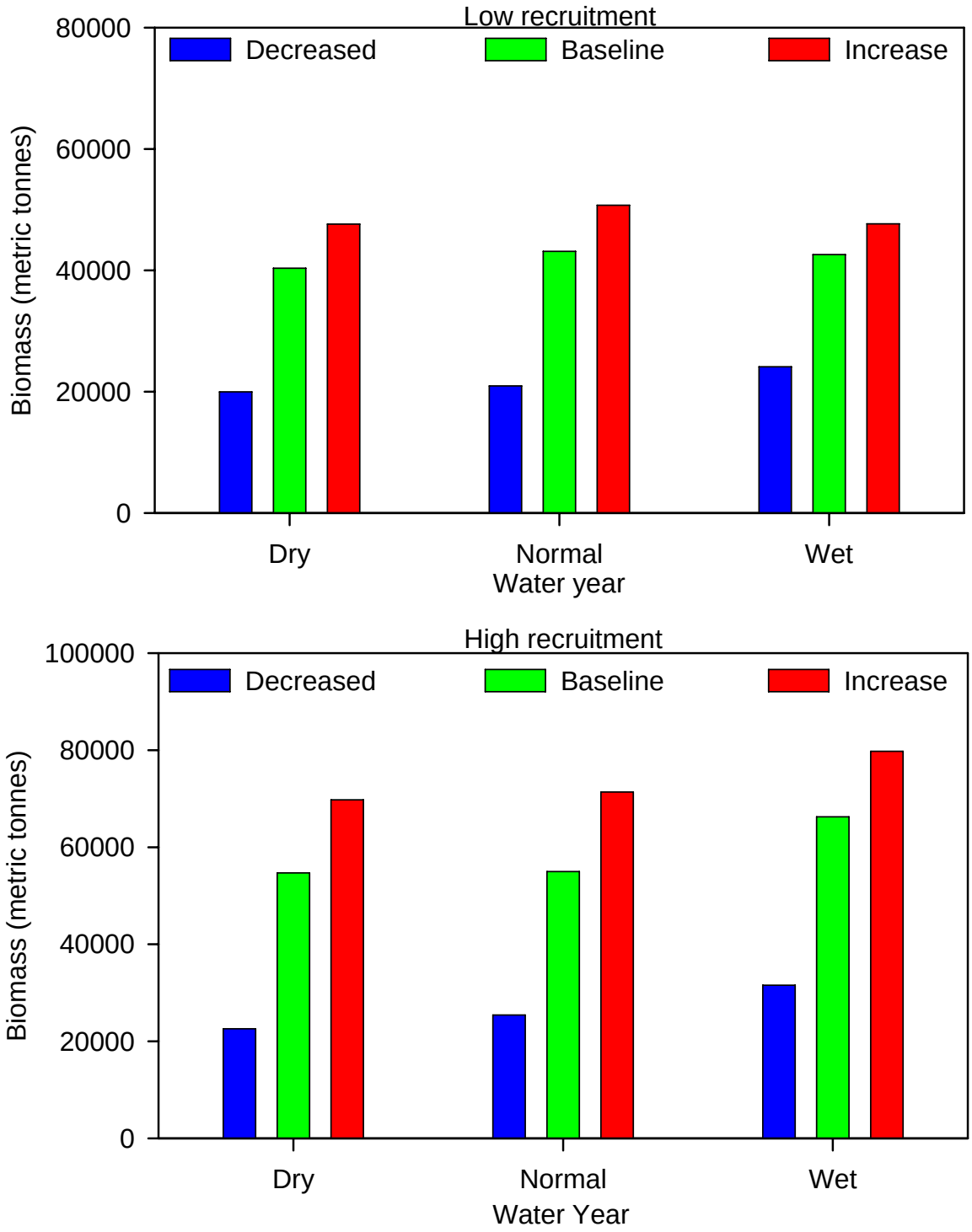

Figure 3.20 October biomass of YOY anchovy for dry, normal and wet years under decreased, baseline and increased nutrient loads for low and high recruitment.

spatial distributions appeared to be in response to the southward expansion of hypoxia in the main channel of the Bay (Figure 3.9). The biggest difference in the predicted spatial patterns of the anchovy occurred between the dry year with decreased nutrient load and the wet year with increased nutrient loads, for both low and high recruitment. The region with the highest densities of anchovy shifted from the region just south of the mouth of the Potomac River to the region between the mouth of the Rappahannock River and the mouth of the Bay. The mean latitudes of age-1 and older shifted southwards from 38.2 degrees North during the dry year with decreased nutrient loads to 37.6 degrees North during the wet year with increased nutrient loads, approximately twice the latitudinal shift predicted between the dry and wet years under baseline nutrient loadings (Figure 3.13).

3.3.4 Kinesis Versus Random Movement

Based on the two cross-bay transects in July, kinesis movement in the vertical direction caused anchovy to avoid areas with low DO (Figure 3.21), and to therefore suffer lower mortality from hypoxia (Figure 3.19). While there were more individuals in both transects under kinesis movement than under random movement (Figure 3.21), a smaller proportion of the individuals were in hypoxic cells. The proportion of mortality that was attributed to hypoxia increased with nutrient loadings for kinesis movement (Figure 3.19). The proportion of mortality attributed to hypoxia for random movement was even higher than that predicted using kinesis movement for the increased nutrient loading under both low and high recruitment.

The effect of the kinesis versus random movement on anchovy biomass depended upon whether anchovy recruitment was low or high (Figure 3.22). When recruitment was low, anchovy biomass was on average 35% higher with kinesis movement; however, simulated anchovy biomass was similar between kinesis and random movement under high recruitment.

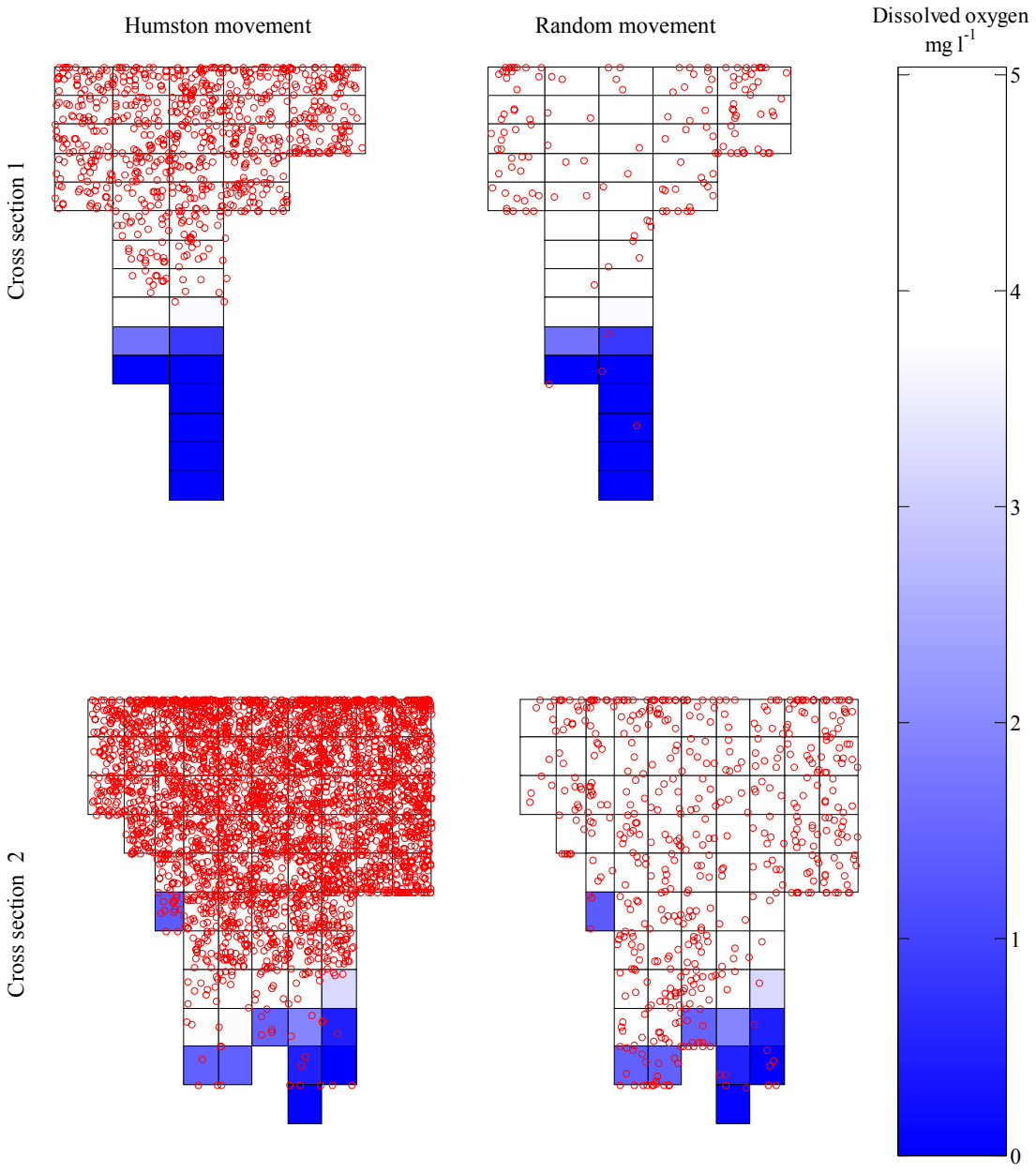

Figure 3.21 Comparison of the vertical distributions of anchovy using kinesis and random movement in two cross-sections of the Chesapeake Bay during July. Location of the anchovy is show with the open red circles. Cell dissolved oxygen concentration is shown by the color of the cell.

Figure 3.22 Biomass of anchovy using kinesis and random movement under baseline nutrient load for low and high recruitment during the three pre-run years and the water years from 1984 to 1993.

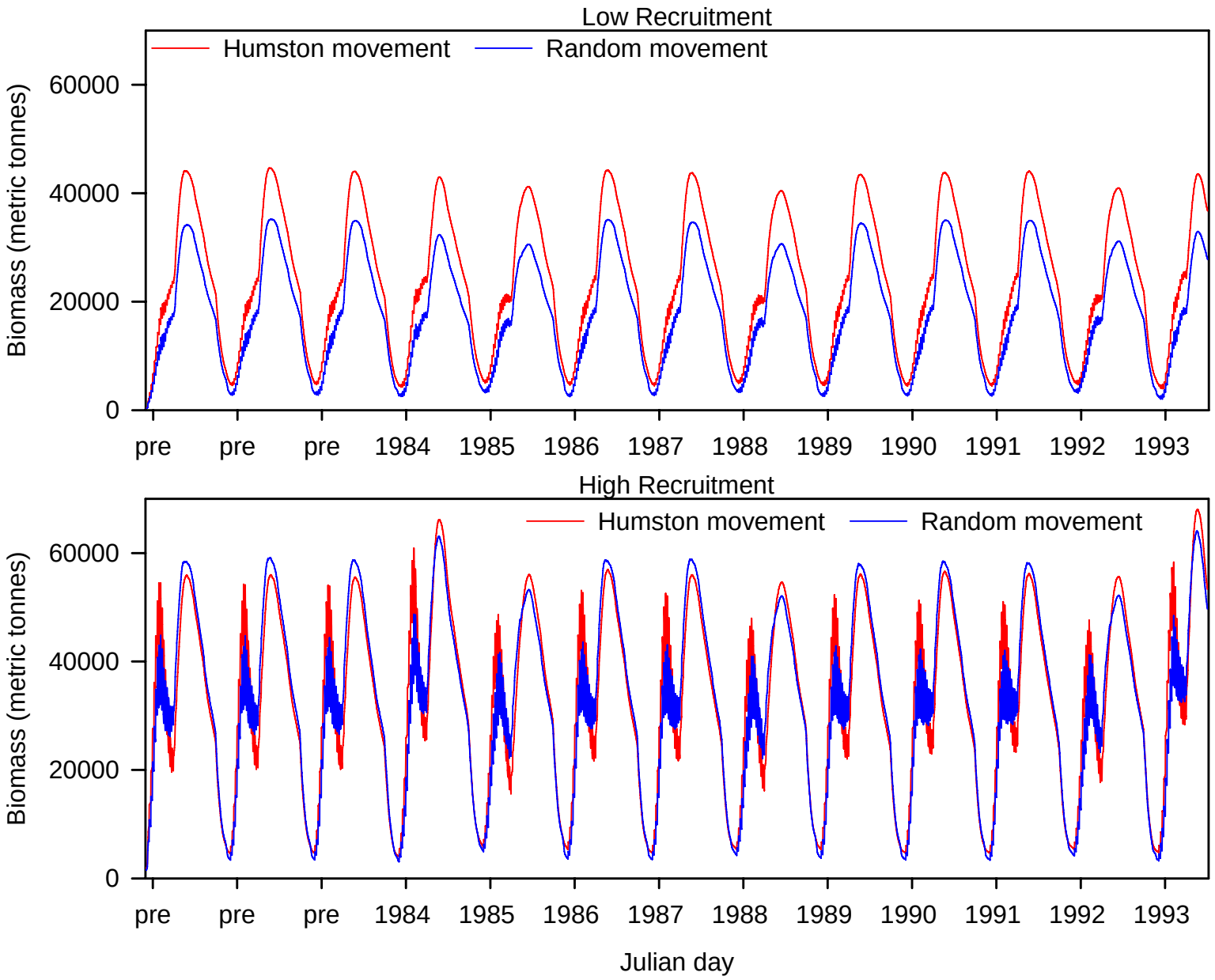
Low Recruitment
Humston movement
Random movement
Biomass (metric tonnes)
60000
40000
20000
0
pre
pre
pre
1984
1985
1986
1987
1988
1989
1990
1991
1992
1993
High Recruitment
Humston movement
Random movement
Biomass (metric tonnes)
60000
40000
20000
0
pre
pre
pre
1984
1985
1986
1987
1988
1989
1990
1991
1992
1993
Julian day

3.4 Discussion

3.4.1 Effects of Nutrient Loadings and Caveats

Decreasing nutrient loads to Chesapeake Bay by 50%, an amount roughly equivalent to the planned reductions under the Chesapeake Bay 2000 Agreement (Kemp et al. 2005, Chesapeake Bay Program 2007), caused large reductions in anchovy length (Figure 3.16) and biomass (Figure 3.20) under both low and high recruitment during all three water years. Increasing Chesapeake Bay nutrient loads by 50% caused a relatively small increase in anchovy sizes and biomass. Luo and Brandt (1993) performed a sensitivity analysis of the bioenergetics model that was used in this study and concluded that the annual growth of anchovy was very sensitive to consumption. The changes in anchovy size and biomass (Figures 3.16 and 3.20) predicted in this analysis for increased and decreased nutrient loadings were a result of the changes in zooplankton density (Figure 3.10 columns), which determined consumption rates. The increase in consumption more than offset any growth reductions (Figure 3.20) and increased mortality due to low DO (Figure 3.19). As long as the kinesis movement kept the juvenile and adult anchovy out of hypoxic water and in cells with sufficient prey, the generally higher zooplankton densities with increasing nutrient loadings (Figure 3.10) overrode any negative effects of the increased hypoxia that was also associated with the increasing nutrient loadings (Figures 3.9 and 3.15).

My result that decreased nutrient loadings from assumed baseline (1984 to1986) levels would decrease anchovy production is consistent with the general idea that adding nutrients can benefit some fish species within certain limits, but the situation specifically in Chesapeake Bay is unclear. Cross-system comparisons have shown that estuarine systems with higher nutrient loads generally have higher biological production (Caddy 1993, Nixon and Buckley 2002). Caddy

(1993) suggests that eutrophication in an ecosystem will initially increase the production of pelagic and demersal fish species. Two examples of systems that showed an increase in fish stocks while eutrophication was occurring are the Black Sea during the late 1970s and 1980s and the Baltic Sea since the end of World War II (Caddy 1993). In general, however, further increases in eutrophication would cause the production of pelagic fish to continue to increase, but the production of demersal fish would likely decline due to an increase in the extent and the duration of hypoxic and anoxic conditions that reduce demersal habitat quality and availability. Eventually, even further increases in nutrient loads will lead to a decline in pelagic fish production as water quality eventually deteriorates and gelatinous predators such as ctenophores and jellyfish become more abundant (e.g. the Black Sea, Caddy 1993).

The data from Chesapeake Bay are inconclusive. In broad terms, commercial catch data shows that the ratio of pelagic to demersal fish harvested (as a percentage of total weight) has been increasing since the 1960s (Kemp et al. 2005), seemingly consistent with increasing eutrophication. However, bay anchovy are not part of the pelagic catch data because they are not fished commercially, and furthermore, long term fishery-independent data on anchovy suggest that the anchovy population has not increased (Houde and Zastrow 1991) and, if anything, the population may be decreasing (Durrell and Weedon 2005). Further complicating the situation is that the increasing ratio of pelagic species in the catch data can be, at least partly, attributed to the decline of some demersal species due to overfishing (not eutrophication), and an increase in pelagic fish catches due to increasing catches of Atlantic menhaden (Kemp et al. 2005).

From a life history perspective, there are several reasons for why bay anchovy might be expected to do well in a reasonably eutrophic system. Bay anchovy are opportunistic life history strategists (Winemiller and Rose 1992). Characteristics of opportunistic fish species include

early maturation, frequent reproduction over an extended spawning period, rapid larval growth, and rapid population turnover rates. Anchovy are "income breeders", as their spawning intensity has been linked to adult ration (Luo and Musick 1991, Wang and Houde 1994, Peebles et al. 1996). Increased nutrient loads should result in increased prey availability, which would result in faster growth of juveniles and adults and increased egg production. Increased food availability would also be expected to boost larval growth, shortening the length of the larval stage during which they experience their highest mortality rates (Houde 1987, Jung and Houde 2004A). A shorter larval stage could have a large effect on the number of individuals surviving to the juvenile stage (Houde 1987). Finally, anchovy are a pelagic fish species and are able to simply swim away from regions that are hypoxic (Kramer 1987, Breitburg 2002, Ludsin et al. *in review*) without facing the additional stress that demersal fish species would likely experience (Eby at al. 2005).

While there is some evidence to support the results of my simulations, they should be viewed with caution because I may have underestimated the effects of low DO on juveniles and adults, ignored the effects of nutrient loadings (hypoxia) on the early life stages of anchovy, and because the modeling was a completely bottom-up analysis. Additionally, my analysis focused on the processes that would affect anchovy growth and production as nutrient loadings changed, rather than on making accurate short-term forecasts on the magnitude of the anchovy response. Only juveniles and adults were simulated in my analysis; recruitment was fixed every year and not related to larval survival nor to the amount of energy gained by adults during the spawning season. I could have underestimated the direct effects of low DO on juveniles and adult anchovy by underestimating exposure in simulations and the DO effects are derived from laboratory experiment on menhaden. Furthermore, unlike juveniles and adults, eggs and larvae of anchovy

have only limited abilities to avoid hypoxia and are more sensitive than juveniles and adults to low DO (Chesney and Houde 1989, Breitburg 2002, Breitburg et al. 2003). Eggs and larvae of bay anchovy have 12-hour LC_{50}s of 2.8 mg O_2 liter^{-1} and 2.4 mg O_2 liter^{-1} (Chesney and Houde 1989). Increasing the nutrient load to the Bay caused an increase in the extent and the intensity of hypoxic conditions in the Bay (Figures 3.9 and 3.15). This can cause a significant increase in egg and larval mortality rates that would decrease recruitment to the 23-mm size, when my simulations started. Breitburg et al. (2003) and Adamack (Chapter 2) simulated the effects of changing nutrient loads on anchovy egg and larval survival in the mesohaline portion of the Patuxent River. Comparing between a 50% decrease in nutrient loads and a 50% increase, Adamack (Chapter 2) found that egg mortality was 2-7-fold higher when nutrient loads were increased, and the response of early larvae was complicated because of shifting degrees of vertical overlap with their invertebrate predators. Ignoring how energy gain affects egg production, and therefore potentially recruitment, suggests the need for caution in interpreting the results of my analyses.

The bottom-up approach used here also ignores the response of the rest of the food web to increasing nutrient loadings and how they would affect anchovy. Bay anchovy are part of fairly complicated food web, involving competition with other forage fish species for zooplankton prey, competition and predation by ctenophores (*Mnemiopsis leidyi*) and jellyfish (*Chrysaora quinquecirrha*) (Breitburg and Fulford 2006), with ctenophores also eating jellyfish (Purcell and Cowan 1995, Purcell and Decker 2005), and predation by striped bass, bluefish, weakfish (Hartman and Brandt 1995) and other piscivorous fish. The spatial distribution and productivity of all of these competitor and predator species are themselves affected by different water years and by the effects of hypoxia (Jung and Houde 2003, Purcell and Decker 2005).

Purcell and Decker (2005) found that the distributions and relative abundances of ctenophores (*Mnemiopsis leidyi*) and jellyfish (*Chrysaora quinquecirrha*) varied in response to water years, and bottom layer DO causes changes in the vertical distribution of fish and gelatinous zooplankton that affects the mortality rates of larval anchovy (Breitburg et al. 1999, Breitburg et al. 2003, Ludsin et al. *in review*). Coutant (1985) documented how hypoxia could likely affect striped bass distributions, and Ludsin et al. (in review) recently suggested that increasing nutrient loadings can concentrate potential predators of anchovy (Ludsin et al. in review). These effects, which were ignored in the model simulations, can potentially affect anchovy survival and growth to a greater extent than the bottom-up effects via zooplankton that were simulated.

3.4.2 Density Dependence and Water Years

Comparisons of anchovy survival (Figure 3.18), lengths (Table 3.6, Figure 3.16), and biomasses (Tables 3.6 and 3.7) between low and high recruitment scenarios indicated that anchovy in model simulations exhibited compensatory density dependence. Compensatory density-dependence occurs if a species' vital rates slows population growth rate at high densities and increases population growth rates at low densities (Rose et al. 2001). Young-of-year anchovy in the low recruitment conditions had slightly higher survival rates from recruitment through October than anchovy under high recruitment (Figure 3.18). This is consistent with the findings of Wang et al. (1997) and Cowan et al. (1999), who used an individual-based anchovy population model configured for a single, well-mixed box for the mesohaline region of Chesapeake Bay. The slight changes in survival were for individuals from recruitment at 23-mm to October; whether the effect would be amplified if the dynamics of the larval stage are simulated dynamically is not clear. Given the small response in survival, more zooplankton

under increasing nutrient loadings led to faster anchovy growth (Table 3.6), and thus larger anchovy (Figure 3.16) and higher biomass (Figure 3.20).

Water years generally had only a small effect on the growth, survival, abundance, and biomass of anchovy (Table 3.6) but had a larger effect on their latitudinal distributions with anchovy on average being located further south during a wet year than a dry year (Figure 3.13). The change in latitudinal distributions is consistent with Jung and Houde (2004B). They suggested that during wet years, anchovy would be located further south than during dry years as their northward movement would be blocked by low DO in the deeper waters of the mid-Bay region. However, they also hypothesized that anchovy should have higher survival rates during wet years than dry years. The higher survival of anchovy during wet years would be due to their concentrated numbers in the lower Bay region satiating their predators, resulting in an increase in their overall survival rate. This potential response of anchovy mortality rates to water years cannot be seen in the current version of the model, as predators are only included in a general size-dependent mortality term.

3.4.3 Kinesis Versus Random Movement

The effectiveness of the kinesis movement model was also related to the density-dependence inherent in model simulations. Under low recruitment, kinesis movement was more effective than random movement at having anchovy avoid low DO (Figure 3.21). The kinesis movement model was likely also more effective at finding areas with relatively high densities of zooplankton as anchovy biomass with low recruitment was higher under kinesis movement (Figure 3.22). This advantage disappeared under high recruitment. The performance of kinesis movement under high recruitment being no better than random movement may have been due to the density-dependent effects of high numbers of anchovy preying upon zooplankton, and

thereby making cells that were good for growth relatively sparse. Median lengths of anchovy under high recruitment simulations were ~ 10 mm shorter than under low recruitment (Figure 3.16). Perhaps the zooplankton density effect in the kinesis movement was not weighted heavily enough in the horizontal movement computations, or anchovy were not allowed to move far enough to discover the relatively fewer good food cells.

The kinesis model was successful in mimicking some of the anchovy distributional patterns observed in Chesapeake Bay related to wet, normal, and dry years. The horizontal distribution of anchovy (Figure 3.13) tended to be farther south during the wet year than in the dry year, as was observed by Jung and Houde (2004B). Comparisons of the predicted latitudinal distribution of anchovy by length-class and water year to field data (Figure 3.14) showed that, for most length-classes, the predicted distributions of anchovy were reasonable.

3.4.4 Summary and Future Directions

I have successfully demonstrated that we have the knowledge and computing power to dynamically couple the 3-dimensional Chesapeake Bay water quality model with a nearly full life-cycle fish growth and population dynamics model of bay anchovy. All model simulations reported in this chapter were run on desktop personal computers. The 13-year simulations using ~100,000 model individuals per simulation year required 3 to 4 days of CPU time. The same simulations, but using ~200,000 model individuals per year, required 7 to 10 days to run. As computing power continues to increase (e.g., multi-core processors, parallel computing), even more complex models, longer simulations, and more complicated simulation experiments will be the norm. Wang et al. (2005) used parallel computing with a spatially-explicit fish model (ALFISH) and achieved a speedup factor of 16 (~11 hours of CPU time per run on a single processor to 39 minutes of CPU time per run on 25 processors). I anticipate that such

improvements in the Chesapeake Bay model coupled to anchovy are possible now, or will be possible very soon.

I believe that there are two high-priority expansions needed to the present model. The first is to continue to develop the model for bay anchovy in Chesapeake Bay by adding the egg and larval stages, allowing anchovy recruitment to vary dynamically in response to changes in adult anchovy sizes and prey ration, and making predation mortality on anchovy dependent on piscivore dynamics. Making these changes to the model would help us to better understand the effects of changes in nutrient loadings on bay anchovy. As part of this expansion and to help guide the expansion, the present version of the model should undergo a more formal skill assessment to examine the model's performance using the data from the TIES and CHESFIMS projects. As a part of this skill assessment, the predicted spatial distribution of anchovy during dry, normal and wet water years would be quantitatively compared to the observed spatial distributions of anchovy during similar water years. The second high-priority expansion of the model is to modify the model to simulate species other than bay anchovy. The structure of the model is such that it should be relatively easy to modify the code to simulate other species. Future analyses should focus on the effects of nutrient loadings on a demersal fish species such as croaker (*Micropoganias undulates*), who are more directly affected by hypoxia (Eby et al. 2005).

My analysis is the first step in a more complicated analysis to assess how changes in nutrient loadings would affect key fish species in the Chesapeake Bay. My results suggest that decreased nutrient loadings from present levels could reduce bay anchovy productivity. But given the many caveats underlying my analysis, I suggest that my results be treated with caution until the effects of nutrient loadings into Chesapeake Bay on fish dynamics are more fully

explored. Expansion of the model and additional analyses are needed to increase the realism in simulations and to confirm that these preliminary results are robust to more complicated (and more realistic) situations and are general for other species.

3.5 References

Adamack, A. T.. 2003. Quantifying habitat quality of larval bay anchovy (*Anchoa mitchilli*) in Chesapeake Bay by linking an individual-based model with spatially-detailed field data. M.S. Thesis, Louisiana State University, Baton Rouge, Louisiana

Baird, D. and R. E. Ulanowicz. 1989. The seasonal dynamics of the Chesapeake Bay ecosystem. Ecological Monographs 59: 329-364

Boesch, D. F., R. B. Brinsfield, R. E. Magnien. 2001. Chesapeake Bay eutrophication: Scientific understanding, ecosystem restoration, and challenges for agriculture. Journal of Environmental Quality 30: 303-320

Brandt, S. B. and D. M. Mason. 2003. Effect of nutrient loading on Atlantic menhaden (*Brevoortia tyrannus*) growth rate potential in the Patuxent River. Estuaries 26: 298-309

Breitburg, D. L.. 2002. Effects of hypoxia and the balance between hypoxia and enrichment on coastal fishes and fisheries. Estuaries 25: 767-781

Breitburg, D. L., K. A. Rose and J. H. Cowan Jr.. 1999. Linking water quality to larval survival: predation mortality of fish larvae in an oxygen-stratified water column. Marine Ecology Progress Series 178: 39-54

Breitburg, D. L., A. Adamack, K. A. Rose, S. E. Kolesar, M. B. Decker, J. E. Purcell, J. E. Keister, J. H. Cowan Jr.. 2003. The pattern and influence of low dissolved oxygen in the Patuxent River, a seasonally hypoxic estuary. Estuaries 26: 280-297

Breitburg, D. L. and R. S. Fulford. 2006. Oyster-sea nettle interdependence and altered control within the Chesapeake Bay ecosystem. Estuaries and Coasts 29: 776-784

Burton, D. T., L. B. Richardson and C. J. Moore. 1980. Effect of oxygen reduction rate and constant low dissolved oxygen concentrations on two estuarine fish. Transactions of the American Fisheries Society 109: 552-557

Caddy, J. F.. 1993. Toward a comparative evaluation of human impacts on fishery ecosystems of enclosed and semi-enclosed seas. Reviews in Fisheries Science 1: 57-95

Cerco, C. and T. Cole. 1993. Three-dimensional eutrophication model of Chesapeake Bay. Journal of Environmental Engineering 119: 1006-1025

Cerco, C. F.. 1995. Response of Chesapeake Bay to nutrient load reductions. Journal of Environmental Engineering 121: 549-557

Cerco, C. and M. Meyers. 2000. Tributary refinements to the Chesapeake Bay Model. Journal of Environmental Engineering 126: 164-174

Cerco, C. F. 2004. Users guide to the CE-QUAL-ICM Eutrophication Model. Environmental Laboratory, U. S. Army Engineer Research and Development Center, Vicksburg, Mississippi

Cerco, C. F. and M. R. Noel. 2004. Process-based primary production modeling in Chesapeake Bay. Marine Ecology Progress Series 282: 45-58

Chesapeake Bay Program. 2007. http://www.chesapeakebay.net. Annapolis, Maryland

Chesney, E. J. and E. D. Houde. 1989. Laboratory studies on the effect of hypoxic waters on the survival of eggs and yolk-sac larvae of the bay anchovy, *Anchoa mitchilli*. In Houde, E. D., E. J. Chesney, T. A. Newberger, A. V. Vazquez, C. E. Zastrow, L. G. Morin, H. R. Harvey, and J. W. Gooch. Population Biology of Bay Anchovy in Mid-Chesapeake Bay. Solomons, Maryland pg. 98-107

Cooper, S. R. and G. S. Brush. 1991. Long-term history of Chesapeake Bay anoxia. Science 254: 992-996

Cloern, J. E.. 2001. Our evolving conceptual model for the coastal eutrophication problem. Marine Ecology Progress Series 210: 223-253

Coutant, C. C.. 1985. Striped bass, temperature, and dissolved oxygen: A speculative hypothesis for environmental risk. Transactions of the American Fisheries Society 114: 31-61

Cowan, J. H. Jr., K. A. Rose, E. D. Houde, S-B Wang and J. Young. 1999. Modeling effects of increased larval mortality on bay anchovy population dynamics in the mesohaline Chesapeake Bay: Evidence for compensatory reserve. Marine Ecology Progress Series 185: 133-146

Cronin, T. M. and C. D. Vann. 2003. The sedimentary record of climatic and anthropogenic influence on the Patuxent estuary and Chesapeake Bay ecosystems. Estuaries 26: 169-209

DiToro, D. 2001. Sediment Flux Modeling. John Wiley % Sons, New York, New York

deYoung, B. M. Heath, F. Werner, F. Chai, B. Megrey, and P. Monfray. 2004. Challenges of modeling ocean basin ecosystems. Science 304: 1463-1466

Dortch, M. R. Chapman and S. Abt. 1992. Application of three dimensional Lagrangian residual transport. Journal of Hydraulic Engineering 118:831-848

Durell, E. Q. and C. Weedon. 2005. Striped bass seine survey juvenile index web page. http://www.dnr.state.md.us/fisheries/juvindex/index.html. Maryland Department of Natural Resources, Fisheries Service

Eby, L. A., L. B. Crowder, C. M. McClellan, C. H. Peterson, and M. J. Powers. 2005. Habitat degradation from intermittent hypoxia: impacts on demersal fishes. Marine Ecology Progress Series 291: 249-261

Fisher, T. R., J. D. Hagy III, W. R. Boynton, and M. R. Williams. 2006. Cultural eutrophication in the Choptank and Patuxent estuaries of Chesapeake Bay. Limnology and Oceanography 51: 435-447

Geometry – Geometric Calculations. 2007. http://people.scs.fsu.edu/~burkardt/cpp_src/geometry/geometry.html

Griffin, J. C. and F. J. Margraf. 2003. The diet of Chesapeake Bay striped bass in the late 1950s. Fisheries Management and Ecology 10: 323-328

Hagy, J. D., W. R. Boynton, C. W. Keefe, and K. V. Wood. 2004. Hypoxia in Chesapeake Bay, 1950-2001: Long-term change in relation to nutrient loading and river flow. Estuaries 27:634-658

Hartman, K. J. and S. B. Brandt. 1995. Trophic resource partitioning, diets and growth of sympatric estuarine predators. Transactions of the American Fisheries Society 124: 520-537

Hermann, A. J., S. Hinckley, B. A. Megrey, and J. M. Napp. 2001. Applied and theoretical considerations for constructing spatially explicit individual-based models of marine larval fish that include multiple trophic levels. ICES Journal of Marine Science 58: 1030-1041

Hewett, S. W. and B. L. Johnson. 1987. A generalized bioenergetics model of fish growth for microcomputers. U. S. Sea Grant, Madison, Wisconsin

Houde, E. D.. 1987. Fish early life dynamics and recruitment variability. American Fisheries Society Symposium. 2: 17-29

Houde, E. D., E. J. Chesney, T. A. Newberger, A. V. Vazquez, C. E. Zastrow, L. G. Morin, H. R. Harvey, and J. W. Gooch. 1989. Population Biology of Bay Anchovy in Mid-Chesapeake Bay. Solomons, Maryland

Houde, E. D. and C. E. Zastrow. 1991. Bay anchovy. *In* Funderburk, S. L., J. A. Mihursky, S. J. Jordan, and D. Riley (eds.). Habitat requirements for Chesapeake Bay living resources, 2nd Edition. Living Resources Subcommittee, Chesapeake Bay Program. Annapolis, Maryland pg 8-1 – 8-14

Humston, R. J. S. Ault, M. Lutcavage, D. B. Olson. 2000. Schooling and migration of large pelagic fishes relative to environmental cues. Fisheries Oceanography 9: 136-146

Humston, R. 2001. Development of movement models to assess the spatial dynamics of marine fish populations. PhD dissertation. University of Miami, Coral Gables, Florida

Johnson, B. H., K. W. Kim, R. E. Heath, B. B. Hsieh, and H. L. Butler. 1993. Journal of Hydraulic Engineering 119:2-20

Jung, S. and E. D. Houde. 2003. Spatial and temporal variabilities of pelagic fish community structure and distribution in Chesapeake Bay, USA. Estuarine, Coastal and Shelf Science 58: 335-351

Jung, S. and E. D. Houde. 2004A. Production of bay anchovy *Anchoa mitchilli* in Chesapeake Bay: Application of size-based theory. Marine Ecology Progress Series 281: 217-232

Jung, S. and E. D. Houde. 2004B. Recruitment and spawning-stock biomass distribution of bay anchovy (*Anchoa mitchilli*) in Chesapeake Bay. Fishery Bulletin 102: 63-77

Kemp, W. M., P. A. Sampou, J. Garber, J. Tuttle, W. R. Boynton. 1992. Seasonal depletion of oxygen from bottom waters of Chesapeake Bay: roles of benthic and planktonic respiration and physical exchange processes. Marine Ecology Progress Series 85: 137-152

Kemp, W. M. 2004. Coupling water quality and upper trophic level modeling for Chesapeake Bay: A planning workshop. U.S. EPA Chesapeake Bay Program Conference Room Annapolis, Maryland

Kemp, W. M., W. R. Boynton, J. E. Adolf, D. F. Boesch, W. C. Boicourt, G. Brush, J. C. Cornwell, T. R. Fisher, P. M. Glibert, J. D. Hagy, L. W. Harding, E. D. Houde, D. G. Kimmel, W. D. Miller, R. I. E. Newell, M. R. Roman, E. M. Smith, and J. C. Stevenson. 2005. Eutrophication of Chesapeake Bay: Historical trends and ecological interactions. Marine Ecology Progress Series 303: 1-29

Kramer, D. L.. 1987. Dissolved oxygen and fish behavior. Environmental Biology of Fishes 18: 81-92

Lett, C., K. A. Rose, B. A. Megrey. *Submitted*. Biophysical models of small pelagic fish.

Ludsin, S. A., D. M. Mason, X. Zhang, S. B. Brandt, M. R. Roman, W. Boicourt, and M. Costantini. *In review*. Indirect effects of coastal hypoxia on planktivore habitat and pelagic food web dynamics.

Lung, W. S. and S. Bai. 2003. A water quality model for the Patuxent Estuary: Current conditions and predictions under changing land-use scenarios. Estuaries 26: 267-279

Luo, J. and S. B. Brandt. 1993. Bay anchovy *Anchoa mitchilli* production and consumption in mid-Chesapeake Bay based on a bioenergetics model and acoustic measures of fish abundance. Marine Ecology Progress Series. 98: 223-236

Luo, J. K. J. Hartman, S. B. Brandt, C. F. Cerco, and T. H. Rippetoe. 2001. A spatially-explicit approach for estimating carrying capacity: An application for the Atlantic menhaden (*Brevoortia tyrannus*) in Chesapeake Bay. Estuaries 24: 545-556

Luo, J. and J. A. Musick. 1991. Reproductive biology of the bay anchovy in Chesapeake Bay. Transactions of the American Fisheries Society 120: 701-710

Mauchline, J.. 1998. The biology of Calanoid Copepods. Advances in Marine Biology 33

Morin, L. G. and E. D. Houde.1989. Hatch-date frequencies and young-of-the-year growth rates of bay anchovy in mid-Chesapeake Bay (Chapter 5).*In* Houde, E. D., E. J. Chesney, T. A. Newberger, A. V. Vazquez, C. E. Zastrow, L. G. Morin, H. R. Harvey, and J. W. Gooch. Population Biology of Bay Anchovy in Mid-Chesapeake Bay. Solomons, Maryland pg. 98-107

Newberger, T. A., E. D. Houde, and E. J. Chesney.1989. Relative abundance, age, growth and mortality of bay anchovy (*Anchoa mitchilli*) in the mid-Chesapeake Bay (Chapter 3).*In* Houde, E. D., E. J. Chesney, T. A. Newberger, A. V. Vazquez, C. E. Zastrow, L. G. Morin, H. R. Harvey, and J. W. Gooch. Population Biology of Bay Anchovy in Mid-Chesapeake Bay. Solomons, Maryland pg. 17-77

Nixon, S. E. and B. A. Buckley. 2002. "A strikingly rich zone" – Nutrient enrichment and secondary production in coastal marine ecosystems. Estuaries 25: 782-796

Peebles, E. B., J. R. Hall, and S. G. Tolley. 1996. Egg Production by the bay anchovy *Anchoa mitchilli* in relation to adult and larval prey fields. Marine Ecology Progress Series 131: 61-73

Powledge, F.. 2005. Chesapeake Bay restoration: A model of what?. BioScience 55: 1032-1038

Purcell, J. E. and J. H. Cowan Jr.. 1995. Predation by the scyphomedusan *Chrysaora quinquecirrha* on *Mnemiopsis leidyi* ctenophores. Marine Ecology Progress Series 129: 63-70

Purcell, J. E. and M. B. Decker. 2005. Effects of climate on relative predation by scyphomedusae and ctenophores on copepods in Chesapeake Bay during 1987-2000. Limnology and Oceanography 50: 376-387

Rabalais, N. N., R. E. Turner, Q. Dortch, D. Justic, V. J. Bierman Jr., W. J. Wiseman Jr.. 2002. Nutrient-enhanced productivity in the northern Gulf of Mexico: past, present and future. Hydrobiologia 475: 39-63

Randall, C. W., Z. Kisoglu, D. Sen, P. Mitta, and U. Erdal.1999. Final report: Evaluation of wastewater treatment plants for BNR retrofits using advances in technology. U.S. EPA Chesapeake Bay Program, Annapolis, Maryland

Rose, K. A., J. H. Cowan Jr., M. E. Clark, E. D. Houde, and S-B Wang. 1999. An individual-based model of bay anchovy population dynamics in the mesohaline region of Chesapeake Bay. Marine Ecology Progress Series. 185: 113-132

Rose, K. A., J. H. Cowan Jr., K. O. Winemiller, R. A. Myers and R. Hilborn. 2001. Compensatory density dependence in fish populations: importance, controversy, understanding and prognosis. Fish and Fisheries 2: 293-327

Runge, J. A., P. J. S. Franks, W. C. Gentleman, B. A. Megrey, K. A. Rose, F. E. Werner, B. Zakardjian. 2004. Diagnosis and prediction of variability in secondary production and fish recruitment processes: developments in physical-biological modeling (Chapter 13), *In* Robinson, A. R. and K. H. Brink (eds). The global coastal ocean: Multi-scale interdisciplinary processes, The Sea, 13: 413-473

Scheffer, M, J. M. Baveco, D. L. DeAngelis, K. A. Rose, and E. H. Van Nes. 1995. Super-individuals a simple solution for modeling large populations on an individual basis. Ecological Modelling 80: 161-170.

Snyder, J. P.. 1987. Map projections – A working manual. Geological Survey Professional Paper, 1395. U. S. Government Printing Office, Washington, D. C.

Wang, D., M. W. Berry, and L. J. Gross. 2005. A parallel structured ecological model for high end shared memory computers. First International Workshop on OpenMP.

Wang S-B and E. D. Houde. 1994. Energy storage and dynamics in bay anchovy *Anchoa mitchilli*. Marine Biology 121: 219-227

Wang, S-B, J. H. Cowan Jr., K. A. Rose and E. D. Houde. 1997. Individual-based modeling of recruitment variability and biomass production of bay anchovy in mid-Chesapeake Bay. Journal of Fish Biology 51(Suppl. A): 101-120

Winemiller, K. O. and K. A. Rose. 1992. Patterns of life-history diversification in North American fishes: Implications for population regulation. Canadian Journal of Fisheries and Aquatic Sciences 49: 2196-2218

Zastrow, C. E., E. D. Houde, and L. G. Morin. 1991. Spawning fecundity, hatch-date frequency and young-of-the-year growth of bay anchovy *Anchoa mitchilli* in mid-Chesapeake Bay. Marine Ecology Progress Series 73: 161-171

CHAPTER 4: GENERAL CONCLUSIONS

In this study, two fish population models were linked to water quality models to predict the effects of changes in lower Patuxent River and Chesapeake Bay water quality on bay anchovy growth and survival. Most water quality models do not include trophic levels higher than zooplankton, while most fish models do not include trophic levels lower than zooplankton. Yet, understanding how changes in nutrient loadings affect fish production requires an integrated approach.

For the Patuxent River portion of the study (Chapter 2), I linked an individual-based predation model of bay anchovy with a Patuxent River water-quality model that itself was linked to a Patuxent watershed land-use model. The output of the watershed model was used as inputs to the water quality model, and the resulting outputs of the water quality model were used as inputs to the anchovy predation model. The coupled models were used to examine the effects of changes in Patuxent watershed land-use (decreased, current, and increased), changes in Chesapeake Bay nutrient loadings at the downstream boundary (decreased, baseline, and increased), and water year (wet and dry) on summertime survival of anchovy egg and larval cohorts.

For the Chesapeake Bay portion of the study (Chapter 3), I dynamically coupled a spatially-explicit, individual-based model of bay anchovy to the 3-dimensional Chesapeake Bay water quality model. The water quality model simulated nutrient recycling, and phytoplankton and zooplankton densities in the spatial grid. The water quality model used output from a hydrodynamics model for advection and dispersion, and was coupled with a sediment diagenesis model to allow for long-term effects of nutrient changes to be simulated. The coupled anchovy and water quality models were used to examine the effects of decreased, baseline, and increased

nutrient loadings on anchovy growth, survival, and biomass for fixed low and high anchovy recruitment. Ten-year simulations using the observed sequence of wet, normal, and dry water years between 1984 and 1993 were performed.

In Chapter 2, I found that Chesapeake Bay water quality had a bigger effect on egg and larval survival in the lower Patuxent River than changes in local Patuxent watershed land-use. The effect of changes in Patuxent watershed land-use on egg and larval survival was small, as the modeled water quality in the lower portion of the Patuxent River was strongly influenced by the water quality of Chesapeake Bay. Patuxent watershed land-use scenarios did have an effect on chlorophyll *a* concentrations and dissolved oxygen concentrations in segments farther upstream, with reduced nutrient loadings resulting in the best water quality and highest dissolved oxygen concentrations. However, most anchovy spawn farther downstream, preferring to spawn in more saline waters (Houde and Zastrow 1991). Additionally, dissolved oxygen concentrations in the upstream segments were not hypoxic and therefore would not affect anchovy growth and survival. Improving Chesapeake Bay water quality increased egg survival but decreased larval survival during June. During July, larval mortality rates were uniformly high, and the effects of changing nutrient loadings on survival could not be determined. The low tolerance of anchovy eggs to hypoxia resulted in eggs being highly vulnerable to the direct effects of hypoxia. In contrast, larval survival was primarily affected by the indirect effects of low dissolved oxygen that altered the degree of spatial overlap between larvae and their invertebrate predators.

In Chapter 3, I successfully coupled a spatially-explicit individual-based bay anchovy population model with the Chesapeake Bay water quality model. Predicted anchovy growth, abundance, and biomass were generally comparable to field data. The kinesis movement model was successful in mimicking some of the anchovy distributional patterns that have been observed

in Chesapeake Bay related to wet, normal, and dry years. Simulations of Chesapeake Bay water quality found that decreasing nutrient loadings to the Bay by 50% would result in large reductions in anchovy lengths and biomass, while having only small positive effects on anchovy survival. Increasing nutrient loadings was found to increase anchovy lengths and biomass, but the effects were smaller than for a decrease in nutrient loadings and sometimes similar to the results predicted under baseline nutrient loadings. Comparisons of anchovy lengths, survival, and biomass between low and high anchovy recruitment scenarios indicated that anchovy exhibited compensatory density-dependent growth. When recruitment was assumed low every year, simulated anchovy grew longer.

There are three major caveats that should be considered when determining the implications of my modeling results. The first caveat, which applies only to the Patuxent model, is that while Chesapeake Bay water quality affected anchovy survival far more than Patuxent watershed land-use, this should not be taken as argument that there is not a need to control nutrient loadings from the local Patuxent River watershed. Reduced nutrient loadings under decreased land-use did improve water quality farther upstream in the Patuxent River, and there are other potential benefits to improved water quality beyond anchovy egg and larval survival. Furthermore, as a tributary of the Chesapeake Bay, Patuxent River nutrient loadings and water quality need to viewed in the context of the entire Bay and efforts for whole-system management.

The second caveat, which applies to both the Patuxent River and the Chesapeake Bay analyses, is that both models assumed simplified initial numbers of individuals for their simulations. Not allowing the initial numbers of individuals in model simulations to vary as a part of the simulations removed potentially important effects of water years on anchovy growth

and survival. In the Patuxent River simulations, predator abundances did not change in response to water years. Purcell and Decker (2005) found that the relative abundances of ctenophores and sea nettles changed in response to water years. Changes in predator abundances would affect anchovy mortality rates. The Chesapeake Bay analysis ignored the effects of hypoxia on the early life stages of anchovy prior to 23-mm juveniles. Small differences in the growth and survival rates of early life stages can have order of magnitude effects on the abundances of later life stages (Houde 1987).

The third caveat, which applies to both models, is that model simulations focused on bay anchovy and greatly simplified the dynamics of other species. Anchovy are a part of a complicated food web that includes competition from other forage fish species for zooplankton prey, competition for zooplankton prey and predation by ctenophores and sea nettles (Purcell and Decker 2005), and predation by pisciviorous fish including striped bass, bluefish, and weakfish (Hartman and Brandt 1995). Research by Jung and Houde (2003) and Purcell and Decker (2005) have shown that the distributions and abundances of the competitors and predators of anchovy vary in their responses to wet versus dry water years and to hypoxic conditions. Allowing predator effects to vary between water years could increase the effect of water years in simulations and affect my conclusions about the effects of changes in nutrient loadings. These differences could have potentially large effects on anchovy growth and survival.

Both models could be improved by making growth and mortality dynamic and dependent upon computed conditions within the models. For example, the Patuxent River anchovy model could be improved if water quality model predictions of chlorophyll *a* were used to adjust growth rates of anchovy. Changes in anchovy growth rates may affect larval mortality rates, as faster growing larvae may have lower overall mortality rates than slower growing larvae (Houde

1987). The Chesapeake Bay anchovy model could be improved if dynamic predators were added to the model. In its current form, the model is a completely bottom-up analysis. Adding a predator would allow for the inclusion of top down effects on anchovy population dynamics.

The biggest improvement that could be made to the two anchovy models would be to combine them into a single model. The counter-acting dependence of egg mortality and larval mortality on nutrient loadings made their separate analyses difficult to combine. The analysis is further complicated by the fecundity of adult anchovy being dependent on food availability as anchovy are "income breeders" (Luo and Musick 1991, Wang and Houde 1994, Peebles et al. 1996). Anchovy spawning intensity could be increased by both increases in food availability and reductions in the number of individuals present. By developing a full-life cycle dynamically coupled population and water quality model we could better determine the long-term population responses of anchovy to changes in nutrient loadings.

Future modeling studies should focus on the development of a full life cycle, dynamically coupled fish population and water quality model for Chesapeake Bay. The current Chesapeake Bay anchovy model should be expanded to include the egg and larval stages of anchovy. Anchovy egg production would be dependent upon simulated spawning stock biomass and daily prey consumption. Egg predation by key anchovy invertebrate and fish predators and egg mortality from exposure to hypoxia and anoxia would determine larval production. A true full life cycle model with anchovy imbedded in a food web would allow for the sometimes counter-acting effects of nutrient loadings among life stages and for the potential for both bottom-up and top-down controls to be integrated into a single model. Anchovy prey and predator abundances and spatial distributions would then both vary in response to water years and changes in nutrient loadings. As a part of the expansion, the present version of the model should undergo a more

formal skill assessment to examine the model's performance using the data from the Trophic Interactions in Estuarine Systems (TIES) and the Chesapeake Bay Fishery-Independent Multispecies Survey (CHESFIMS) projects. Future analyses could use the present model to simulate the population response of more benthic-oriented species such as croaker (*Micropoganias undulates*), which might be more sensitive to the hypoxia aspects of changes in nutrient loadings than anchovy (Eby et al. 2005).

In summary, this study showed that the response of anchovy to changes in nutrient loadings was dependent on the life stage being examined. Patuxent River simulations (Chapter 2) found that anchovy egg survival increased when nutrient loads were reduced, while larval survival decreased. Additionally, it was found that changes in Chesapeake Bay water quality affected egg and larval survival more than Patuxent watershed land-use. Chesapeake Bay simulations (Chapter 3) found that juvenile and adult anchovy had slower growth and lower biomass when nutrient loadings were reduced. Both sets of results should be treated with caution as there are a number of caveats that could affect the robustness and realism of the results. Finally, I demonstrated that it is both feasible and desirable to dynamically couple a near full-life-cycle, spatially-explicit, individual-based anchovy population model with the Chesapeake Bay water quality model. Future studies should focus on expanding this model to include the full life-cycle of anchovy imbedded in a food web.

4.1 References

Eby, L. A., L. B. Crowder, C. M. McClellan, C. H. Peterson, and M. J. Powers. 2005. Habitat degradation from intermittent hypoxia: impacts on demersal fishes. Marine Ecology Progress Series 291: 249-261

Hartman, K. J. and S. B. Brandt. 1995. Trophic resource partitioning, diets and growth of sympatric estuarine predators. Transactions of the American Fisheries Society 124: 520-537

Houde, E. D.. 1987. Fish early life dynamics and recruitment variability. American Fisheries Society Symposium. 2: 17-29

Houde, E. D. and C. E. Zastrow. 1991. Bay anchovy. *In* Funderburk, S. L., J. A. Mihursky, S. J. Jordan, and D. Riley (eds.). Habitat requirements for Chesapeake Bay living resources, 2nd Edition. Living Resources Subcommittee, Chesapeake Bay Program. Annapolis, Maryland pg 8-1 – 8-14

Jung, S. and E. D. Houde. 2003. Spatial and temporal variabilities of pelagic fish community structure and distribution in Chesapeake Bay, USA. Estuarine, Coastal and Shelf Science 58: 335-351

Luo, J. and J. A. Musick. 1991. Reproductive biology of the bay anchovy in Chesapeake Bay. Transactions of the American Fisheries Society 120: 701-710

Peebles, E. B., J. R. Hall, and S. G. Tolley. 1996. Egg Production by the bay anchovy *Anchoa mitchilli* in relation to adult and larval prey fields. Marine Ecology Progress Series 131: 61-73

Purcell, J. E. and M. B. Decker. 2005. Effects of climate on relative predation by scyphomedusae and ctenophores on copepods in Chesapeake Bay during 1987-2000. Limnology and Oceanography 50: 376-387

Wang S-B and E. D. Houde. 1994. Energy storage and dynamics in bay anchovy *Anchoa mitchilli*. Marine Biology 121: 219-227

VITA

Aaron Thomas Adamack was born in Fernie, British Columbia, Canada, on January 17, 1976, the son of Beverly E. Adamack and Dr. Thomas L. Adamack and the brother of Denene C. Adamack. He attended school in Fernie, British Columbia, before moving to Kelowna, British Columbia, where he attended Mt. Boucherie Secondary School, graduating in 1994. He then attended Okanagan University College from 1994-1996 before transferring to the University of British Columbia, which he attended from 1996-1999, and received a Bachelor of Science in animal biology. He entered the Department of Oceanography and Coastal Sciences at the Louisiana State University in August 1999 as a graduate research assistant under the direction of Dr. Kenneth A. Rose and received a Master of Science degree in oceanography and coastal sciences in December 2003. Aaron has continued working as a graduate research assistant under the direction of Dr. Kenneth A. Rose and will be receiving a Doctor of Philosophy degree in oceanography and coastal sciences in August 2007. Ironically, having spent the last eight years living in Louisiana and studying Chesapeake Bay in Maryland and Virginia, upon completing his degree, Aaron will be moving to Michigan to begin work as a post-doctoral researcher with Dr. Doran Mason at the Great Lakes Environmental Research Laboratory and the Cooperative Institute for Limnology and Ecosystems Research studying fish and shrimp in coastal Louisiana.